Foreland evolution of Blåisen, Norway, over the course of an ablation season

Alexander Foyn

Dissertations in Geology at Lund University,
Master's thesis, no 585
(45 hp/ECTS credits)

Department of Geology
Lund University
2020

Foreland evolution of Blåisen, Norway, over the course of an ablation season

Master's Thesis

Alexander Foyn

Department of Geology
Lund University
2020

Contents

Abbreviations

DEM = Digital Elevation Model
GIS = Geographical Information Systems
GPS = Global Positioning System
LIA = Little Ice Age
SfM = Structure from Motion
UAV = Unmanned Aerial Vehicle

Cover Picture: Thawing winter snow on Finsevatnet in June 2019, view looking out from Finse towards Hardangerjøkulen, with Blåisen visible in the background. Photo: Alex Foyn

Foreland evolution of Blåisen, Norway, over the course of an ablation season

ALEXANDER FOYN

Foyn, A., 2020: Foreland evolution of Blåisen, Norway, over the course of an ablation season. *Dissertations in Geology at Lund University*, No. 585, 71 pp. 78 hp (45 ECTS credits)

Abstract: This study presents a detailed investigation into the evolution of sedimentary landforms over an ablation season at Blåisen, an outlet of the Hardangerjøkulen Icecap, Norway. The two visits to Blåisen, one each side of the ablation season, allowed the preservation and evolution of the landforms to be studied. Much research is conducted studying glacial landforms, which are key in our understanding of past and future ice behaviour. This is important in researching the past, present and future response of the cryosphere to climate forcing, and the impact of such changes. A smaller portion of glacial geomorphological studies are now conducted using predominantly fieldwork with even fewer making repeated visits to sites in short succession. Many now use remote sensing which, while being a powerful tool to understand ice behaviour, means that smaller scale features (both in the temporal and spatial sense) may be missed. An awareness of what may be missing when studying forelands that are a few years to many millennia old is important to gaining a more holistic understanding of the ice behaviour and the processes occurring. This study focuses on the younger landforms in the immediate vicinity of the ice margin. GPS mapping, field observations and Structure from Motion Photogrammetry was used over two visits to Blåisen in June and September to identify four such landform types: snowbank squeeze moraines, flutes, minor moraines and an ice-cored wedged shaped ridge system (called a sediment wedge in this study after its characteristic shape).

The foreland of Blåisen was characterised by a number of areas where a reverse bedrock was present (bedrock that slopes in the opposite direction to ice flow); this had the effect of inhibiting drainage leading to saturated sediments around the ice margin. These sediments are easily deformable, so play an important role in the formation of the Snowbank Squeeze Moraines, Flutes, Minor Moraines in particular. The processes of formation are explored using the geomorphological and sedimentological evidence to devise genesis and evolution models for each landform type. The model for the formation of the sediment wedge presents freeze-on as a prominent mechanism, facilitating the transport of debris in a band from the base of the glacier to the margin where, due to differential melting, the underlying ice is isolated from the rest of the glacier. Snowbank Squeeze Moraines were observed as ridges of sediment protruding out of the snow in June formed by the deformation of sediments between the ice margin and the winter snowbank lying over the margin. The ‘squeeze’ form of snowbank moraines has not been widely documented in part due to their poor preservation, illustrated by the lack of remaining evidence for them in September. Few flutes were recorded aside from those mapped in September, indicating that either in past seasons, conditions had not been favourable for formation, or that preservation was poor. The latter is supported by the lack of remaining evidence of the snowbank squeeze ridges in September. The poor preservation of these landforms highlights how they may be missed in other studies and the need for further research in this area.

Keywords: Geomorphological Mapping, Structure from Motion, Glacial Landforms, Ice-Marginal Landforms, Landform Preservation, Hardangerjøkulen, Norway

Supervisor: Sven Lukas

Subject: Quaternary Geology

Alexander Foyn, Department of Geology, Lund University, Sölvegatan 12, SE-223 62 Lund, Sweden. E-mail: alex.foyn@btopenworld.com

Utvecklingen under en ablationssäsong av Blåisens förland, Norge

ALEXANDER FOYN

Foyn, A., 2020: Utvecklingen under en ablationssäsong av Blåisens förland, Norge. Examensarbeten i geologi vid Lunds universitet, Nr. 585, 71 sid. 78 hp (45 ECTS credits)

Sammanfattning: Denna studie presenterar en detaljerad undersökning av utvecklingen av sedimentära landformer under en ablationssäsong vid Blåisen, en del av Hardangerjøkulen, Norge. Två besök vid Blåisen, i början och i slutet av ablationssäsongen, gjorde det möjligt att studera hur landformerna bevaras och utvecklas. Det pågår mycket forskning om glaciala landformer som är en nyckel till förståelse av hur tidigare och framtida isar fungerar. Detta är en viktig del inom forskningen om hur kryosfären har reagerat, reagerar och kommer att reagera på klimatförändringar och vilka effekter de ger. En mindre andel av de glacialmorfologiska studierna är nu övervägande baserade på fältarbete, och inom ännu färre görs upprepade besök på samma plats med korta tidsintervall. Flertalet forskare använder nu fjärranalys som, även om det är ett kraftfullt verktyg för att förstå isdynamik, innebär att företeelser i mindre skala (både i tidsmässig och rumslig mening) kan missas. För att få en helhetsförståelse för isdynamiken och de processer som äger rum är det viktigt med en medvetenhet om vad som, beroende på metod, kan undgå upptäckt när man studerar glaciala förland som är några år till tusentals år gamla. Denna studie fokuserar på yngre landformer i omedelbar närhet av isfronten. GPS-kartläggning, fältobservationer och Structure-from-motion- fotogrammetri användes under två fältbesök vid Blåisen i juni och september 2019 för att identifiera fyra sådana landformstyper: snödrivepressade moräner (Snowbank Squeeze Moraines), moränsträngar, mindre moräner och ett system av kilformade ryggar med iskärnor (kallat sedimentkil i denna studie efter dess karakteristiska form).

Blåisens förland kännetecknades av ett antal områden där berggrunden lutade mot glaciären (berggrund som lutar i motsatt riktning mot isflödet); detta hindrade dräneringen vilket ledde till att sedimenten vid iskanten blev vattenmättade. Dessa sediment är lättdeformerade och spelar en viktig roll i bildandet av snödrivepressade moräner, moränsträngar och särskilt de mindre moränerna. Bildningsprocesserna utforskas med hjälp av geomorfologiska och sedimentologiska observationer för att utforma bildnings- och utvecklingsmodeller för varje landformstyp. Bildningsmodellen för sedimentkilen tar upp tillfrysning som en framträdande mekanism, och som underlättar materialtransport från glaciärens bas till kanten där den underliggande isen isoleras från resten av glaciären genom olikformig avsmältning. De snödrivepressade moränerna observerades som ryggar av sediment som stack ut ur snön i juni och var bildade genom deformation av sediment mellan iskanten och den driva av vintersnö som låg över iskanten. Den "pressade" formen hos snödrivemoränerna har inte kunnat dokumenteras i detalj, delvis på grund av deras dåliga bevarande, vilket illustreras av att det inte fanns kvar några spår av dem i september. Få moränsträngar observerades förutom de som kartlades i september. Det visar att antingen hade förhållandena inte varit gynnsamma för bildandet av moränsträngar under tidigare säsonger eller så var bevarandegraden dålig. Det sistnämnda stöds av bristen på kvarvarande bevis för snödrivemoränryggarna i september. Den dåliga bevarandegraden hos dessa landformer belyser hur de kan missas i andra studier och visar på behovet av ytterligare forskning inom detta område.

Nyckelord: Geomorfologisk kartläggning, struktur från rörelse, glaciala landformer, Ismarginala landformer, Landformsbevarande, Hardangerjøkulen, Norge

Handledare: Sven Lukas

Ämnesinriktning: Kvartärgeologi

Alexander Foyn, Geologiska institutionen, Lunds Universitet, Sölvegatan 12, 223 62 Lund, Sverige. E-post: alex.foyn@btopenworld.com

1. Introduction

1.1. Background

Glaciers and other large ice bodies play a crucial role, both as controls and reactive components within the earth system and impact all life on earth directly or indirectly (Abram et al., 2019). Climatologically, feedback mechanisms in the cryosphere can accelerate climate change and its impacts (Kaser, 2001; Bishop et al., 2004; Box et al., 2012). The cryosphere is an integral part of the short and longer-term hydrological cycle, a key factor governing sea level variation (Meier, 1984; Meier et al., 2007; Radić and Hock, 2011; Marzeion et al., 2017) and water supply to many regions of the world (Kaser et al., 2010; Chevallier et al., 2011). Ice also has a prominent role in erosion rates, a central factor in sediment and nutrient supply to lower lying and agricultural regions (Allison and Kepple, 2001; Mukherjee et al., 2009) and the longer-term landscape evolution (Brozović et al., 1997; Bishop et al., 2001; Jamieson et al., 2008; Mukherjee et al., 2009). The study of glaciers and the wider cryosphere is therefore of vital importance in understanding how the climate has changed in the past, its present changes, and the impacts this will have (IPCC, 2019). The evolution of glaciers and glacial landscapes forms an important part of this understanding, particularly for the accurate representation of past ice behaviour, indicating how glaciers may respond in the future.

Through erosional and depositional landforms and sediments, glaciers leave their mark on the landscape. Particularly through ice-marginal landforms such as moraines, it is possible to reconstruct previous margin positions (Evans and Benn, 2014; Bennett and Glasser, 2009; Benn and Evans, 2010). By mapping former ice margin positions, the Equilibrium Line Altitude of former glaciers can be calculated for palaeoclimate research (Benn and Evans, 2010). The Equilibrium Line Altitude is the hypothetical line across a glacier which divides the accumulation and ablation zones, where the net annual mass balance (i.e. the change in a glacier's mass over a given time period) equals zero. There is a vast body of literature documenting glacial forelands (e.g. Stokes et al. 2013; Bendle et al. 2017; Pearce et al 2018). However, much of this relies predominantly on remote sensing (e.g. Hughes et al. 2014; Chandler et al. 2016a; Evans et al. 2016; Stroeven et al. 2016; Margold et al. 2018) or uses relict forelands (e.g. Benn and Ballantyne, 2005; Chiverrell and Thomas, 2010; Chandler and Lukas, 2017; Margold et al., 2018). While these studies are all highly valuable for furthering our understanding of glaciers and their behaviour, more poorly preserved landforms may be overlooked. These landforms are underrepresented in the literature because they are either too small to be identified in all but the most detailed aerial imagery and Digital Elevation Models (DEMs), or more frequently, the preservation duration is too short to allow for documentation. If a study uses satellite imagery for example, a landform could be created and lost between satellite passes. Similarly, the palaeoglacial studies can only be based on the evidence that is preserved, normally limited to the largest landforms with many smaller features potentially lost in the intervening period between formation and documentation.

There is therefore still a need to study contemporary glaciers in the field rather than solely using remote sensing. While remote sensing has many advantages for example, the ability to study large areas and the greater sense of perspective this offers (Pellikka and Rees 2009), the investigation is limited in the scale of the landforms that can be studied by the resolution of the data. Additionally, not being present in the field prevents the study of sedimentology in tandem with the geomorphology, a vital aspect of understanding landform genesis and preservation potential.

1.2. Aims

To address the gap in the literature identified above, the primary aim of this study is to investigate newly forming and exposed landforms in the foreland of Blåisen over an ablation season (the portion of the year where ablation exceeds accumulation, i.e. the summer months) in order to best document the genesis and evolutionary changes of these landforms over a short time span. This will be done by contrasting field observations and geomorphological mapping conducted at the start of summer (June) with those made towards the end of summer in September. This primary aim encompasses several objectives:

- Firstly, to explore the use of Structure from Motion (SfM) modelling to aid the characterisation of landforms and how they develop over the ablation season.
- Secondly, to map the immediate foreland in detail, both in June and September to study changes at the margin.
- Thirdly, to investigate the possible formation and preservation potential of glacial landforms along the margin using field observations and SfM models from each side of the ablation season.

2. Study Area

Blåisen is an outlet glacier situated on the northeastern side of the Hardangerjøkulen icecap, which itself lies in Hordaland county, in central southern Norway. Hardangerjøkulen is a small icecap or plateau icefield, at approximately 69.2km^2 in area, it represents Norway's sixth-largest ice mass (Andreassen et al., 2012). Topographically it ranges from 1863m to 1066m above sea level at the terminus of the Rembesdalskåka outlet glacier on the eastern side of Hardangerjøkulen (Weber et al., 2019). Blåisen by comparison terminates at approximately 1424m above sea level. The glacier's gradient averages around 8-10% but steepens towards the margin.

The glacier was selected as it presented a relatively accessible glacial foreland, only five kilometres from the village of Finse, itself on the railway line between Oslo and Bergen, making it easy to access with equipment. Secondly, there have been few studies made on Blåisen to date; these will be outlined in this section. Glacial retreat at Blåisen has been shown to be accelerating (Weber et al., 2019), making it a suitable site to study landforms as they are created and evolve.

The topography of the glacial foreland is complex and dominated by the influences of bedrock and meltwater shown in Figure 1a. Broadly, the margin falls away slightly to the northwest in the direction of Midtdalsbreen **[1]** with more undulating bedrock dominating the immediate foreland topography to the south **[2]**. A large ridge dissects the east of the foreland **[3]**, separating a smaller subsidiary portion of the glacier to the southeast **[4]**. The main meltwater portal **[5]** is currently located in a localised lower area roughly midway across the foreland. Beyond the study area to the northeast, the foreland is dominated by braided meltwater systems **[6]** which predominantly drains in a northwards direction.

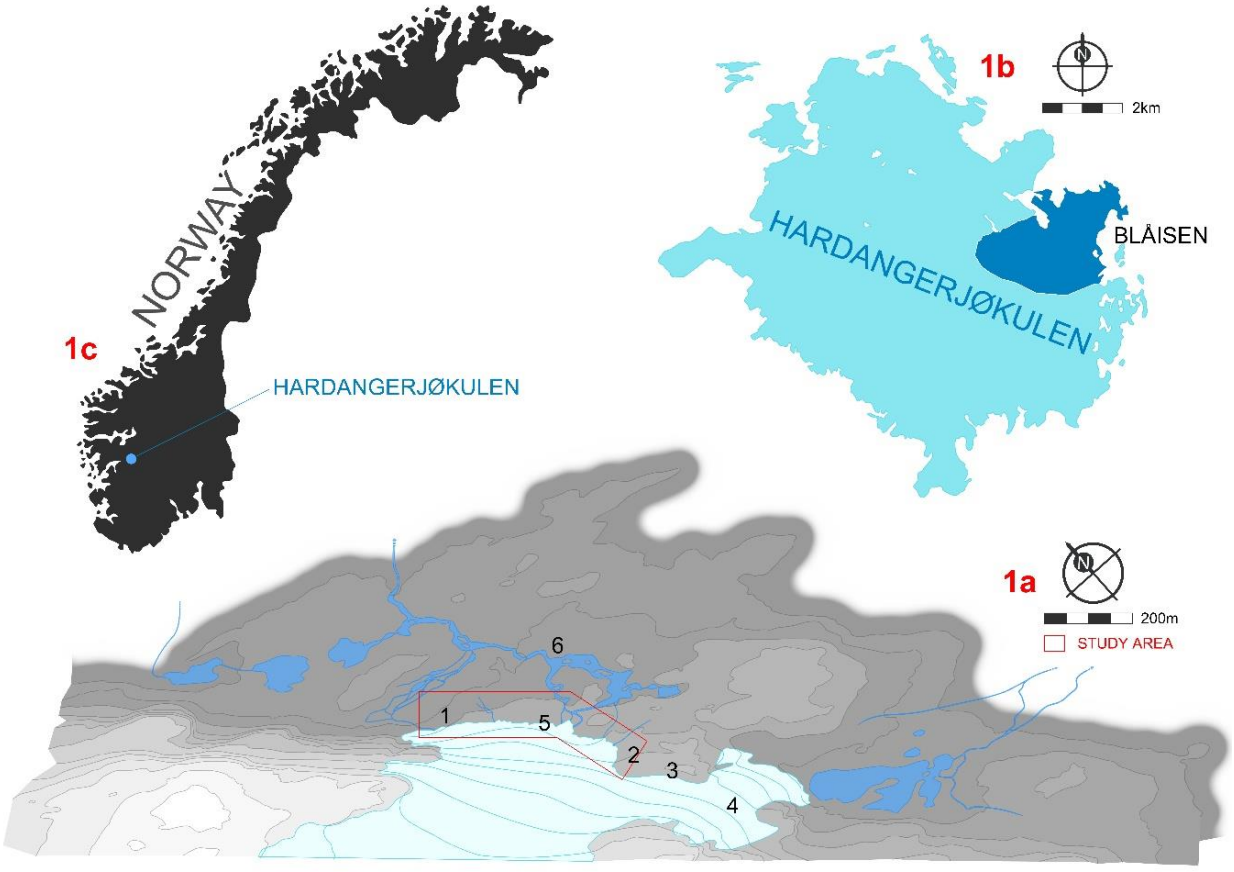

Figure 1a *- Figure showing the broad foreland topography of Blåisen immediate foreland, numbering relates to features described in the above paragraph (topography data from Kartverket, glacier position from NVE, 2013 and drainage from satellite imagery acquired from http://norgeibilder.no/). The study site is shown in red.* ***Figure 1b*** *(inset) - shows the Hardangerjøkulen icecap (data from NVE, 2013) with Blåisen and its approximate catchment in blue.* ***Figure 1c*** *- (inset) shows the location of Hardangerjøkulen icecap within Norway.*

To address the project aims, the investigation focuses on the first 100m of Blåisen´s foreland. Older, larger features, further from the present glacier snout having already been studied, most recently by Weber et al. (2019) following the earlier work of Andersen and Sollid (1971). Field studies focused on the main Blåisen snout: the smaller eastern portion of the glacier, separated by an outcrop of rock, was not included in this study due to its inaccessibility, lying at higher elevation and further from shelter, and the very extensive snow cover in the area during the first visit in June.

Existing Studies of Blåisen and Hardangerjøkulen

Existing research on Hardangerjøkulen is relatively sparse with less than a dozen papers written in English covering the icecap and surrounding area (Andreassen et al., 2012). Based on sedimentological and geomorphological evidence, the present icecap has existed since the Mid-Holocene, ~4.8–3.4 ka BP, following several ice-free periods after the breakup of the continental ice sheet ~9.1 ka BP (Dahl and Nesje, 1994; Nesje et al., 1994; Dahl and Nesje, 1996).

The sedimentological and geomorphological evidence is supported by several investigations employing modelling to examine the past changes and future response to climate change (Giesen, 2009; Giesen and Oerlemans, 2010; Åkesson, 2014; Åkesson et al., 2017). These studies have found that under a linear climate forcing, the Hardangerjøkulen icecap can grow from ice-free conditions at the time indicated by the sedimentological studies, to a maximum extent during the Little Ice Age (LIA) (Åkesson et al., 2017). For Blåisen, the LIA outermost moraines were constrained to ca.1750 (using Lichenometry) and now lie roughly 1km from the 2019 glacial margin (Andersen and Sollid 1971; Nesje and Dahl, 1991). Lichenometry is the use of estimated lichen growth rate to determine the age that a surface (bolder or bedrock) has been exposed (Trenbirth & Matthews, 2010). The modelling studies also show that the present-day icecap is highly vulnerable to changes in mass balance (Åkesson et al., 2017), with projections predicting the disappearance of the icecap by 2100 (Giesen and Oerlemans, 2010). This is supported by the observational and geomorphological evidence which has shown sustained and, in the last 30 years, accelerating retreat since the LIA (Nesje and Dahl, 1991; Andreassen et al., 2005; Nesje et al., 2008; Weber et al., 2019).

The most recently published paper at the time of writing by Weber et al. (2019) investigates in detail the retreat of Hardangerjøkulen since the LIA. Ice-marginal features such as moraines, glacial deposition limits, trimlines, and erosion and weathering boundaries were mapped using historical maps, satellite imagery and fieldwork for ground-truthing. Weber et al. (2019) provide the most comprehensive geomorphological mapping around the icecap to date. The work shows an a-synchronous pattern of moraine formation over time, whereby few to no moraines are found dating to after ~1923-1929, only restarting from the 1990s. The exception to this are the outlets of Blåisen and neighbouring Midtdalsbreen, the latter restarting in the 1950s. Blåisen is the only outlet where moraine formation was continuous. Weber et al (2019) hypothesises that this may be linked to sediment availability, and potentially a function of inefficient glaciofluvial transport of material away from the margin.

Focusing on the existing literature for Blåisen, only two papers have investigated the geomorphology in any detail, Andersen and Sollid (1971) and the aforementioned paper by Weber et al. (2019). Of these, only Andersen and Sollid (1971) has studied the geomorphology in conjunction with the sediments. Their paper, which incorporated several other outlets of Hardangerjøkulen including Midtdalsbreen, used Lichenometry to date mapped landforms and provides the earliest record in English of the Geomorphology around Blåisen, summarising the previous Norwegian work. The paper is approaching 50 years old in 2020, with a great deal more foreland exposed now than when the paper was published. For this reason, it is of limited use within the study area of this investigation. However, Andersen and Sollid (1971) include detailed geomorphological and sedimentological description of the landforms they encountered, more so for Midtdalsbreen than Blåisen, but which provided a valuable inventory of landforms around Hardangerjøkulen which this study used as a guide for the fieldwork. This includes extensive fluting at both Blåisen and Midtdalsbreen, and a detailed description of the types of moraines found. Some smaller moraines close to the margin of Midtdalsbreen are interpreted as ‘Annual’ Moraines, described as consisting of clayey sediments and glaciofluvial material. Ice-cored moraines were also observed and described as deriving from frozen-on bands of sediment, transported to the glacier surface along shear zones where it buries ice/snow at the margin, with differential melting leading the moraine formation. This is supported by a more recent study by Reinardy et al. (2013) at Midtdalsbreen, which details a similar process but emphasises the role of freeze-on within seasonal cyclicity.

The paper by Weber et al. (2019) provides the most recent mapping of both Blåisen and Hardangerjøkulen. However, this was performed as part of a large-scale project with the focus on landforms that can be used to constrain the extent of Blåisen for the use of modelling the evolution of Hardangerjøkulen and predict its future, not as part of a study investigating glacial-sedimentary

processes and landform genesis. The fieldwork was conducted with the purpose of ground-truthing the satellite imagery, so the smaller scale geomorphology, too small to be seen by satellite, is largely absent from the mapping. Similarly, features with short 'lifespans' (i.e. the duration that landforms are in existence before degradation makes them indistinguishable, and the extent to which they are preserved) are not included due to the coarse temporal resolution of the imagery/DEM. Despite this, the mapping by Weber et al. (2019) does supply a comprehensive wider geomorphological framework for this investigation and context for the rest of Hardangerjøkulen.

3. Methods

In the methods section, the distinction is made between the conventional methodology that was employed and how it was adapted for certain tasks during this investigation. This study will take holistic approach in mapping all geomorphological landforms in the foreland while also noting changes in topography, underlying bedrock and observations on sedimentology and processes. In recent years, there has been a shift towards a greater reliance on remote sensing in mapping with the use of DEMs and aerial imagery with fieldwork used more in the ground truthing process (Stokes et al., 2013; Bendle et al., 2017; Pearce et al., 2018; Chandler et al., 2016a; Evans et al., 2016a). This process particularly lends itself to the study of large-scale paleo-glaciated environments such as the mapping of past ice sheet extents and flows (Hughes et al., 2014; Stroeven et at., 2016; Margold et al., 2018). However, for this smaller scale investigation on Blåisen, the ongoing state of flux in the foreland with the continuous creation and destruction of landforms over a short timescale of a few months meant that the use of existing imagery and DEMs, more suited to static environments, would be inappropriate. Therefore, this study takes a largely 'classical' approach to mapping using predominantly field-based methods, with Geographical Information Systems (GIS) used in the post fieldwork phase to assemble the data.

3.1. Field Methods

To address the aims, two periods of fieldwork took place, one in the early ablation season between the 14th-19th of June 2019. The second, towards the end of the ablation season from the 9th-14th of September 2019. During the latter trip, work was significantly hampered by poor weather conditions which reduced the amount of time that could be spent in the foreland. The following section describes the field methods performed and provides justification for any modifications made to the standard practice described by Chandler et al (2018).

3.1.1. Geomorphological Mapping

Mapping at Blåisen was largely reliant on Global Positioning System (GPS) to mark out geomorphological features that were described in the field. During both field visits, the margin of the glacier was the first feature to be mapped, which allowed the site as a whole to be surveyed before geomorphological mapping commenced. During the June fieldwork, the glacier terminus was covered in a large quantity of snow making it was impossible to locate the ice margin under the snow. Therefore, the snow and ice margin were mapped as one entity without distinguishing between the two.

Ridges were recorded by marking GPS points on a Garmin GPSMAP 64s along the ridge crests following a similar process to that described in the literature (e.g. Bradwell et al.,2013; Brynjólfsson et al., 2014; Małecki et al., 2018). Mapping was carried out systematically starting at one side of the glacier foreland and working across. As already stated in the site description, mapping focused on the 100 m of foreland closest to the glacier, bearing the youngest landforms. To distinguish between tightly spaced landforms, where possible nearby features were mapped in differing directions so that the GPS numbering could be used to separate the features (as in Figure 2). GPS data were continually loaded into Google Earth at the end of each day in the field as a means to quickly check that the targeted area of Blåisen's foreland were being covered by the ongoing mapping and that no areas were being missed.

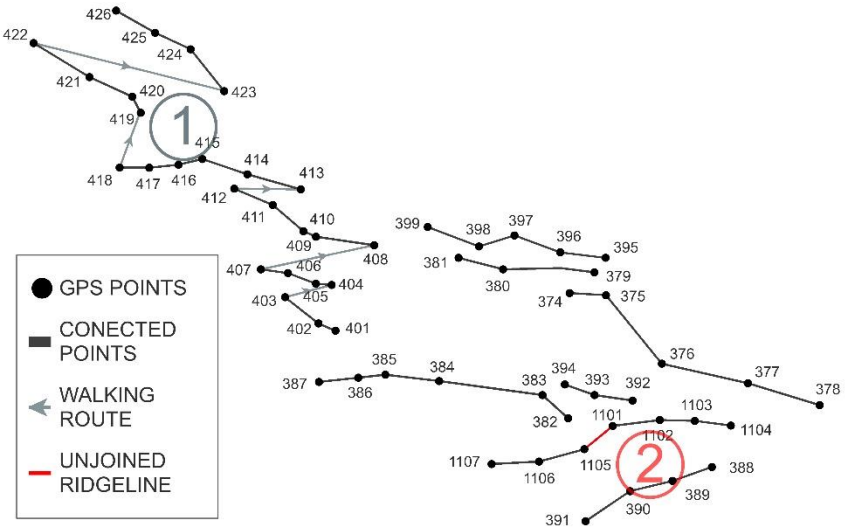

Figure 2 *- An illustration of how the numbering of the GPS points was used to distinguish between tightly spaced ridgelines by mapping nearby ridges in opposite walking directions* ***[1]****. The red line* ***[2]*** *shows how this same method could be used to separate discontinuous ridgelines using the point numbering.*

Aside from the GPS data, non-quantitative data were collected in the field in the form of georeferenced photographs: some of specific features for the purpose of drawing diagrams and sections, and some contextual. Field notes were taken in video format as this allowed features to be simultaneously pointed out and described from multiple angles and their context to be shown all within one recording.

3.1.2. Structure from Motion Data Collection

A regular digital camera was used on a locked setting to prevent automatic image adjustment which might otherwise affect the colour of the model. As the image capturing was carried out without the use of an Unmanned Aerial Vehicle (UAV), two small sites (approximately 40m^2) were selected as opposed to the photogrammetry being carried out across the whole foreland. A far greater area is captured in a single image from a UAV compared to image capture on the ground. Therefore, the number of images versus area covered is far less efficient in the latter, impacting on computing memory required in the processing stage. This study focusing instead on two sites in greater detail rather than the whole foreland (James and Robson, 2012).

After an initial survey of the whole foreland, two sites were selected in June near the snow margin which both typified the geomorphology found across the foreland, and presented interesting development potential over the course of the melt season; these are displayed in Figure 3. Approximately 270±70 photos were taken for each site during each timeframe resulting in four separate data sets. Photos were taken in a broadly systematic pattern by walking transects where the terrain allowed, however deviations were frequent in order to adequately capture the more complex features with varying surface aspects.

Ground control points were used on easily distinguishable landmarks most commonly large, distinctively coloured boulders within the SfM sites. The control points were recorded on GPS with descriptions and photographs of the location taken so that they could later be identified in the 3D model. At least three control points were used for each site to allow for scaling of the SfM models.

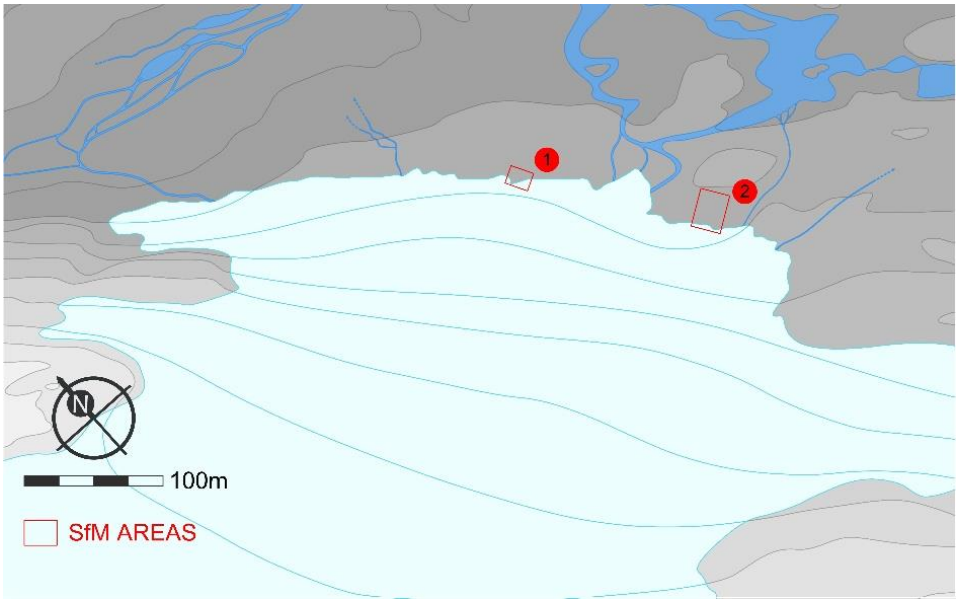

Figure 3 *- Map showing locations of the SfM sites within the foreland of Blåisen*

3.2. Data Processing

3.2.1. Mapping

The GPS data was initially loaded into Google Earth while the fieldwork was in progress. Google Earth was then also used post-fieldwork to delineate the GPS points to recreate the features mapped in the field, this process is shown above in **Figure 2** and follows an increasingly common method of the use of Google Earth for vectorisation (Margold and Jansson, 2011; Margold et al., 2011; Fu et al., 2012). The imagery has been removed from behind the data because it was found to be incorrectly georeferenced within Google Earth, (evident when comparing the available recent historical imagery from the last few years in Google Earth). This is an issue that could be misleading when attempting to make geomorphological interpretations and which has previously been highlighted by existing studies (Mather et al 2015; Wyshnytzky 2017). The delineated geomorphology shapefiles (approximately 234 features from June and a further 188 features from September), were exported into ArcGIS so that correctly georeferenced backing satellite imagery could be added to aid interpretation and form the basis for the delineation of contextual landscape features such as the approximate water courses for the final mapping figure. This was then exported into Vectorworks SP5 (Vectorworks Inc., 2017) where coarse topographic data for the land and icecap was added from Kartverket - Norwegian Mapping Authority to form the base for the geomorphological mapping. The delineated geomorphology was then added and annotated with the aid of field notes and photographs.

3.2.2. Structure from Motion Photogrammetry

Structure from Motion (SfM) achieves the reconstruction of a 3D surface using a series of overlapping images taken from slightly varying offsets, similar to the principles of stereoscopic photogrammetry (Westoby et al., 2012) illustrated below in Figure 4. Points from sets of adjacent photos can be matched using feature-matching algorithms developed in the 1980s (Förstner, 1986) which have since been widely used in photo panoramic software. The geometry of the resulting collection of matched points and their positions relative to the cameras can be triangulated simultaneously '*using a highly redundant, iterative bundle adjustment procedure*' (Snavely, 2008 in Westoby et al., 2012: 301) creating a spatially accurate point cloud similar to that generated by terrestrial laser scanning.

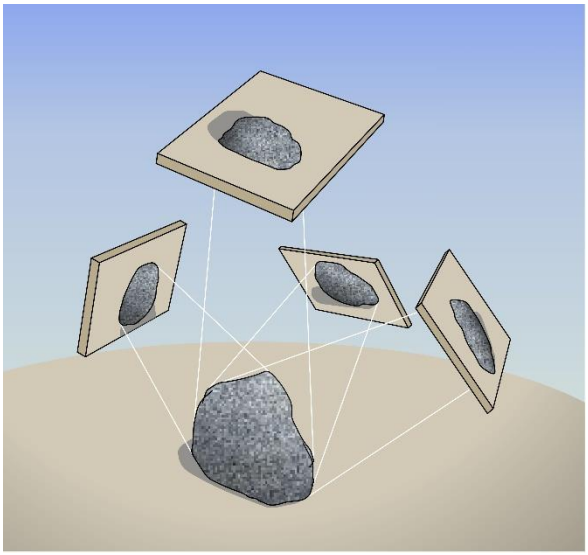

Figure 4 *- Conceptual diagram showing how a 3D object is captured from different angles to prior to creating the point cloud.*

The use of SfM in the geosciences has been increasingly employed over the last decade) particularly as a low-cost alternative to laser scanning methods (Westoby, 2012). SfM also avoids many of the issues that inhibit ground-based laser scanning such as the requirement of a stable static platform and the time required in the laser to pan; in areas where the ground is unstable such as on beaches or water logged glacial margins, SfM is advantageous (James & Robson, 2012).

The SfM process was conducted in Agisoft Metashape 1.6.2 (Agisoft LLC, 2019), the most popular software of its type at the time of writing (Chandler et al., 2016a; Evans et al., 2016a; Ely et al., 2017; Allaart et al., 2018; Chandler et al., 2018; Ewertowski et al., 2019), and followed its basic workflow guideline for creating a 3D mesh (3D polygonal model) shown below and corresponding to Figure 5.

1. align photos → *2. build dense point cloud* → *3. build mesh* → *4. generate texture*

1. Photo alignment quality was set to high, with a key point limit of 40,000 and a tie point limit of 4000. The resulting cloud of tied points (between 100,000 to 500,000 points) was then clipped to the desired area to remove obvious outliers and artefacts, such as background mountains in some of the photos.

2. A dense point cloud recording true colour was generated by interpolating between the original points. The quality set varied of the number of points in the original cloud. Large clouds on higher quality exceeded the available computer RAM, therefore the quality was lowered for the larger clouds; for the example below (Fig. 5) high quality was used resulting in a dense point cloud of over 19 million points. The depth filtering was set to mild to take account of the small variations in topography.

3. A mesh was then constructed using the points of the dense point cloud. For the surface type, arbitrary surface type was selected as it gives better results for smaller areas. Had a UAV been used, height field surface type would have been selected at this stage as it is suited to processing aerial photography and requires a lower amount of memory so allows for larger data set processing. As the photographs were taken from ground level, so covering a smaller area, arbitrary surface type processing was used because it does not assume that the surface modelled should have relatively low relief.

4. The final stage was to add texturing. As the photos for each model had been taken each within a short time period with constant lighting, colour calibration was not required. Generic texture mapping mode was used where no prior assumption is made, and the colours of the original photos were used for texturing.

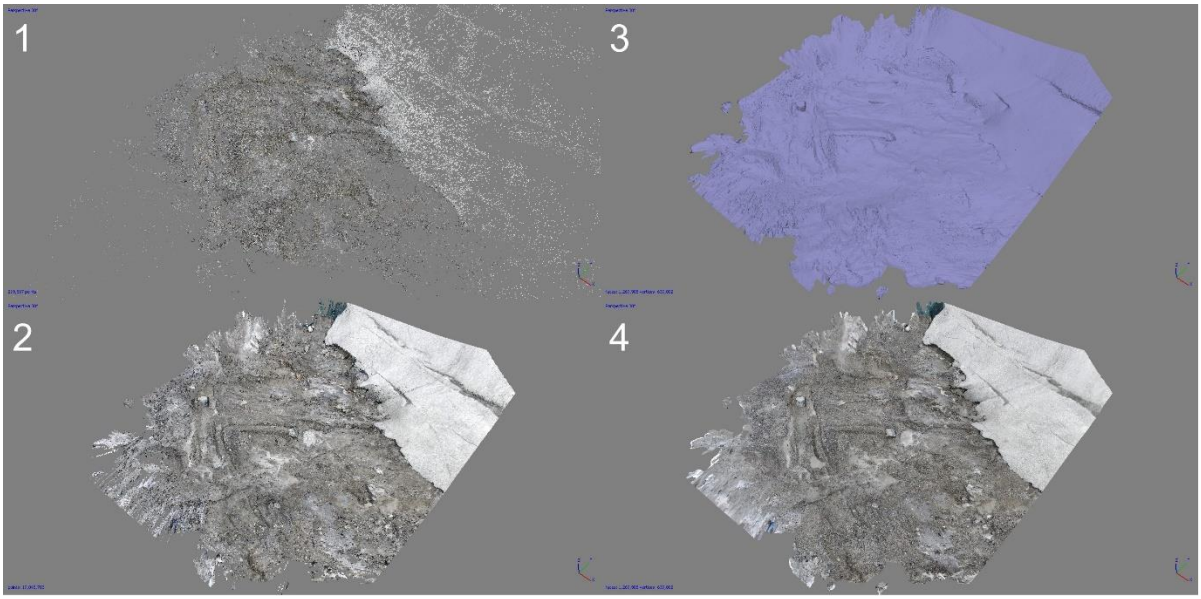

Figure 4 *- Showing the stages of generating the SfM surfaces, numbering relates to the workflow stages described above.*

The model was then exported into ArcGIS to create a DEM while the original model on Agisoft was used to aid interpretations and process observations. The model was exported as a mesh - Virtual Reality Modeling Language File (.wrl) - and converted to a TIN shapefile within ArcGIS. This was then converted to a raster from which DEM analysis such as slope and aspect could be performed.

One set of DEMs from Site 2 were differenced using the Raster Calculator function to show quantifiable changes in the foreland in terms of elevation gained or lost. This was only carried out on one of the two sets, as the September DEM of the first site was of insufficient quality to difference with its corresponding DEM from June.

3.2.3. Sedimentary Exposures

Several exposures were recorded in the field, focusing on particular landforms that were difficult to interpret from the geomorphology alone. It is important to stress these were not accurate logs in the classical sense, i.e. accurately recording the dip, orientation of clasts and thicknesses of individual sediment layers. The purpose of these sections was to focus on landform formation processes rather than a specific focus on the sediment properties themselves. Thus, photographs with a known object for scale were used over the more traditional methods of measuring and sketching, as time in the field was a constraint and the details of sections were not prioritised. These photos were vectorised and coloured on Vectorworks SP5 (Vectorworks Inc., 2017) to make some structural elements clearer; as much detail was retained as possible, as to not compromise the more subtle sedimentary structures. These exposures were then annotated and can be found in results section 4.3. Unfortunately, due to poor weather limiting time in the field in September, all of the exposures were made during the June visit.

4. Results

The results are divided into five sections. The first section outlines the landforms and geomorphological features observed and mapped in the field and interprets them, categorising the features into the geomorphological landforms identified in the literature. Section two shows the results from the SfM modelling, displaying the models themselves and the generated DEMs. The fourth section displays and describes the sedimentary exposures while the final section documents the changes in the foreland by comparing photos taken in June and September. The forth section displays 'before and after' photos of approximately the same perspective of the foreland taken from the same GPS locations in June and September to provide visual evidence of the wider foreland changes including some of the areas focused on in the previous sections. The final section compiles these observations and interpretations into two geomorphological maps, for June and September respectively, which can be directly compared to show changes in the foreland.

4.1. Geomorphological Observations & Interpretations

The following section describes the observed landforms in a very broad sense in terms of geometry and distribution across the foreland, before interpreting and categorising them. The geomorphological map is presented in section 4.6.

4.1.1. Ridges perpendicular to ice flow

Observations

Ridges perpendicular to the flow of Blåisen were the most commonly occurring feature observed in the foreland during both field visits. Typically, these ranged in size from approximately 1 m in height and 3-4 m in width down to small alignments of clasts perched on exposed bedrock, less than 10 cm in height and 20-30 cm wide. Lengths also varied from <1 m up to ~100 m.

In terms of distribution, the longer ridges (not the largest in height or width) are mainly found on the north-western side of the foreland where the ground slopes gently away from the glacier to the northwest, viewed from a distance in Figure 6d. Here they extend for up to 100 m in length with a 'medium' cross sectional size (height x width) when compared to the rest of Blåisen, averaging up to 50 cm in height by 1-2 m width and are occasionally dissected by meltwater channels (Fig. 6c).

Further east across the foreland, but west of the main meltwater outlet ([5] Fig. 1a), the ridges become larger and more hummocky. The underlying bedrock also had a greater influence in modifying the topography and protrudes in three distinct ridges in this area. The bedrock ridges are aligned perpendicular to ice flow and dipping gently towards the glacier. They are divided by small elongated ponds and have hummocky sediment ridges of up to a metre in height superimposed on them (Fig. 6a). This area is shown on the map in Figure 6 marked by the letter 'a' in the June map.

Beyond the main meltwater portal, the ridges are much smaller and at times difficult to distinguish in the field, with heights of up to 10 cm and widths of less than 20-30 cm. They are also observed to be more closely spaced and shorter in length to the extent that some ridges overlap one another as shown in Figure 6b; this is in contrast to the north-western foreland where the spacing is greater at 3-10 m.

An important observation from September was that the ice margin itself was not in contact with the bedrock, with the ice in many areas sloping upwards away from the bedrock/sediment like the prow of a boat. This was particularly prevalent in areas where there was a reverse slope at the margin. In some areas the gap between the ice and substratum was sufficient to walk under while stooping and extended back into the glacier for many tens of metres. This observation is mentioned here because within these 'ice caves' small ridges in the underlying sediment were observed; in contrast to the foreland, these 'subglacial' ridges are composed of much finer sorted sediment.

Interpretation

The ridges perpendicular to flow are interpreted as minor moraines. The term 'Minor Moraines' is reasonably fluid, with a number of different names appearing in the literature to describe closely-spaced smaller end moraines; 'small' in this instance refers to ridges under 4 m high (Wyshnytzky, 2017). The ridges in this study were all very small, under 100 cm in height, and were found occurring in high frequency, with spacing ranging from multi-crested moraines with the crest separated by a few centimetres, up to the larger ridges found in the north-western side of the foreland and depicted in Figure 6d. This interpretation is supported by observations by Andersen and Sollid (1971) and Reinardy et al. (2013) who also identified similar small ridges in the foreland of neighbouring Midtdalsbreen as minor moraines. Both of these papers called such moraines 'annual moraines'; other terms have been used such as 'minor recessional moraines' (Christiansen, 1956) and more widely, 'annual or sub-annual moraines' (Worsley, 1974; Birnie, 1977; Sharp, 1984; Ono, 1985; Boulton, 1986; Gordon and Timmis, 1992; Krüger, 1995; Evans et al., 1999a; Evans et al., 1999b; Bradwell, 2004; Evans and Hiemstra, 2005;

Beedle et al., 2009; Lukas, 2012; Schomacker et al., 2012; Bradwell et al., 2013; Chandler et al., 2016a; Chandler et al., 2020), however the latter term requires proof that the ridges have indeed formed annually for this term to be applied. As no dating was carried out to test whether they have formed annually, even if this may be likely, this study will use the term minor moraines.

Figure 6 *(Overleaf) Map panels show the ridges perpendicular to ice flow mapped by GPS from June and September, it is important to note that the mapping in September focused more on the newly exposed areas, morphology recoded in June was largely not rerecorded in September, except as reference. Mapped bedrock and local slope direction are shown for context. The photos* ***a-d*** *show varying perpendicular ridges observed in the foreland, described in the text above with the photo location marked on the June map.* ***6a*** *- set of ridges on the lee side of a bedrock outcrop.* ***6b*** *- very small ridges, less than 15cm in close succession; Sven Lukas and Lena Uldal Hansen for scale.* ***6c*** *- long ridge dissected by meltwater stream.* ***6d*** *- long ridges on northwest of foreland viewed from a distance.*

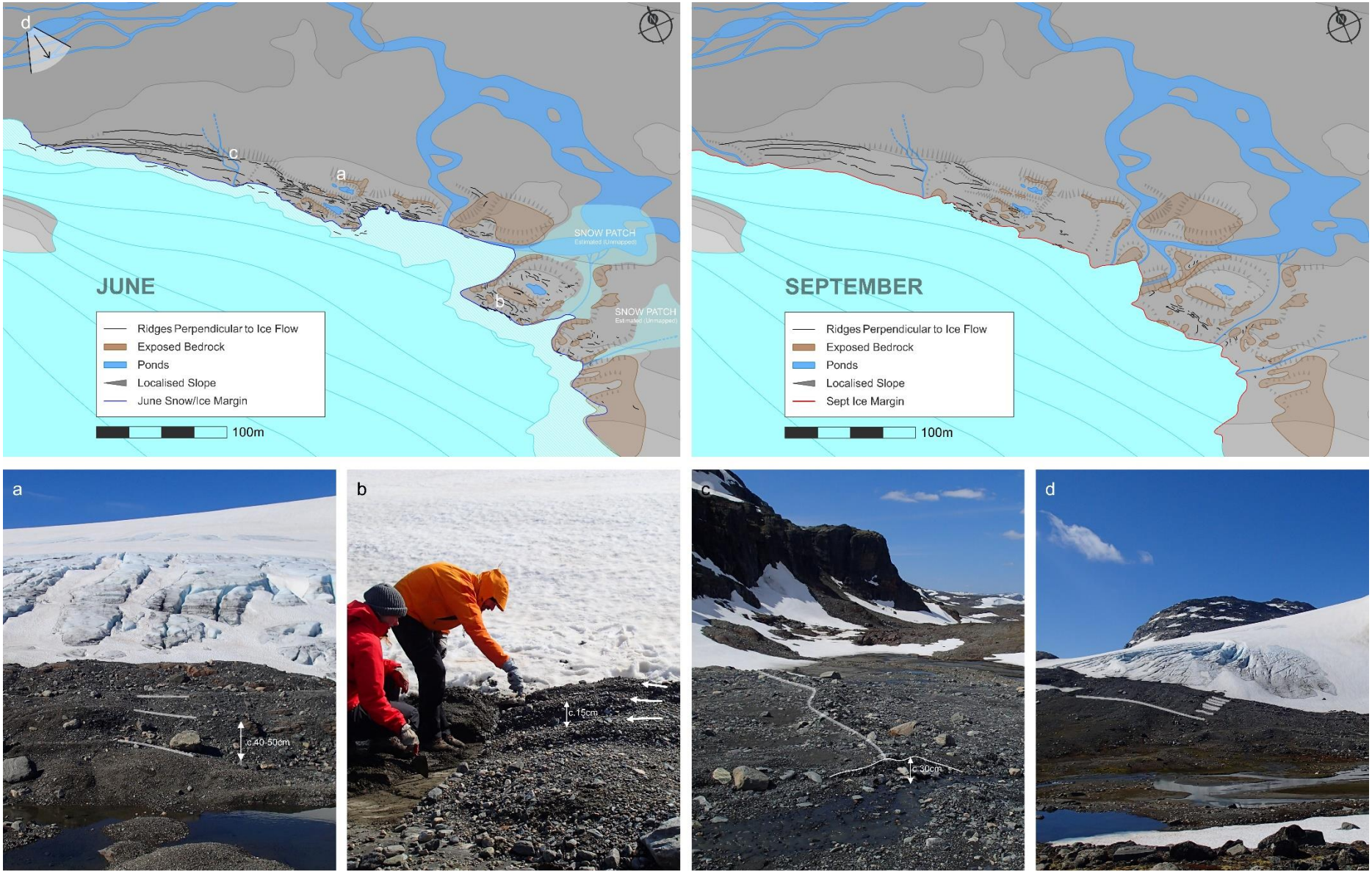
d
c
a
b
SNOW PATCH
Estimated (Unmapped)
SNOW PATCH
Estimated (Unmapped)
JUNE
Ridges Perpendicular to Ice Flow
Exposed Bedrock
Ponds
Localised Slope
June Snow/Ice Margin
100m
SEPTEMBER
Ridges Perpendicular to Ice Flow
Exposed Bedrock
Ponds
Localised Slope
Sept Ice Margin
100m
a
c.40-50cm
b
c.15cm
c
c.30cm
d

4.1.2. Ridges parallel to ice flow

Observations

Ridges found parallel to ice flow were less numerous than those observed perpendicular to it, and they were notably confined more to the southern side of the foreland; here more of these features were recorded during the September fieldwork in the newly exposed areas. Their occurrence was noted in two main circumstances, either in the lee of protruding features like outcrops or boulders or sub-parallel to slope contours and near the lateral margins of the glacier.

These features were mapped for June and September in the same fashion as section 4.1.1 (Fig. 7) with photographic examples of their occurrences displayed in a-d. The landforms in Figures 7c & 7d both broadly fall into the first category identified above, located in the lee of obstacles to ice flow: bedrock outcrops or boulders. Figure 7d illustrates the latter particularly well with a prominent ridge directly following a large boulder. In terms of distribution, ridges behind bedrock outcrops were most commonly identified in the area around where the photograph in Figure 7c was taken and further from the ice margin. The former type, ridges behind boulders (Fig. 7d), were found mostly along the glacier margin with many more mapped in the areas newly exposed after the summer melt.

An example of the second type of ridges parallel to ice flow, those near the lateral margins, is depicted in Figure 7b, with the ridge following the contour slope lines along the ice margin. It is notable that the ridges tend (with some exceptions) to have asymmetric cross-sections with a more gentle distal slope and steeper proximal slope. This type of ridge was mainly confined to a small area on the steep northward facing slope at location ‘b’ in Figure 7.

A third occurrence of ridges were observed, characterised by very low amplitude ridges which emerged directly from the snowbank in front of the glacier (Fig. 7a). This was the least-commonly occurring type of ridges orientated parallel to ice flow, confined to a few instances along the ice margin of the north-eastern side of the glacier. It was observed that these ridges crudely aligned with some of the crevasses in the glacier ice.

Interpretation

Using the grouping above, the first category can be identified as flutes. Flutes, or Fluting, are described as elongated, streamlined sediment ridges, aligned parallel to ice flow direction (Boulton, 1976; Rose, 1989; Gordon et al., 1992; Benn, 1994). They can vary from a few decimetres to several meters in height and width; and up to hundreds of meters long (Hoppe and Schytt, 1953; Ottesen and Dowdeswell, 2006; Evans et al., 2009; Roberson et al., 2011). They are found in almost all glacial settings including marine environments (Ottesen and Dowdeswell 2006) and surging glaciers (Evans and Rea, 1999; Evans and Rea, 2003). Their long-term preservation potential is relatively low, therefore they are less frequent in paleo settings (Glasser and Hambrey, 2001; Evans and Twigg, 2002). Extensive fluting is noted by Andersen and Sollid (1971) and Weber et al. (2019) in the forelands of both Blåisen and Midtdalsbreen. The flutes observed in this study fit this description: being elongated ridges, aligned parallel to ice flow with many also exhibiting an initiation; Figure 7b displays a textbook example of this.

The second category is interpreted as lateral moraines. Their occurrence was restricted to the margin of Blåisen and the asymmetric geometry matches that described by Lukas et al. (2012). Lateral Moraines are ridges that form on the flanks of glaciers, aligned roughly parallel to ice flow direction. An extensive body of literature has documented both paleo and active lateral moraines in a variety of environments (Boulton and Eyles, 1979; Eyles, 1979; Eyles 1983; Benn and Ballantyne, 1994; Bennett et al., 2000; Burki et al., 2009; Bennett et al., 2010; Hanáček et al., 2011; Borisov et al., 2017) with many studies focusing on the Alps (Eyles, 1979; Small, 1983; Lukas and Sass, 2011; Lukas et al., 2012; Eichel et al., 2018).

Earlier studies concluded that lateral moraines formed largely by the dumping of supraglacial sediments along the margins (e.g Boulton, 1978; Boulton and Eyles, 1979; Eyles, 1979, Eyles 1983) with the delivery of material onto the glacier surface predominantly through debris falling from the valley sides. Through the late 1980s studies provided evidence of a more complex procedure of englacial transport whereby debris is buried in the accumulation zone and transported down-glacier, eventually remerging near the terminus (Small, 1983; Small, 1987). This material melted out and was deposited on the proximal side of the lateral moraine during the ablation season. Over successive cycles, the lateral moraine could be built up by the stacking of this material. Lukas et al (2012) developed this into a synthesised conceptual model where material is delivered by englacial debris bands to the margins by freeze-on and/or shearing and thrusting mechanisms. The melting out of this material results in the formation of debris cones. The input of material from supraglacial sources, i.e. rockfalls for example, varies greatly depending on the glacier in question. Successive retreats and advances can build up stacked debris flows on the distal side of the moraine with glaciotectonisation of the older sediments. On the proximal slope, a band of subglacial till is deposited and can be thickened with successive glacial advances. Dead ice can also be incorporated on the proximal side as proximal sediments collapse back in the direction of the

glacier (Lukas et al., 2012; Borisov et al., 2017). Although these ridges are smaller than those documented by Lukas et al (2012), sedimentological evidence would have provided more conclusive diagnostic features such as clast alignment and stacking. However, there were no sedimentology sections taken for these landforms to support this interpretation, so the interpretation was as much process of elimination in that they did not have the diagnostic features of flutes, rather than very strong characteristic features of Lateral Moraines.

The final category is interpreted based on its alignment with the crevasse shown in Figure 7a, from this it is proposed that the feature is a laterally aligned crevasse fill ridge deposit, however sedimentological evidence is lacking to support this.

Figure 7 *(Overleaf) Map panels show the ridges parallel to ice flow mapped by GPS from June and September, it is important to note that the mapping in September focused more on the newly exposed areas, morphology recoded in June was largely not rerecorded in September, except as reference. The photos* ***a-d*** *show varying parallel ridges observed in the foreland relating described in the text above with the photo location marked on the June map (the exception being 7d).* ***7a*** *- wide, amplitude ridge emerging directly from the snow in front of, or lying over, the ice margin.* ***7b*** *- asymmetric ridge along the lateral margin of the glacier, roughly perpendicular to the slope.* ***7c*** *- long ridges protruding from the melting snow in the lee side of a bedrock hillock.* ***7d*** *- prominent ridge on the lee side of a bolder, further similar ridges in the background; Lena Uldal Hansen and Mateusz Zawadzki for scale.*

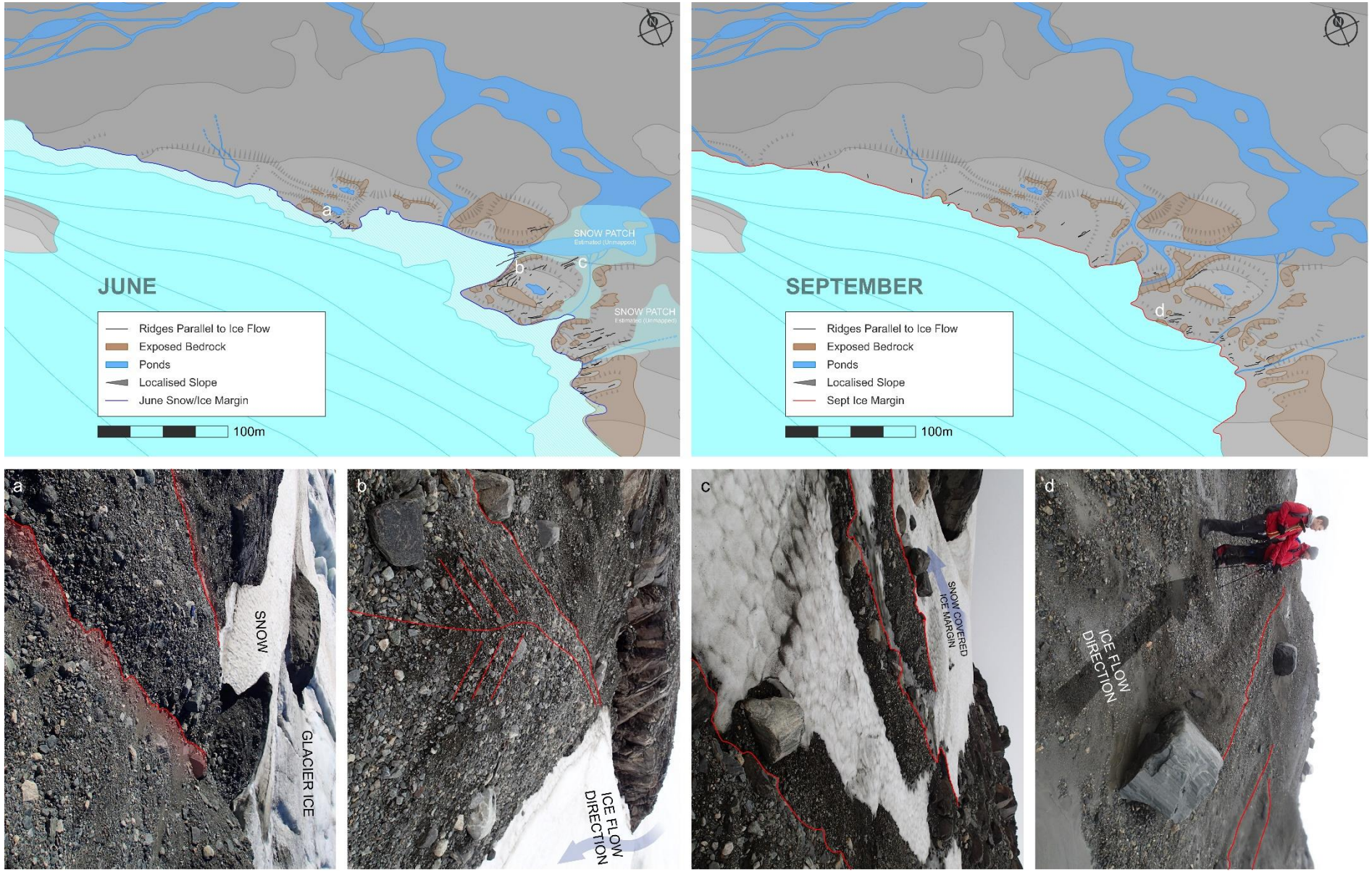
JUNE
Ridges Parallel to Ice Flow
Exposed Bedrock
Ponds
Localised Slope
June Snow/Ice Margin
100m
SNOW PATCH
Estimated (Unmapped)
SNOW PATCH
Estimated (Unmapped)
a
b
c
SEPTEMBER
Ridges Parallel to Ice Flow
Exposed Bedrock
Ponds
Localised Slope
Sept Ice Margin
100m
d
a
SNOW
GLACIER ICE
b
ICE FLOW DIRECTION
c
SNOW COVERED ICE MARGIN
d
ICE FLOW DIRECTION

4.1.3. Snow/ice margin landforms

Observations

The final grouping of features are the 'wedge' shaped features and smaller ridges found in a few isolated incidences along the glacier margin or within the snow/ice margin mapped in June and September (Fig. 8). All of these marginal landforms are found in the north-west area of the foreland, east of the main meltwater outlet. The first of these features depicted in photograph 8a taken in June, is roughly wedge-shaped with a planar shallow sloping top/back and a steeper front lying approximately 120cm above the snow in June. The photographs in Figure 8a show the change between June and September; mainly visible in the snow thaw exposing more of the 'wedge' feature. Figure 8c shows a different angle taken in September, looking east from the same point that the Figure 8a photos were taken; it shows the sediments lying above glacial ice, previously obscured under snow.

This landform was also the focus of Site 1 of the SfM 3D modelling so the geometry is displayed and described in greater detail in section 4.2; cross sections were also recorded from each side of the landform, the sedimentology descriptions can be found in section 4.3 with discussions on its formation and development found in section 5.

To the east of the large wedge, a similar feature was observed, although this was orientated more parallel to ice flow than the feature described in the above paragraph (Fig. 8b). The photographs show that the landform's structure altered markedly between June and September; in June it appeared as a series of two or three stacked 'wedges' orientated perpendicular to ice flow, similar to wedge 8a. By September, this form seemed to have changed, with the shape much less defined, comprising a hummocky ridge.

An elongated ridge was observed in June in the east of the foreland, with Figures 8d & 8e depicting the view from each end. The ridge appears along the boundary between the snowbank and the glacier ice with a band of sediments and ice lying acutely to the near horizontal ice at a near vertical angle, appearing like an anticlinal fold, split along its apex (Fig. 8e).

Interpretation

The interpretation of these features is complex and, at this stage, trying to categorise them into conventional landform types would not be beneficial, without recourse to the sedimentary architecture. The feature that has been described as a 'Sediment Wedge' (Fig. 8a) and the similar feature to the east (Fig. 8b) is explored further in the discussion (Section 5) as it is one of the main focuses of the sections looking at the sedimentological structure in Section 4.3, as well as forming a key part of Site 1 SfM model in section 4.2. The landform in Figure 8d & 8e is interpreted as forming from the squeezing of sediments between the glacier and the combined ice and snow band, based on similar observations made by Birnie (1977) who describes them as Snowbank Push Moraines. This process, and how it may relate to the minor moraines, is further discussed in Section 5 using evidence from a section recorded from the landform shown in section 4.3.

Figure 8 *(Overleaf) Map shows locations of ice marginal features referred to in the text above, mapped by GPS from June and September. Photos* ***8a*** *and* ***8b*** *show landform changes from June to September taken from the same point marked by their corresponding letters on the map. 8c shows a different perspective taken in September of the same feature as* ***8a*** *but taken looking east (to the right in* ***8a****).* ***8d*** *is taken looking NE over an elongated ridge with 8e taken from the opposite end giving a view of the internal structure.*

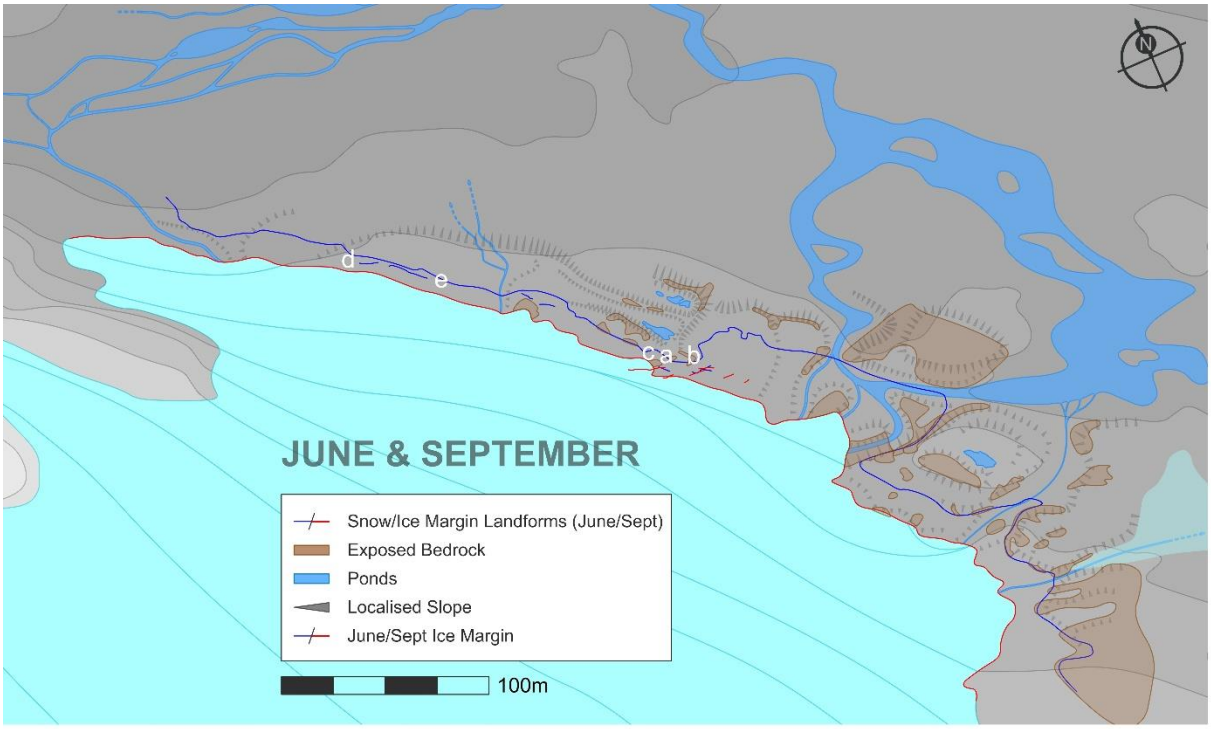
d
e
c a b
JUNE & SEPTEMBER
Snow/Ice Margin Landforms (June/Sept)
Exposed Bedrock
Ponds
Localised Slope
June/Sept Ice Margin
100m

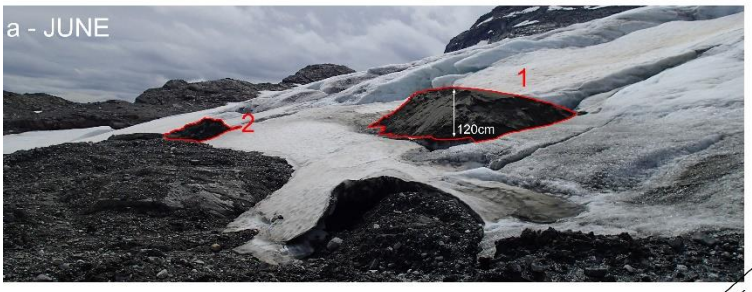
a - JUNE
1
2
120cm


c (SEPT)

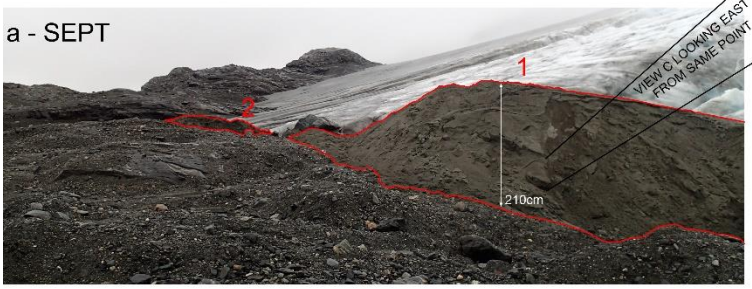
a - SEPT
1
2
210cm
VIEW C LOOKING EAST FROM SAME POINT


d (JUNE)

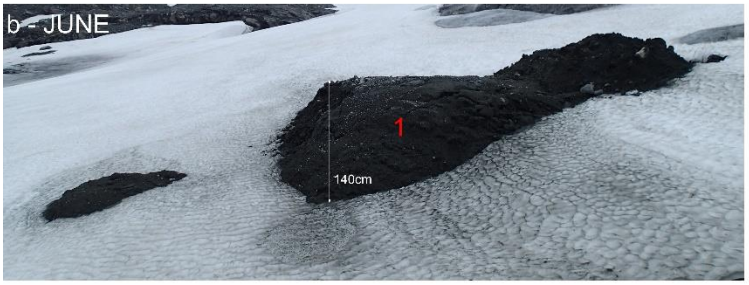
b - JUNE
1
140cm


e (JUNE)

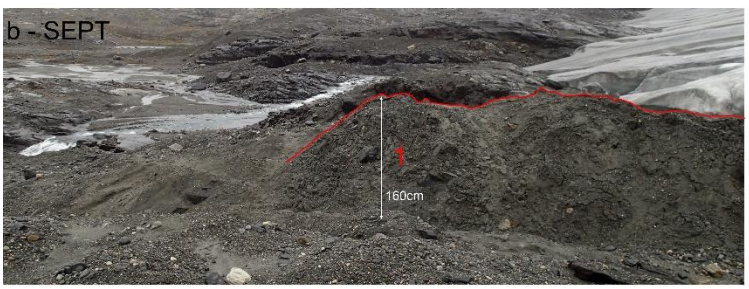
b - SEPT
1
160cm

4.2. Structure from Motion (SfM)

4.2.1. SfM models

In this section, the four SfM models are presented for Site 1 and Site 2 in June and September respectively. As mentioned in the methods section, the sites were selected in order to both represent the geomorphology present in the foreland, and which presented interesting development potential over the course of the melt season between June and September. Site 1 was selected to focus on the possible evolution of the sediment wedge and surrounding area, while site 2 focused on the development of a series of multi-crested minor moraines on the snow margin. The locations of both sites can be found in Figure 3. For each model, parts D and E of each figure show the models compared to a photograph taken from roughly the same position both to give context to the model and also as an illustration of the model's accuracy, an aspect considered further in section 5.2. There are clear examples of the landforms interpreted in Section 4.6, for example a flute with initiating boulder (Site 2, Fig. 12). The models were used in tandem with the mapping data and photographs to aid interpretations. The ability to zoom in and out and quickly change perspective was invaluable, particularly where the complex geometry of the large sediment wedge in Site 1 and its evolution shown in Figures 9 & 10 below was concerned.

The Site 1 models show an ice marginal retreat of between 20-30 m, exposing a far greater quantity of sediment in September, extending away from the original wedge in a band around 25-30 cm thick out to the west. This change is perhaps best illustrated by Figure 16, where the two Site 1 DEMs are scaled and overlaid to show this change. Another observation when comparing the Site 1 models is a small ridge in the September model located approximately two metres north in front of the sediment wedge, which can be viewed in Figure 10A marked with a red asterisk. This aligns with the position of the snow/ice margin in June where the margin protrudes (Fig. 9D, E). There is evidence of further ridges both parallel and perpendicular to the ice in the newly exposed area in September; however, the model is not of sufficient quality to identify them. The poor weather conditions during the second visit including heavy driving rain meant that water droplets collected on the camera lens while the SfM photos were being taken. This resulting in blurred patches in the photos that were perpetuated into the model; this is particularly prevalent on the periphery of the model where there are missing data patches and blurred texturing.

For Site 2 the differences were less dramatic. Here, the ice margin retreated just over ten meters, exposing more minor moraine ridges. When the site 2 was selected, it was thought that the series of multi-crested minor moraines may have formed recently (over the past two to three years), due to their proximity to the margin, so that the landforms may evolve in terms of preservation over the ablation season. However, the multi-crested minor moraines remained largely unchanged as the margin retreated. The retreat exposed at least four minor moraine ridges meaning that this initial assumption was incorrect. If it was that these ridges were annually formed, as described by Andersen and Sollid (1971) and Reinardy et al (2013) on Midtdalsbreen, this would put the age of multi-crested minor moraine at around five years old, and possibly older. Prominent flutes were recorded in the exposed area, particularly the large flute with the proximal boulder shown in Figure 12D is an excellent example of a typical flute configuration (Boulton, 1976; Benn, 1994; Eklund and Hart, 1996). The flutes are particularly interesting in that when viewed in the model, they are not perpendicular to the minor moraines as might be expected; this orientation is also apparent in the geomorphological map (Fig. 25) but was not obvious from the ground.

Site 1 - June

Figure 9
***9A** - Overhead view of the model, of Site 1 in June with north arrow and scale*

***9B** - Isographic view looking west*

***9C** - View looking east down the margin, highlighting the topographic change and the slope of the snow/ice margin*

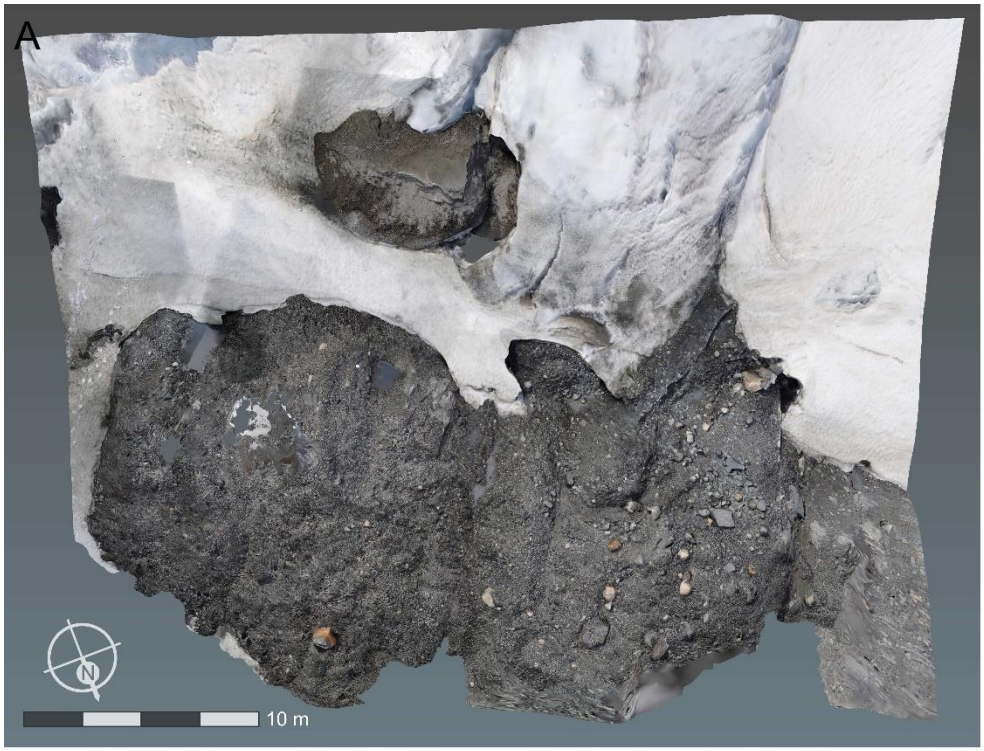

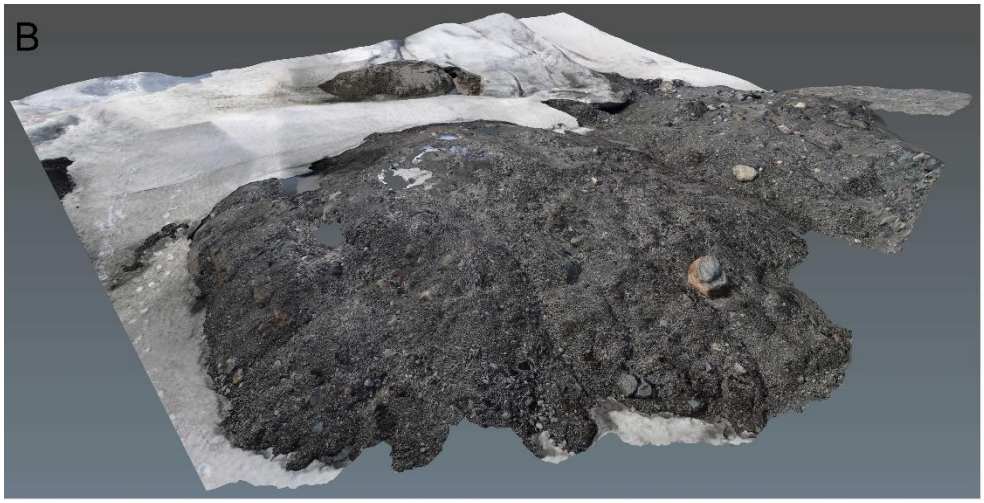

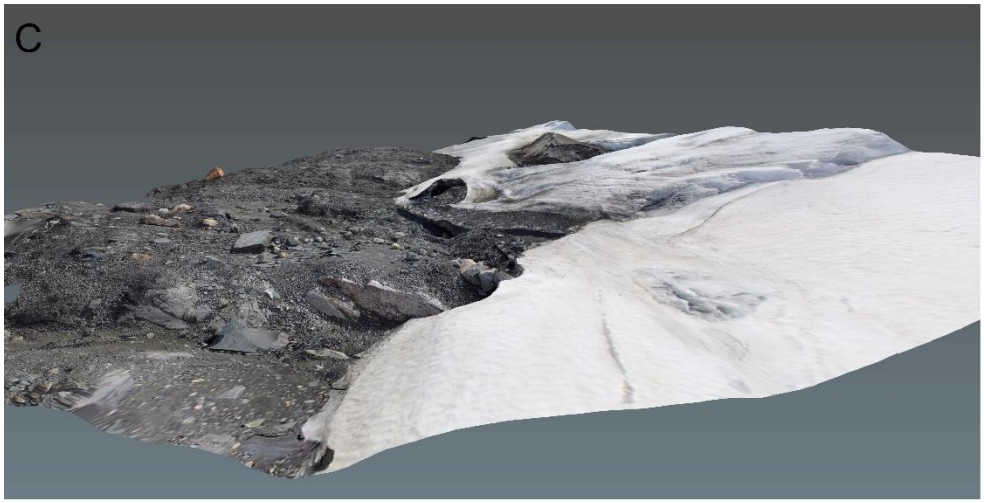

(Overleaf)

***9D** - D_1 shows the model compared to a photograph D_2 taken from roughly the same position*

***9E** - E_1 shows the model compared to a photograph E_2 taken from roughly the same position*

D2
D1
D2
E1
E2
E2

Site 1 - September

Figure 10
10A *- Overhead view of the model of Site 1 in September, with north arrow and scale (note the slightly different orientation and scale when compared to the June model)*

10B *- View looking directly towards the margin 'front on'*

10C *- Isographic view looking west comparable to XB*

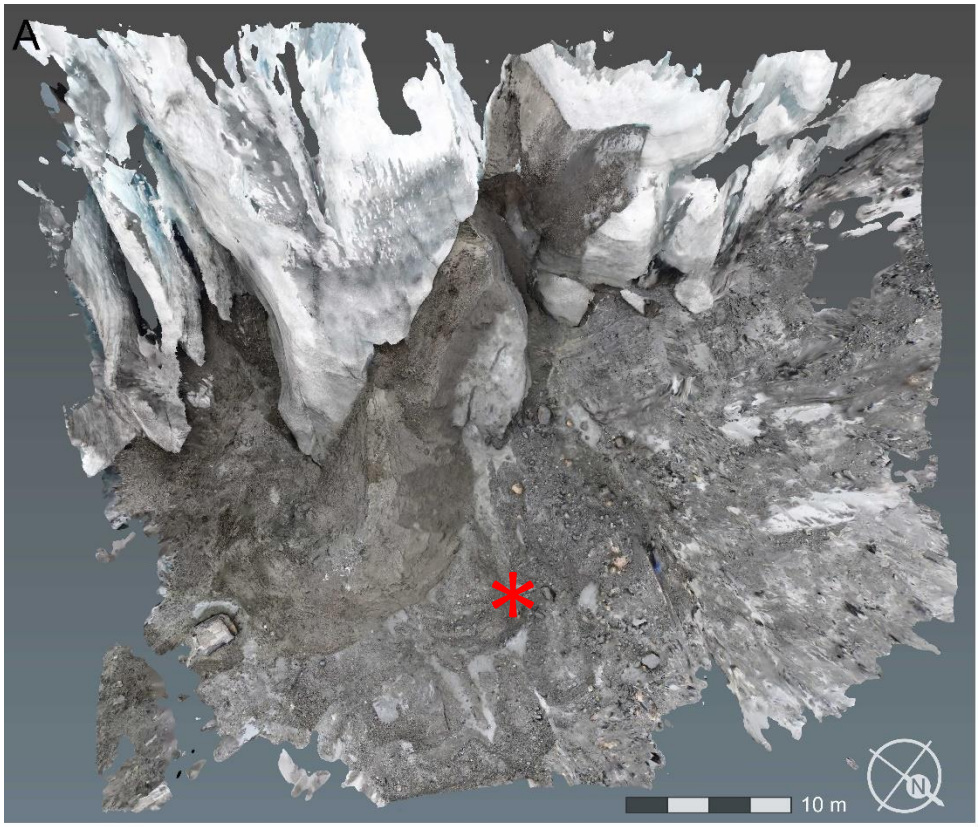

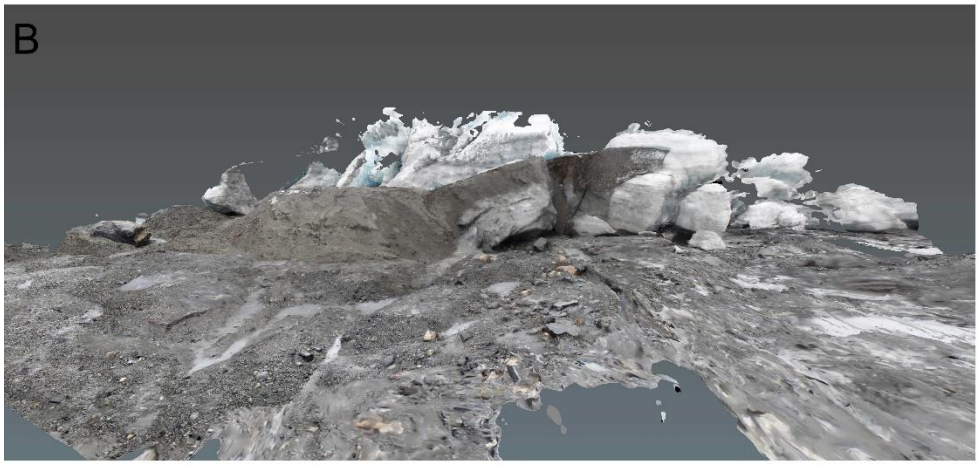

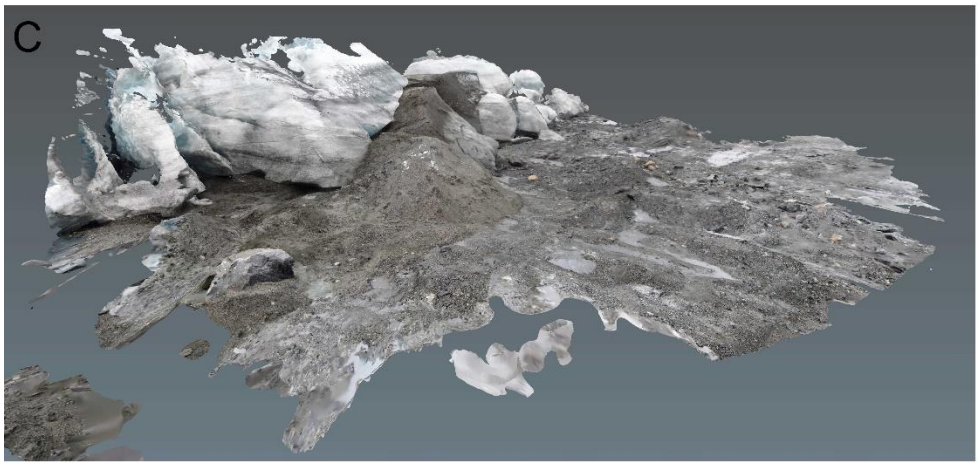

(Overleaf)

10D *- D_1 shows the model compared to a photograph D_2 taken from roughly the same position*

10E *- E_1 shows the model compared to a photograph E_2 taken from roughly the same position*

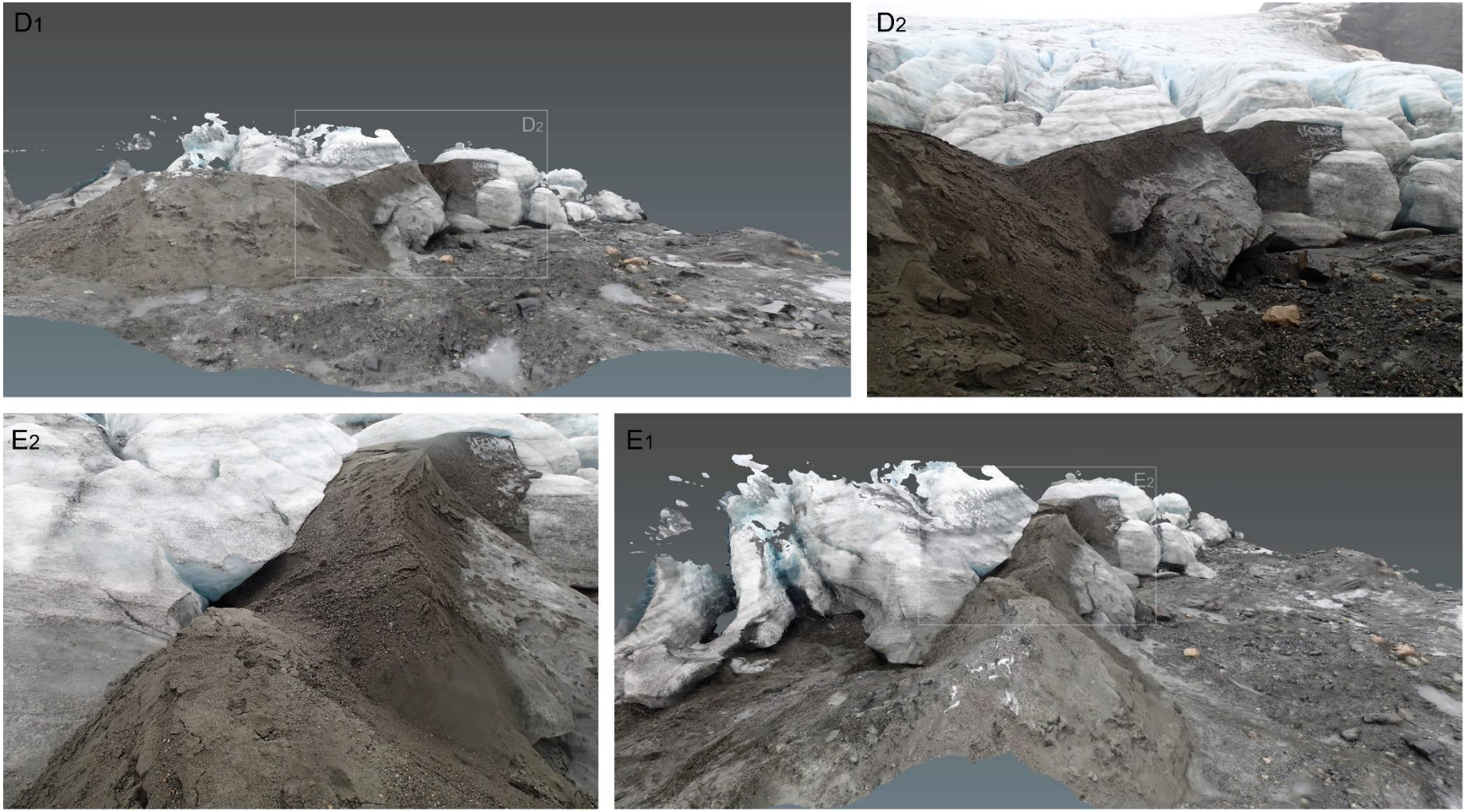
D1
D2
D2
E2
E1
E2

Site 2 - June

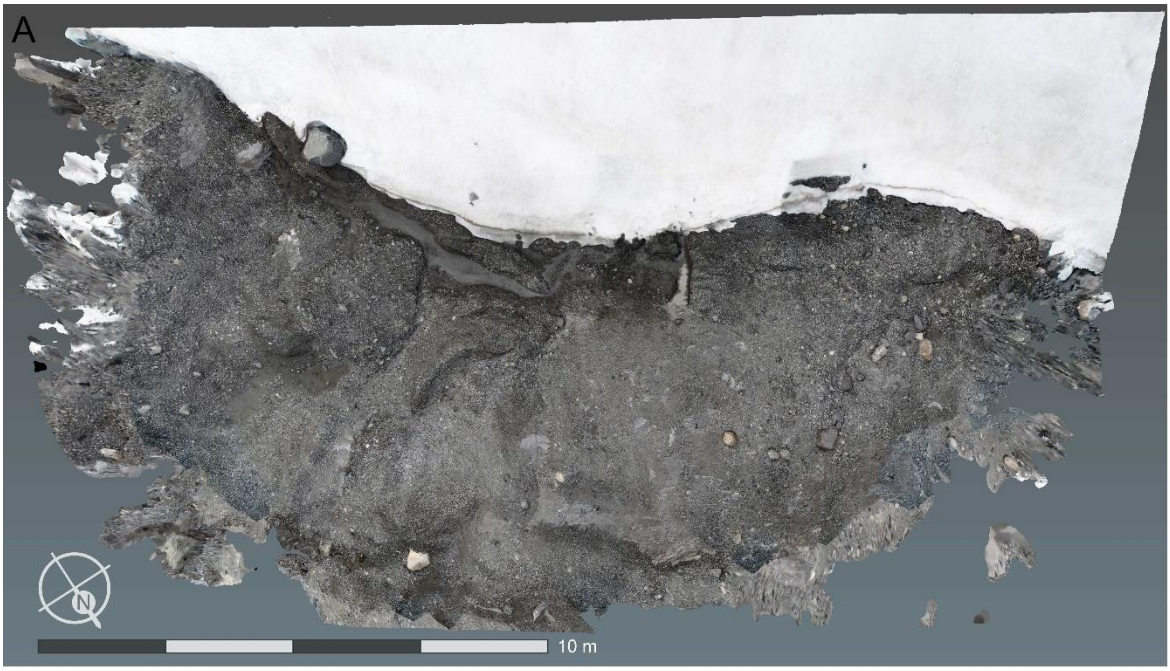

Figure 11
11A *- Overhead view of the model of Site 2 in June, with north arrow and scale*

11B *- Isographic view looking west*

11C *- View looking down the margin*

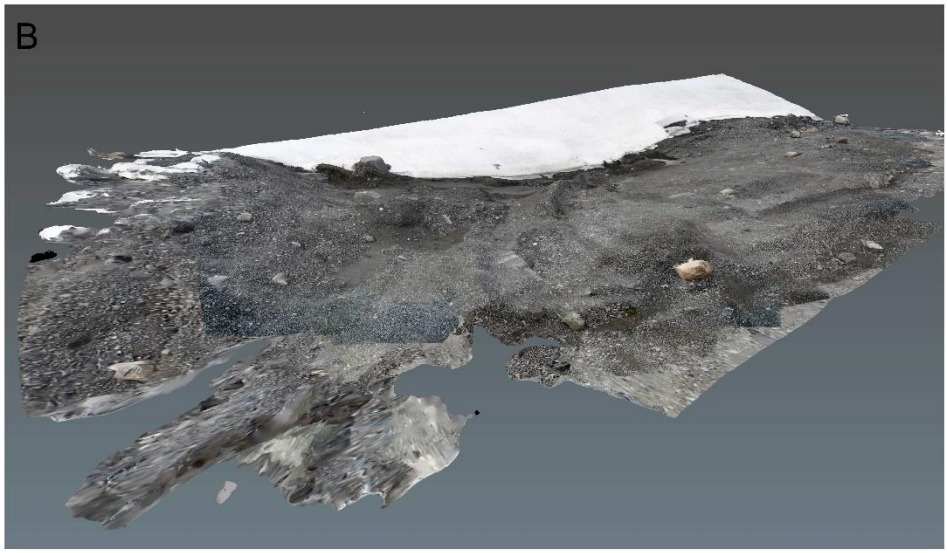

(Overleaf)

11D *- D_1 shows the model compared to a photograph D_2 taken from roughly the same position*

11E *- E_1 shows the model compared to a photograph E_2 taken from roughly the same position*


D1
D2
D2
E2
E1
E2

Site 2 - September

Figure 12
12A *- Overhead view of the model of Site 2 in September, with north arrow and scale (note the slightly different orientation and scale when compared to the June model)*

12B *- Isographic view looking west*

12C *- View looking directly towards the margin 'front on'*

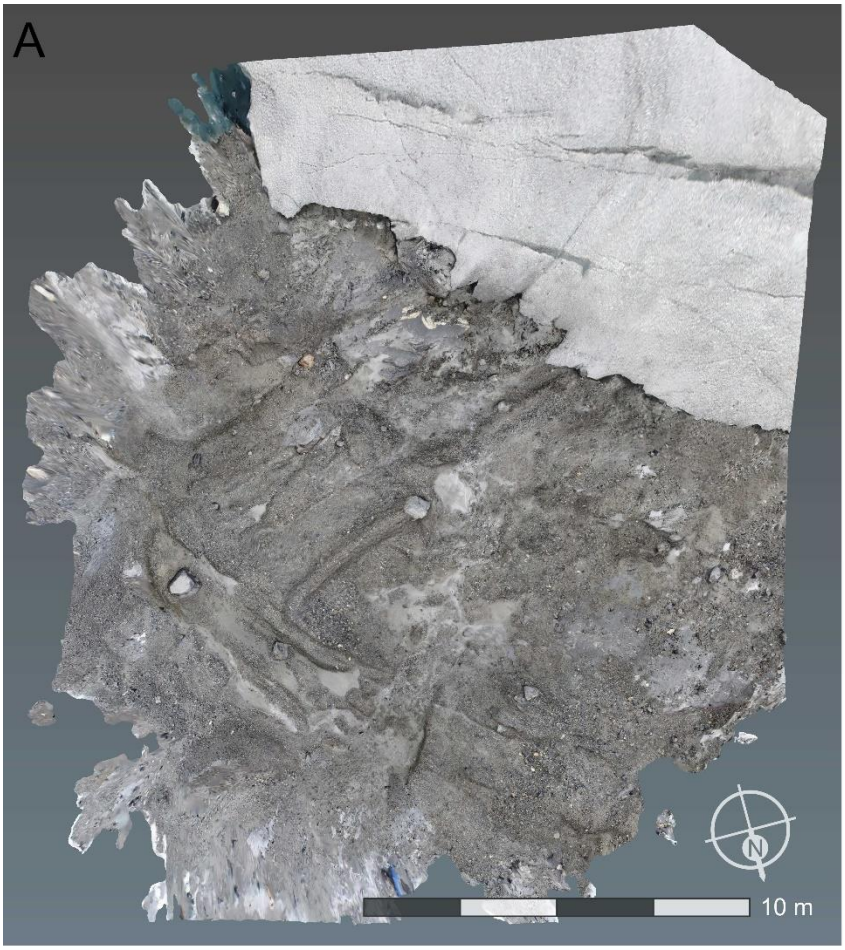

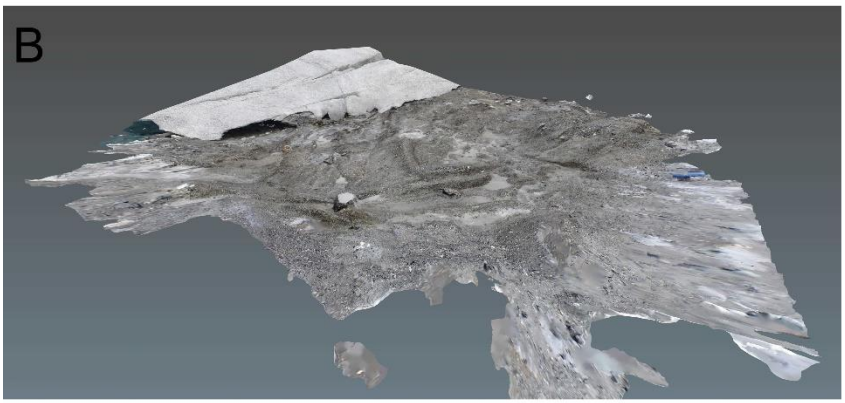

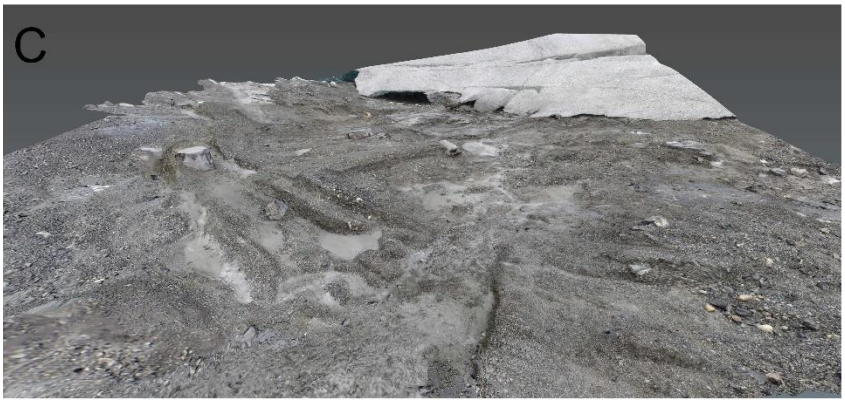

(Overleaf)

12D *- D_1 shows the model compared to a photograph D_2 taken from roughly the same position*

12E *- E_1 shows the model compared to a photograph E_2 taken from roughly the same position*

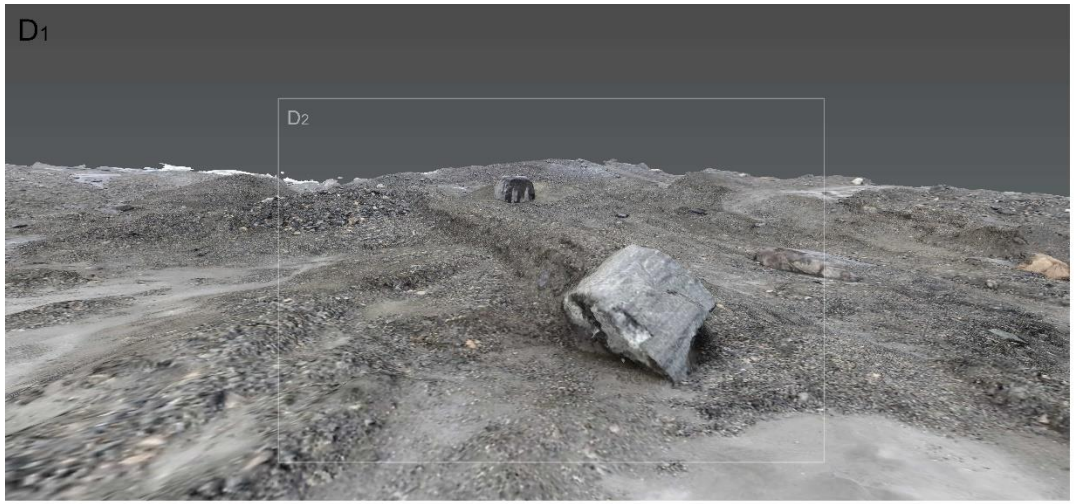
D1
D2


D2


E2

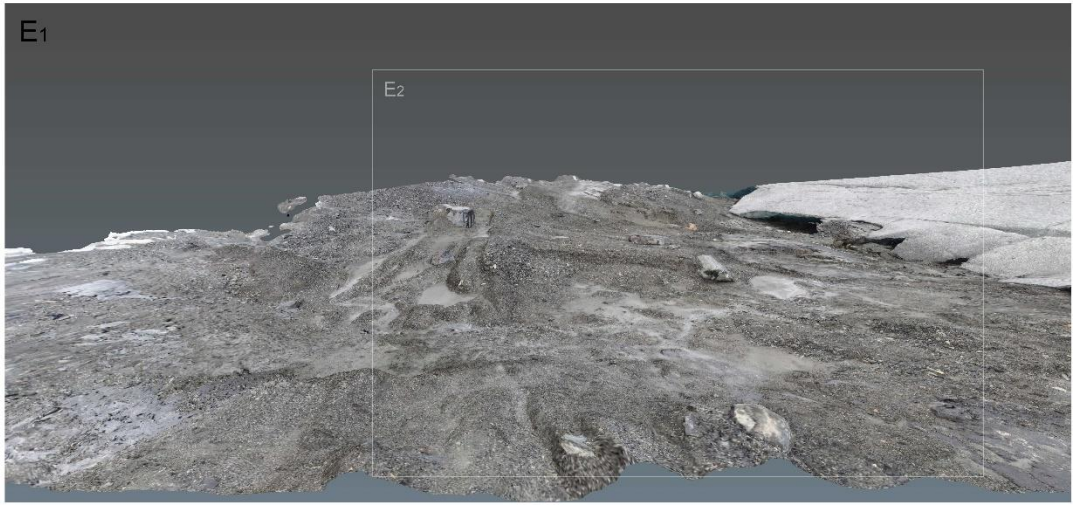
E1
E2

4.2.2. SfM DEMs

As outlined in the methods, the SfM models were imported into ArcGIS and converted into TIN based DEMs presented below (Fig. 13, 14) with hillshading applied to highlight the changes in surface elevation and slope. The DEMs help visualise the landforms as they present the modelled terrain with the focus on the elevation rather than texturing. The texturing, while aiding the identification of different surface types (e.g. snow or ice or sediment), can detract from the landform geometry. The DEMs were referenced alongside the SfM model figures in the section above describing the changes between June and September, so to avoid repeating what has already been outlined this section will focus on the differencing performed on the DEMs.

Due to the poor weather during the second visit in September, the corresponding DEMs are of notably reduced quality, particularly the model from Site 1 in September for the reasons described above (Section 4.2.1). The September DEM quality, and extensive changes at Site 1, meant that it could not be accurately aligned with the June DEM. Only Site 2's DEMs were used for differencing which was in an attempt show quantifiable changes in the foreland in terms of elevation gained or lost. This is presented in Figure 15, showing relatively minor changes, the largest being the loss of the snow cover resulting in a maximum elevation change of just under half a metre. The other elevation changes are negligible, particularly when considering the accumulated error of both the elevation and process of generating the SfM models.

Although the Site 1 DEMs could not be aligned by GPS they could be aligned approximately by manually matching points on the geomorphology. Although less accurate, this allowed for the two sites to be directly compared without the DEM differencing shown in Figure 16. This enabled the comparison of the sediment wedge between June and September, which shows the original wedge as forming part of a much larger structure. The original wedge appeared to be aligned roughly perpendicular to ice flow whereas the September DEM revealed that the alignment is oblique to the ice margin. The form of the original wedge changed markedly over the melt season, but the 'new' wedges retain a wedge morphology with more acute angles, giving it a 'fresher look'. Another observation is that the position of the crevasses in June align with the breaks in the wedge observed in September (Fig. 16**)**. As detailed in the SfM models section, the retreat of the margin also left a prominent ridge marking where the margin had been in June (Fig. 16).

Figure 13 *(Overleaf)* ***Site 1 SfM generated DEMs*** *- This shows the two DEMs from site 1 from June and September, note the slightly different scale and orientation. They can be found scaled and overlaid in Figure 16.*

Figure 14 *(Overleaf x2)* ***Site 2 SfM generated DEMs*** *- As in Figure 13, the DEMs from Site 2 are presented from June and September; they are at the same scale but are orientated slightly differently in order to fit on the page.*

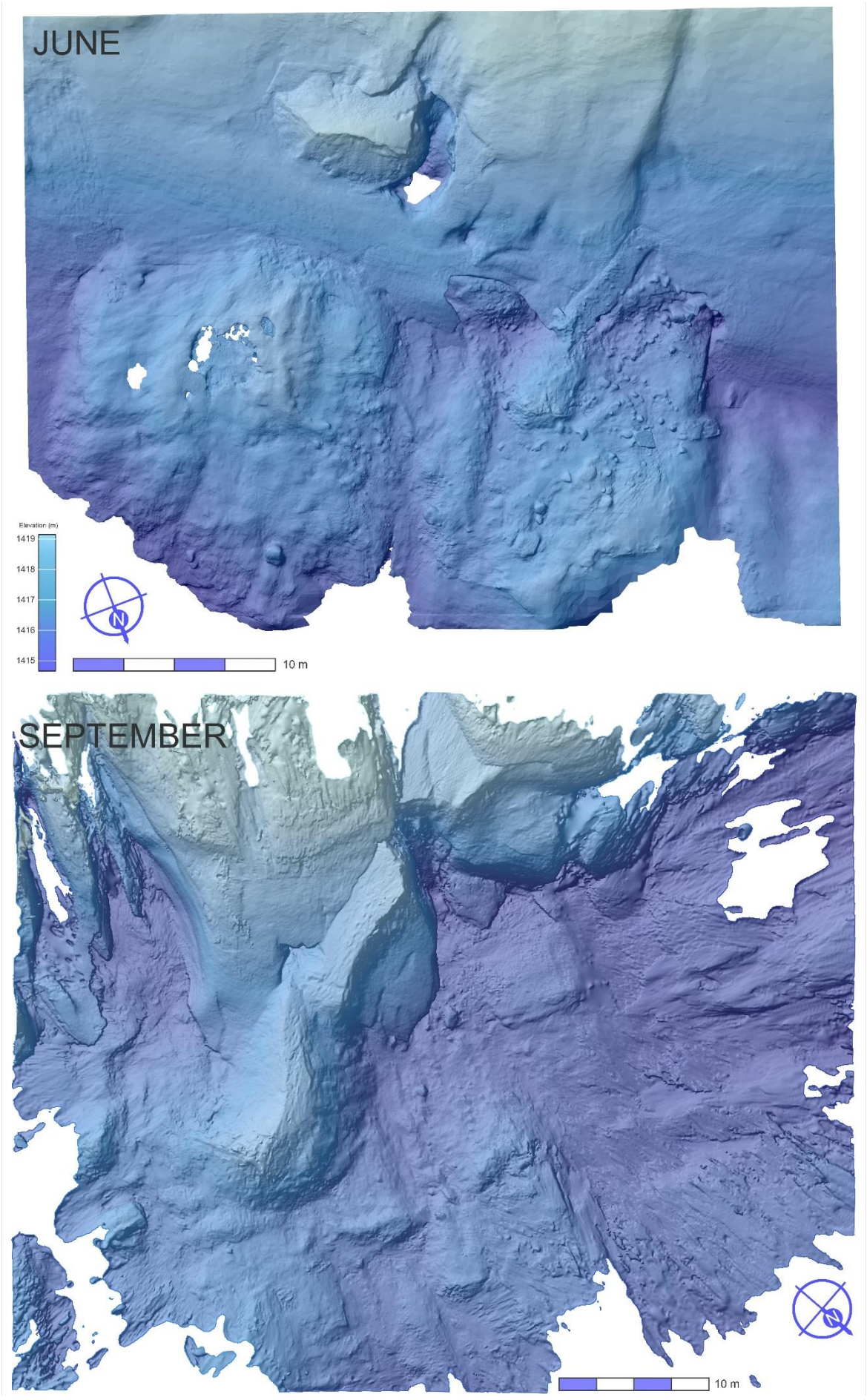
JUNE
Elevation (m)
1419
1418
1417
1416
1415
N
10 m
SEPTEMBER
N
10 m

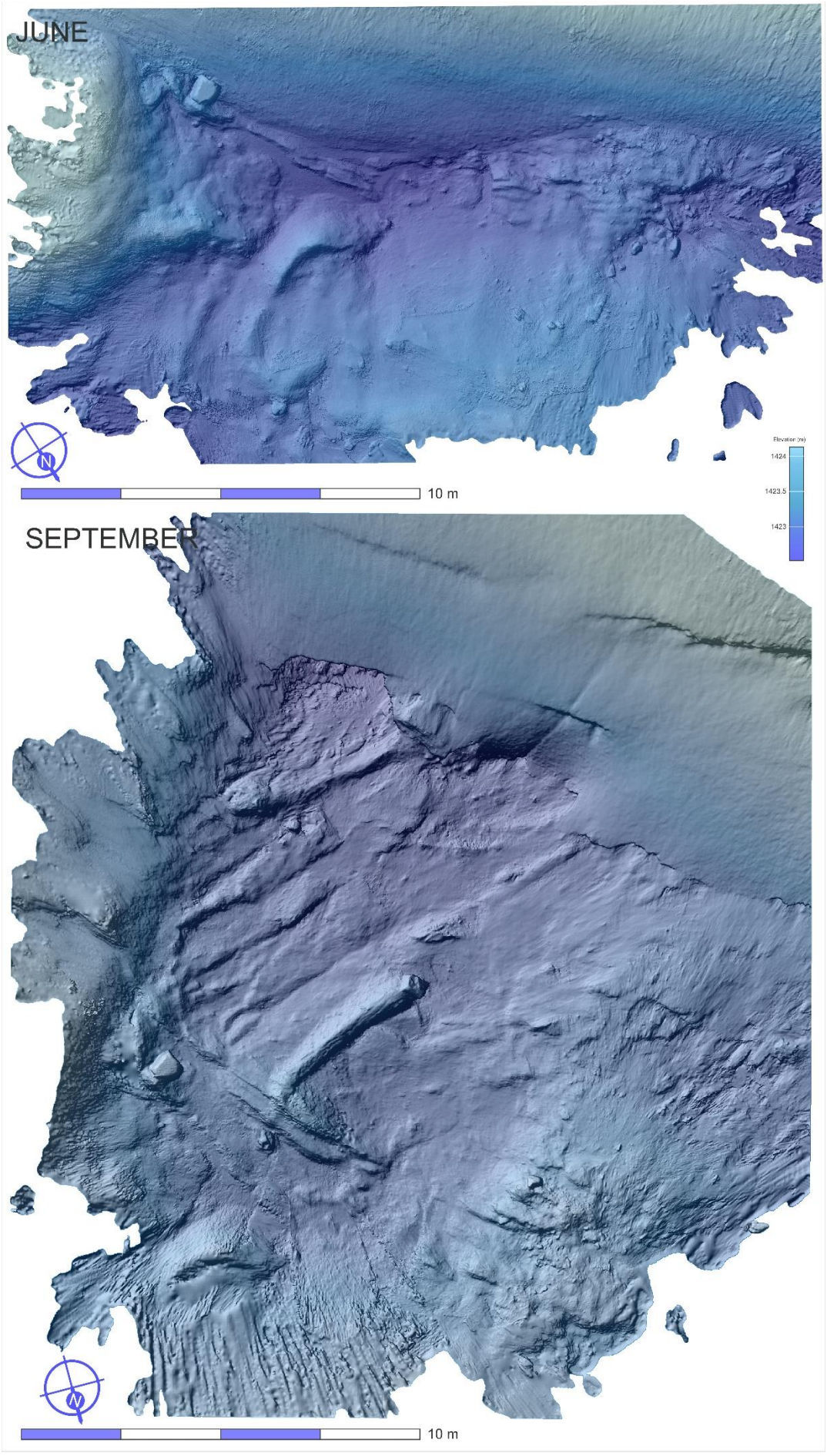
JUNE
Elevation (m)
1424
1423.5
1423
10 m
SEPTEMBER
10 m

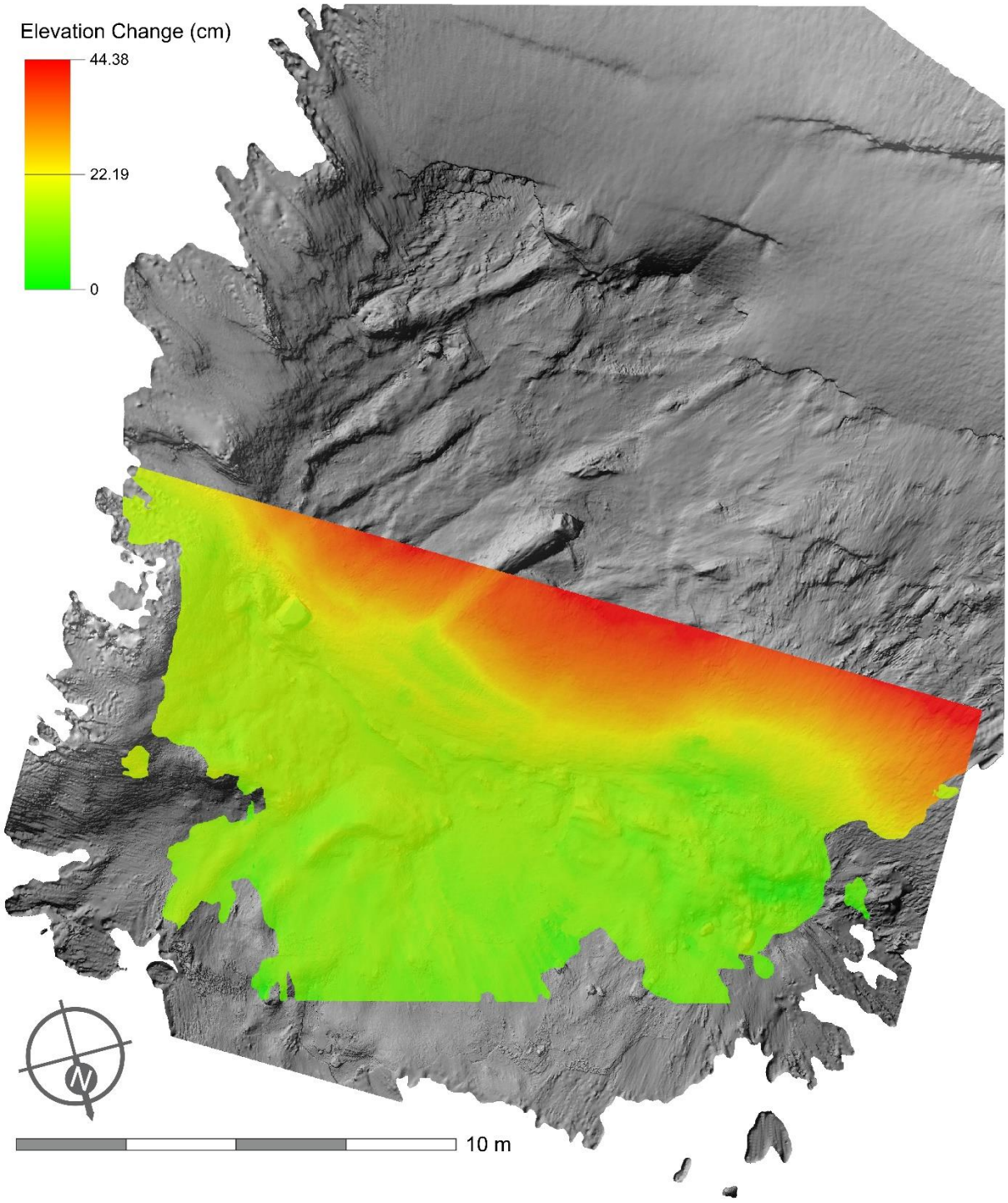

Figure 15 *- This figure shows Site 2 SfM generated DEMs overlaid over each other with the calculated difference shown by the colour scale in the area where the two overlap. Green indicates no change with red being the areas of greatest change.*

Figure 16 *(Overleaf) - Shows the two DEMs from Site 1 roughly scaled and aligned. The upper panel shows the June DEMs with white lines highlighting the features of note; the September DEM is faded in the background for reference. The lower panel shows the September DEM with the white lines retained to show the position of feature in June; the June DEM is also left faded in the background for reference of its position.*

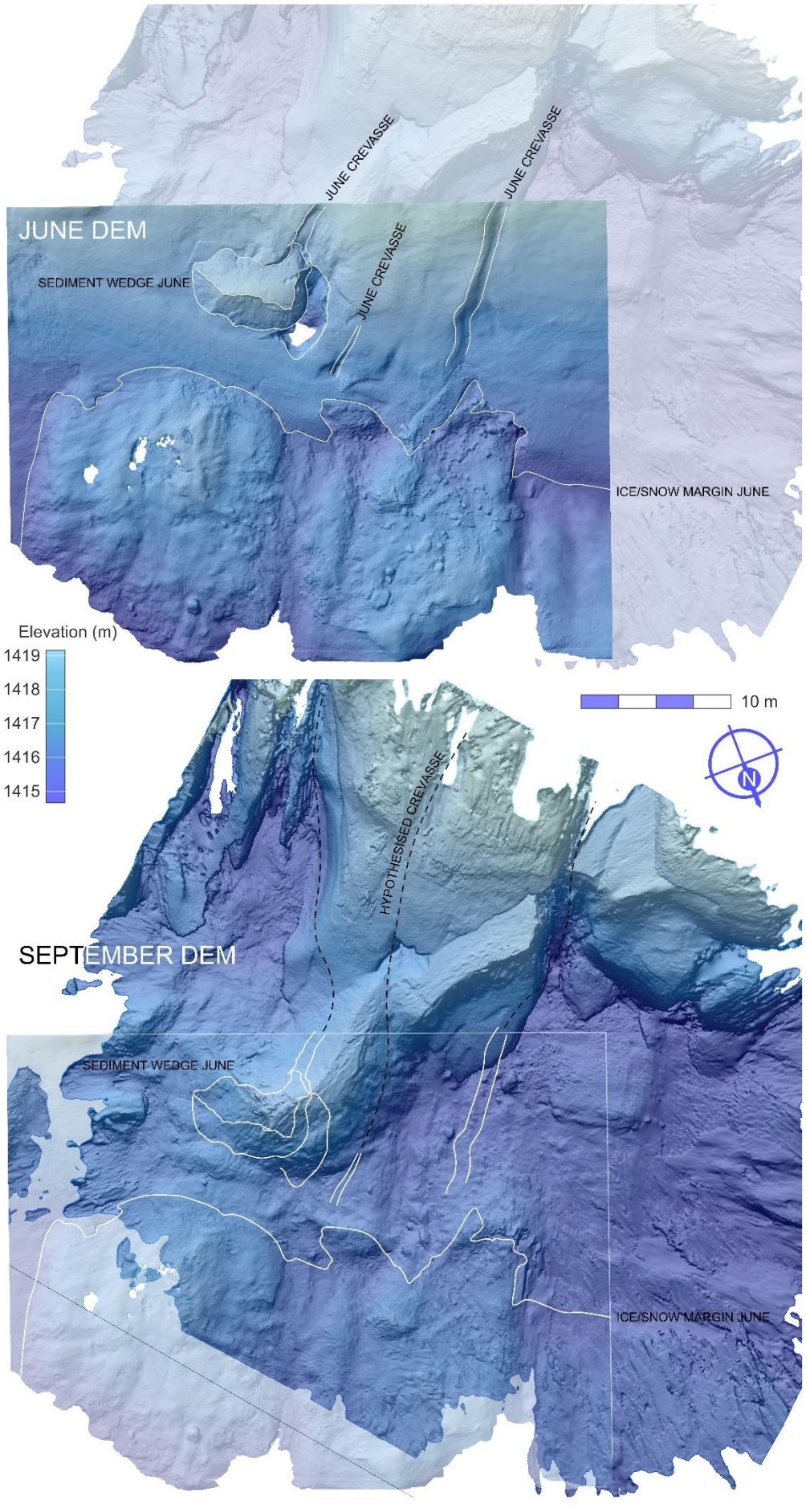
JUNE CREVASSE
JUNE CREVASSE
JUNE CREVASSE
JUNE DEM
SEDIMENT WEDGE JUNE
ICE/SNOW MARGIN JUNE
Elevation (m)
1419
1418
1417
1416
1415
10 m
N
HYPOTHESISED CREVASSE
SEPTEMBER DEM
SEDIMENT WEDGE JUNE
ICE/SNOW MARGIN JUNE

4.3. Sedimentary exposures

In total, seven sedimentary exposures were recorded from either natural exposures or were dug in the field in order to investigate the mechanisms forming specific landforms. This included an exposure focusing on one of the snowbank push ridges; four sections investigating the sediment wedge structures; and one documenting an exposure into the side of the glacier where a lateral depression between the ice and the bedrock revealed a cross section through the ice down to the bed. The final exposure focused on the eastern wedge described in section 4.1.3 and depicted in Figure 8B**.** Due to poor conditions constraining time in the foreland in September, all of the sections were made during the June visit which prevents the investigation of how these structure may have developed over the melt season.

4.3.1. Snowbank ridge

A natural exposure in June was used to document the structure of the snowbank push ridge, where a crevasse intersected with the ridge [60° 33.766'N, 07° 30.167'E], shown below in Figure 17. This presented a profile through the feature which otherwise appears from the surface as a small blocky ridge protruding from the snow near the glacier margin. The ridge extended for approximately 25 m parallel to the ice margin. Similar ridges can be identified in the background of Figure 17. The surrounding foreland slopes back towards the glacier in a reverse slope and comprises of uneven, poorly sorted blocky sediments, in a thin layer overlying bedrock, as visible in the background of Figure 17.

The exposure revealed thin glacial ice separated from the underlying sediments by a 30-40 cm gap on the up-glacier side. On the down-glacier side, a slab of what appears to be ice or compacted snow lies at a steeper angle relative to the ice margin, around 50° compared to the shallow glacier slope of 15-20°. Both sides of the ridge are overlain by snow; however, the down-glacier side appears more ‘dirty’, covered in a mix of finer sediments and subangular pebbles. Between the two sides a ridge was observed composed of a blocky, unsorted diamicton, ranging from silts up to small sub-angular boulders. The ridge in places protruded above the snow line sending material cascading down the distal side of the ridge and onto the snow on the down-ice side.

Figure 17 *(Overleaf) - Presenting the natural exposure cross section through the snowbank ridge. Part A shows an alternative view looking northwest for context; Part B shows the photo that the illustration was based on for comparison; Part C shows the illustration of the section with annotations*

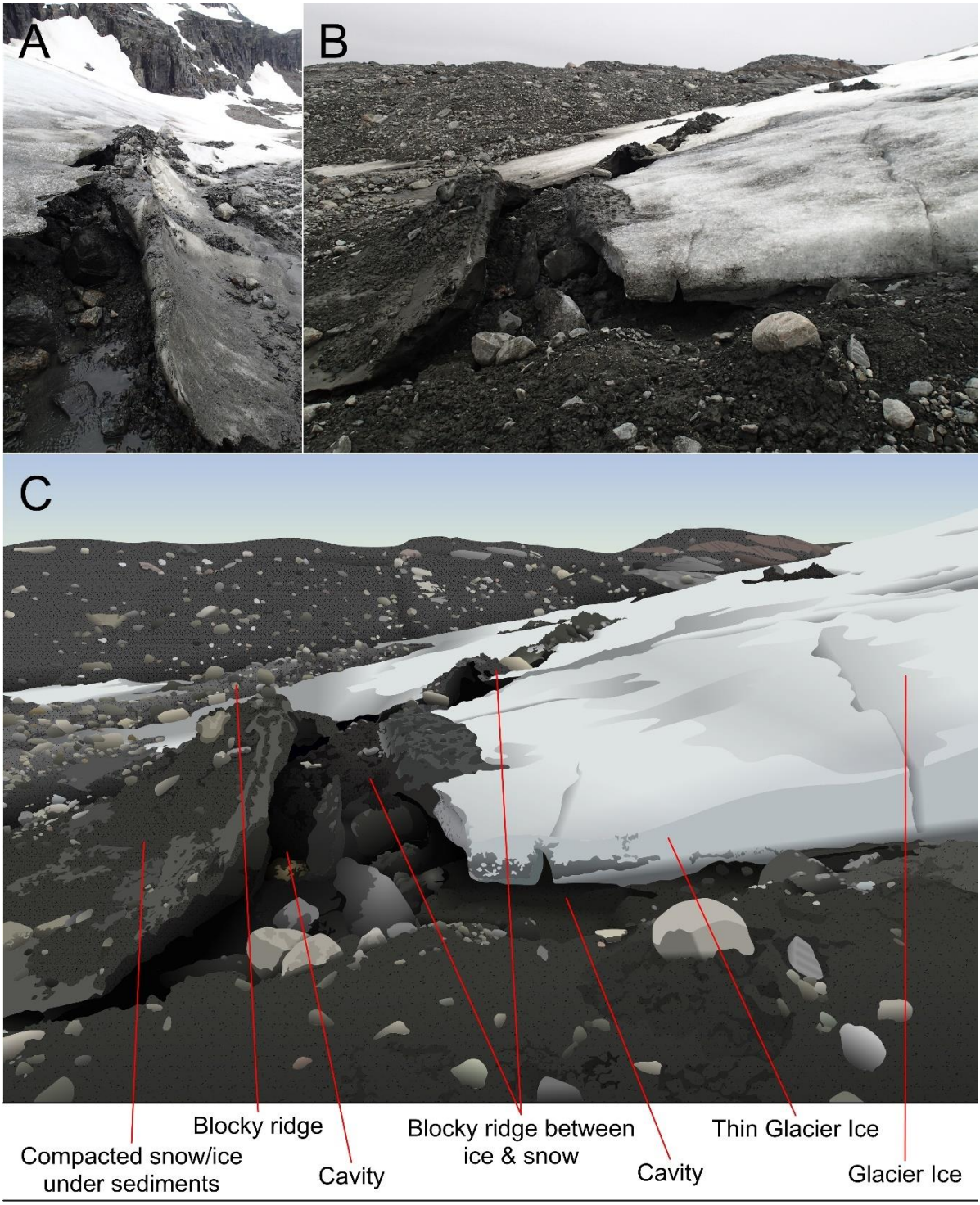
A
B
C
Compacted snow/ice under sediments
Blocky ridge
Cavity
Blocky ridge between ice & snow
Cavity
Thin Glacier Ice
Glacier Ice

4.3.2. Sediment wedge

The sediment wedge was recorded from several angles to best illustrate the observed structure in 3D. The top of the wedge slopes gently towards the glacier with a slight drooping at each end so that it resembles half a hyperbolic paraboloid shape, or roughly the shape of a pringle cut in half lengthways (Fig. 18A). The front of the wedge slopes is at a much steeper angle, almost meeting the upper surface at a right angle, and is composed of loose cascading debris on the surface. The western side of the wedge is dominated by a deep crevasse shown under the View 3 arrow in Figure 18B, this was too deep to photograph to the left of the arrow, resulting in the grey area of no data.

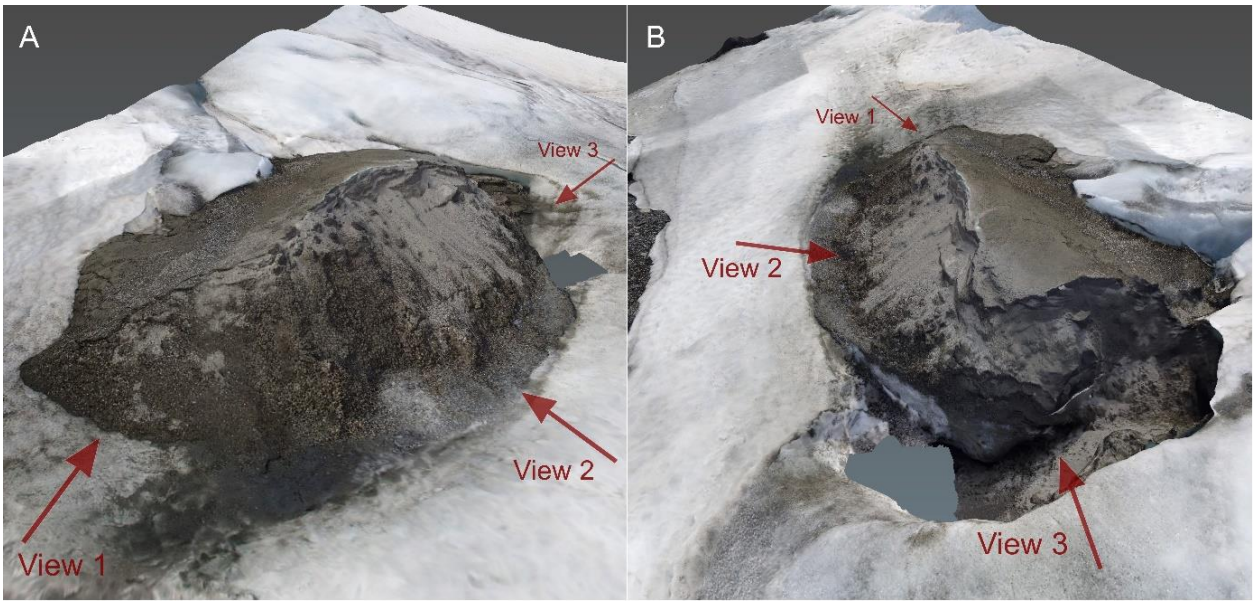

***Figure 18** - This figure helps illustrate the complex geometry of the sediment wedge and depicts where each of the 3 exposures were made shown below in Figure 19. This uses the SfM model from Site 1 which was made before the exposures were created, so it is valuable in that it shows the wedge before it was disturbed. This is particularly important for view 1 (the first panel in Figure 19) which shows the original sediment cover over the underlying glacier ice. View 4 was made looking the opposite way to View 3.*

Four exposures were created within the sediment wedge, one on each of the exposed faces (Fig. 18). View 1 (Fig. 19), shows the first section made dug into the eastern side of the wedge. Around 20 cm of well-sorted brown/yellow gravels sands in a uniformly thick band overlay ice. This sediment was poorly consolidated and faintly laminated, aligned parallel to the top surface of the wedge which sloped gently towards the ice at between 15-20°. The sediment lithology was unique compared to the rest of the foreland, which was typically poorly sorted dark grey sediments. The upper surface of the wedge exhibits some sorting with a patch of coarser grained sediments, gravel up to 10 mm in size, in a belt 30-40 cm behind the ridge crest. Along the ridge crest, the surface is fractured by micro scarps perpendicular to the front of the wedge, particularly at the end nearest where the section was made. Before the section was excavated the face of the wedge was composed of slump debris cascading down the side of the wedge, as such the sediment was highly fissile and easy to remove. The back side of the wedge also exhibited cracks, however these appear to be dendritic in form.

The second panel of Figure 19, (view 2, Figure 18), shows the distal slope or front of the wedge. A section just over a metre was dug into the front slope although half of this comprised of a debris fan of excavated material that collected at the bottom of the section due to the fissile nature of the sediments. The section exposed alternating thin bands of coarser gravels and thicker bands of sand. Sediments finer than coarse sand grain size (0.5–1 mm) were absent. At least five gravel bands up to 3 cm thick were observed with the upper and lower contacts between bands relatively sharp. The gap between the gravel bands varied but also appeared to reduce towards the surface. The bands were not aligned to the surface of the sediment wedge instead dipping very slightly to the east while the top of the wedge sloped towards the west, however this was not measured accurately in the field.

The final panel from Figure 19, is the view 3 directly opposite to view 1 (shown in Figure 18), looking at the wedge from the western side. Due to the crevasse down the western side of the wedge the section could not be examined in detail. However, sediment falling into the

crevasse had left a near-vertical exposure that is recorded in the final panel. The repeating bands of coarser gravels and sands are recorded again, although they are observed dipping in opposing directions underneath the crestline of the wedge, shallowly towards the glacier on the proximal side but more steeply away from the glacier on the distal side. At the point where the two meet, it is difficult to determine whether the sediments are folded, and the bands of gravel are continuous, or if some form of offset exists. The ice observed in the first panel is again visible towards the bottom of the crevasse around two meters below the top of the wedge, out of frame of the photograph and section illustration in Figure 19. The ice may be present closer to the surface lying under the sediment cascading down the side of the landform, as slump obscured up to 80% of the wedge on this side, however the exposure was not accessible to clear and test if this was the case.

Figure 19 *(Overleaf) - This figure runs over the following 4 pages, each panel presenting one of the sections from the sediment wedge, described above and depicted in Figure 18. For each panel, Part A shows the overhead view of the sediment wedge from the SfM model with an indication of the area that the section covers; Part B shows the photo (or stitched photos) that the illustration was based on for comparison; Part C shows the illustration of the section with annotations.*

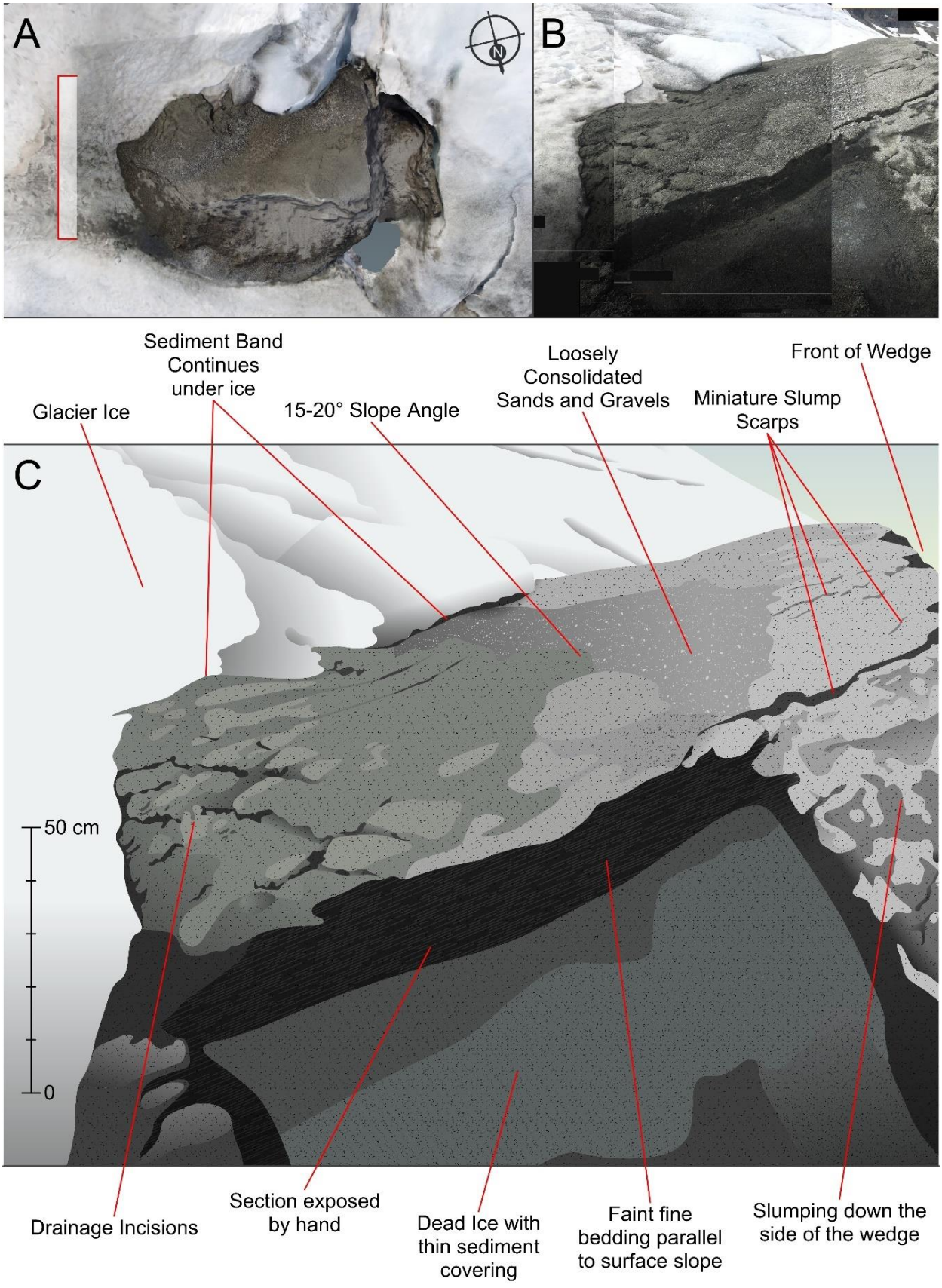
A
B
C
Sediment Band
Continues
under ice
Glacier Ice
15-20° Slope Angle
Loosely
Consolidated
Sands and Gravels
Miniature Slump
Scarps
Front of Wedge
50 cm
0
Drainage Incisions
Section exposed
by hand
Dead Ice with
thin sediment
covering
Faint fine
bedding parallel
to surface slope
Slumping down the
side of the wedge

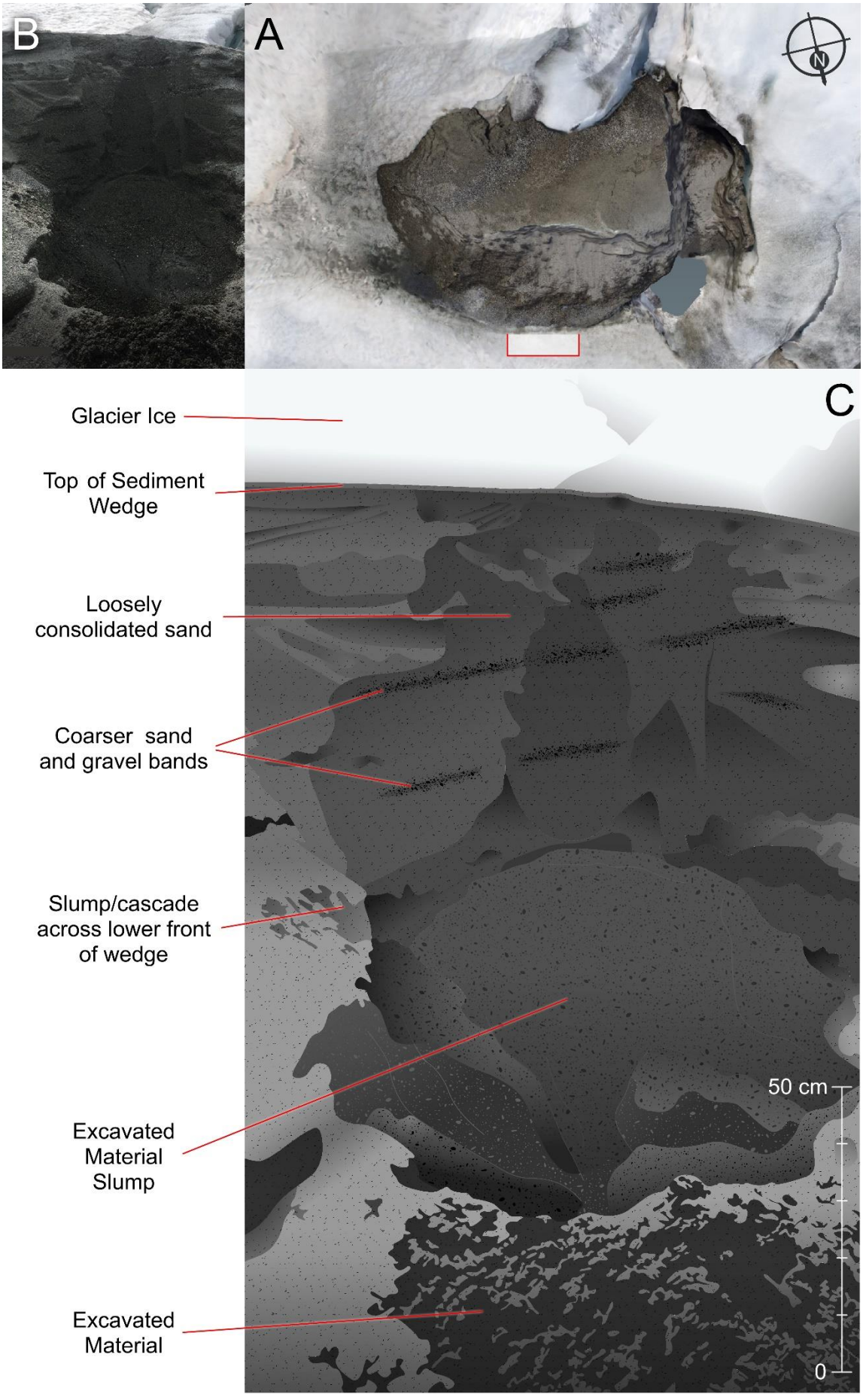
B
A
N
C
Glacier Ice
Top of Sediment Wedge
Loosely consolidated sand
Coarser sand and gravel bands
Slump/cascade across lower front of wedge
Excavated Material Slump
Excavated Material
50 cm
0

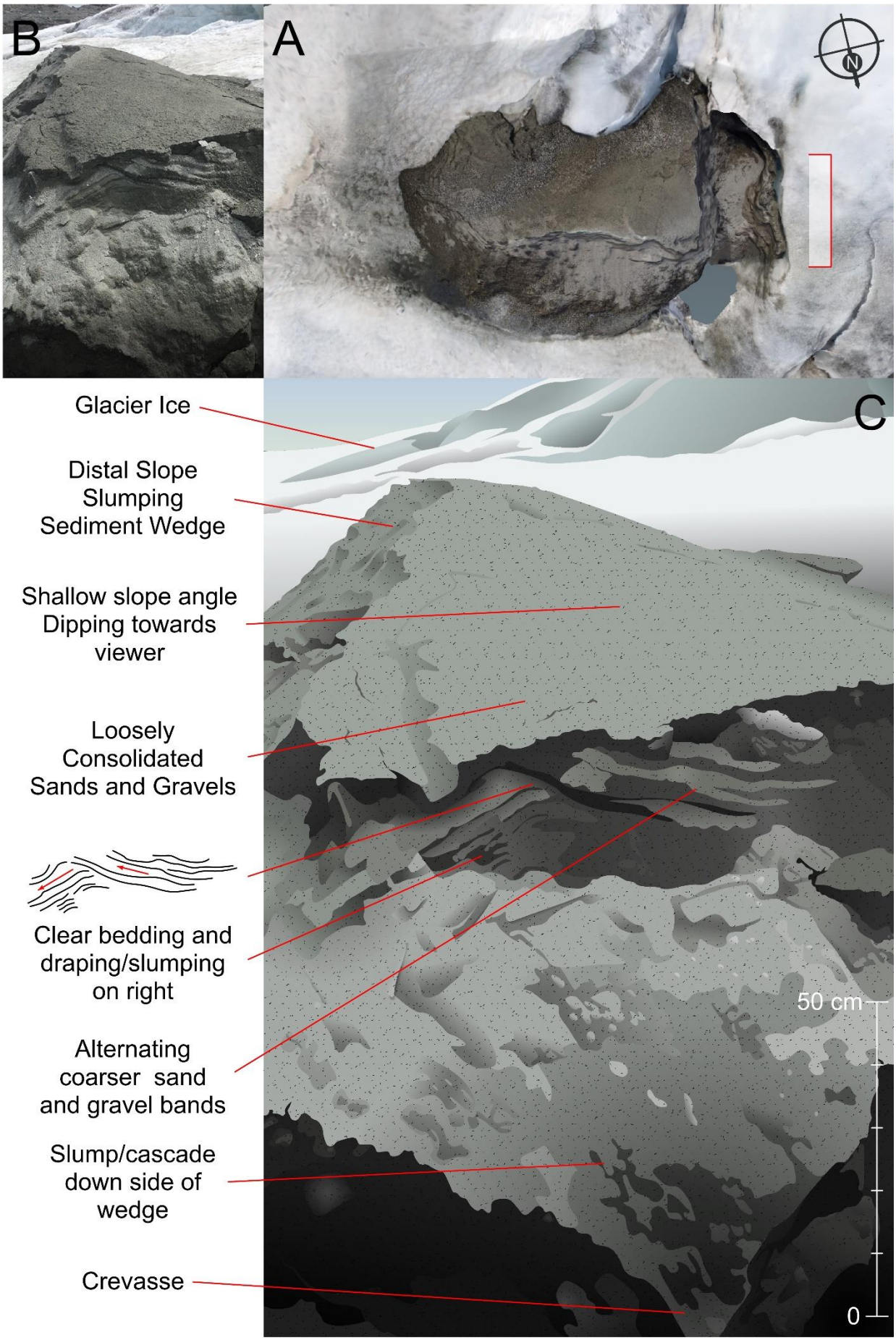
B
A
N
C
Glacier Ice
Distal Slope
Slumping
Sediment Wedge
Shallow slope angle
Dipping towards
viewer
Loosely
Consolidated
Sands and Gravels
Clear bedding and
draping/slumping
on right
Alternating
coarser sand
and gravel bands
Slump/cascade
down side of
wedge
Crevasse
50 cm
0

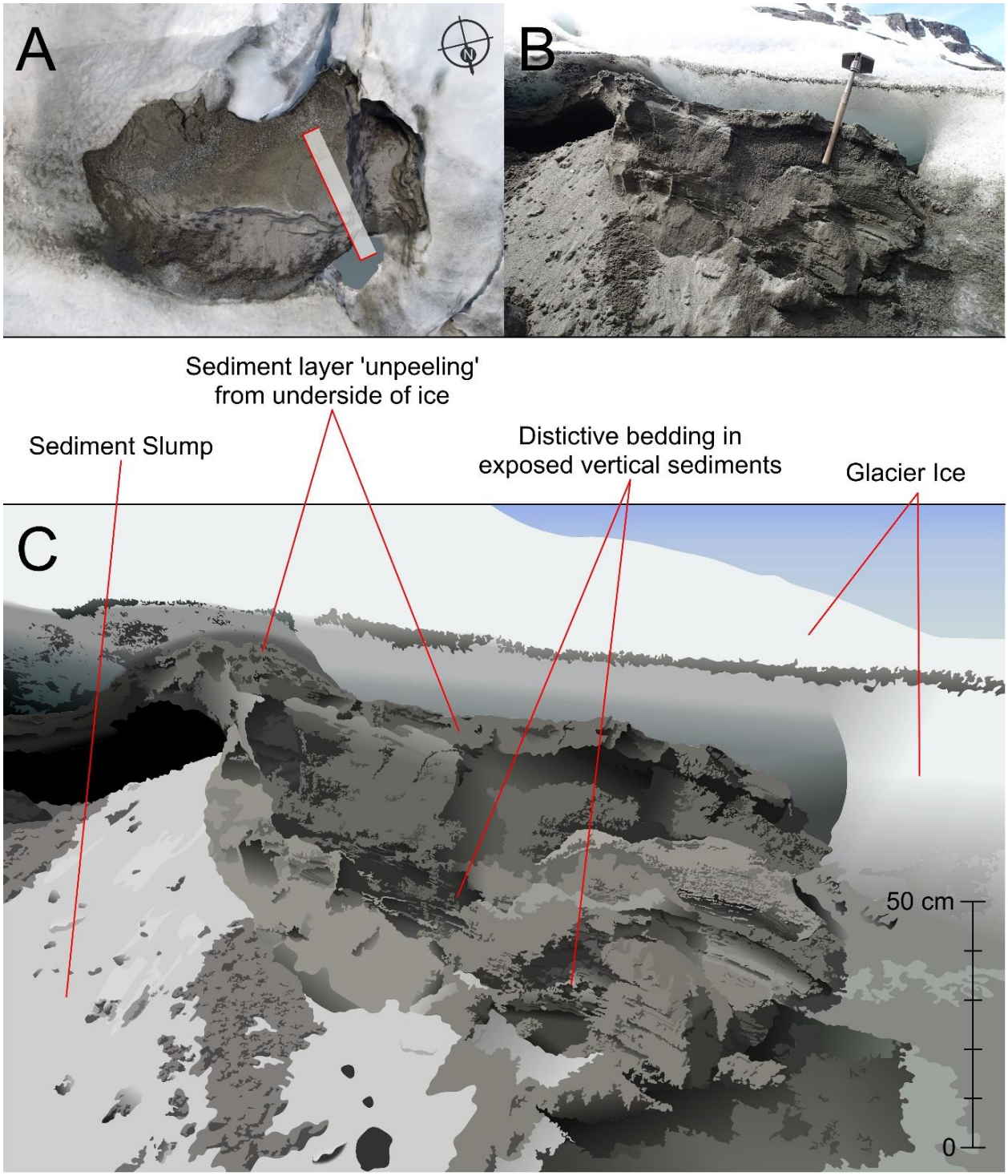
A
B
Sediment layer 'unpeeling'
from underside of ice
Sediment Slump
Distictive bedding in
exposed vertical sediments
Glacier Ice
C
50 cm
0

4.3.3. Debris septum at glacier bed

On the southern side of the protruding area of the ice margin, a large elongated depression at [60° 33.676'N, 7° 30.373'E] was observed, aligned parallel to ice flow between the bedrock and glacier ice with overlying snow (Fig. 20D). This made it possible to view a cross section through the side of the glacier and showed that much of the protruding area of the margin was underlain by glacier ice rather than being just of large snowbank that had accumulated in the low ground around the main meltwater portal (Fig. 20B). Approximately 6 m of snow lay above 2 m of glacier ice. A small crevasse angled at ~45° from the glacier bed sloped down glacier and appeared at least partially filled with sediment. The sediment was poorly sorted and did not exhibit any obvious structure (Fig. 20A). Grain size ranged from coarse sand up to larger subangular clasts (>10 cm). The ice was not in contact with the bedrock, separated by a narrow 10-20 cm crack from which the sound of gushing water could be heard. The bedrock below the feature was covered in a thin layer of sediment, however it was unclear if this had originated from the crevasse feature or the cliff above shown in Figure 20D. Upon returning to the site in September, the margin had retreated at least a further 10 m up glacier from this point leaving no evidence of the feature. It was observed the main meltwater portal emerged from the glacier just under the cliff so was the source of the noise heard in June.

Figure 20 *(Overleaf) - Presenting the exposure from the base of the ice. Part A shows a wider view for context; Part B shows the photo that the illustration was based on for comparison; Part C shows the lateral depression in relation to the glacier; Part D shows the illustration of the section with annotations.*

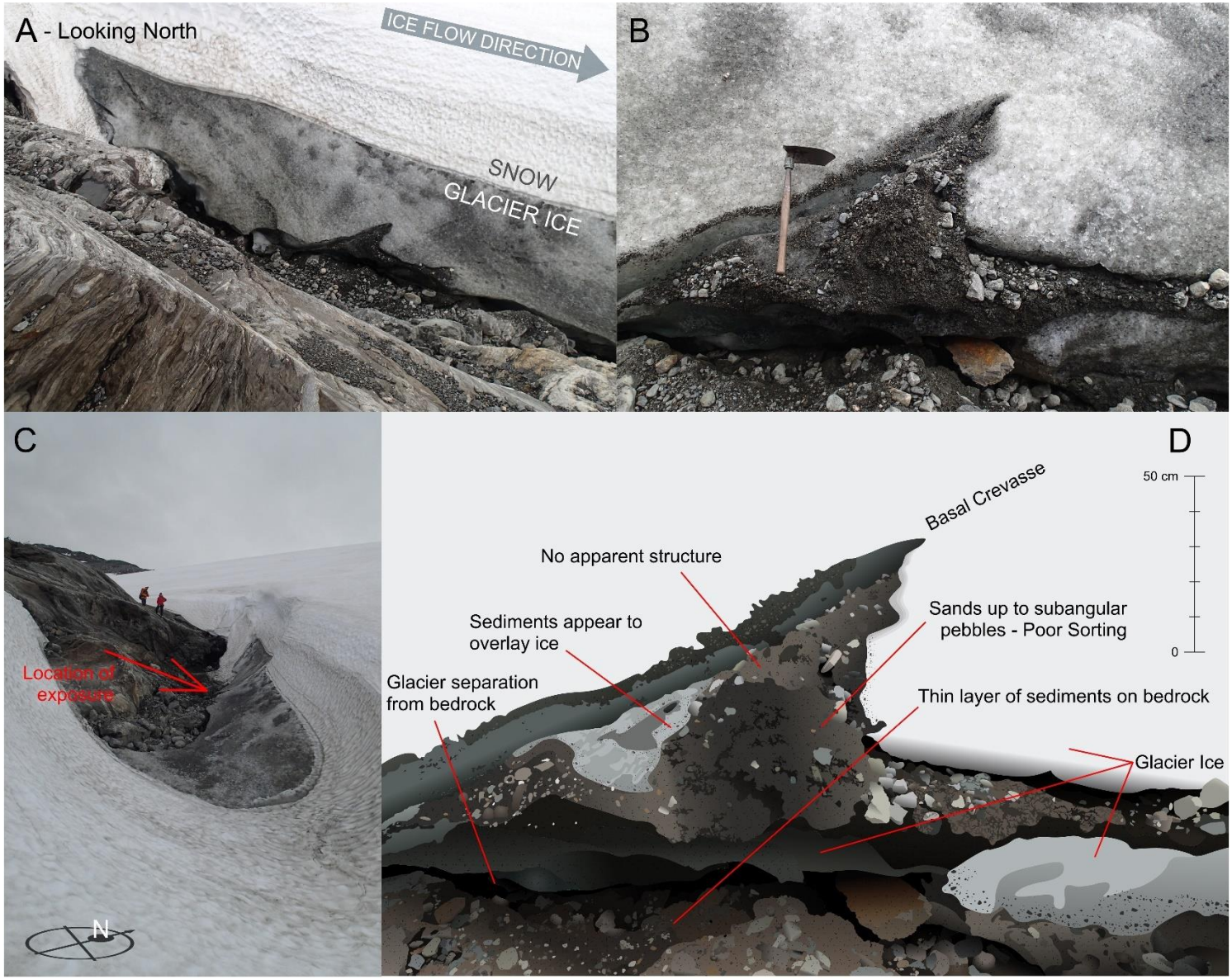
A - Looking North
ICE FLOW DIRECTION
SNOW
GLACIER ICE
B
C
Location of exposure
N
D
50 cm
0
Basal Crevasse
No apparent structure
Sediments appear to overlay ice
Sands up to subangular pebbles - Poor Sorting
Glacier separation from bedrock
Thin layer of sediments on bedrock
Glacier Ice

4.3.4. Eastern Wedge

An exposure was dug into the end of the lateral wedge landform (Fig. 8B) to the east of the main wedge that was the focus of section 4.3.3. The ridge as described in section 4.1.3, was surrounded by snow and was similar to the large sediment wedge (Fig. 8A) in morphology but orientated laterally to the ice flow direction as opposed to perpendicular. Figure 21 displays at least three bands of fine silty sediment each with fine bedding; the thickness is uneven varying from 5-10 cm. Between these finer bands, poorly sorted coarser sand was observed as well as an irregular distribution of clasts which appeared to increase in size lower in the exposure. The beds dipped towards the south, in the direction of the glacier, and were crudely aligned to the slope of the proximal side of the ridge. It was observed that the dipping of the beds was not uniform but appeared to increase in steepness towards the upper distal side, forming a gentle concave curve. On the distal side, these bands appeared somewhat deformed and slightly displaced, potentially showing the presence of a small fault or slumping. Ice was observed at the base of the landform, although it could not be determined whether this had derived from the glacier or was overridden compacted snow.

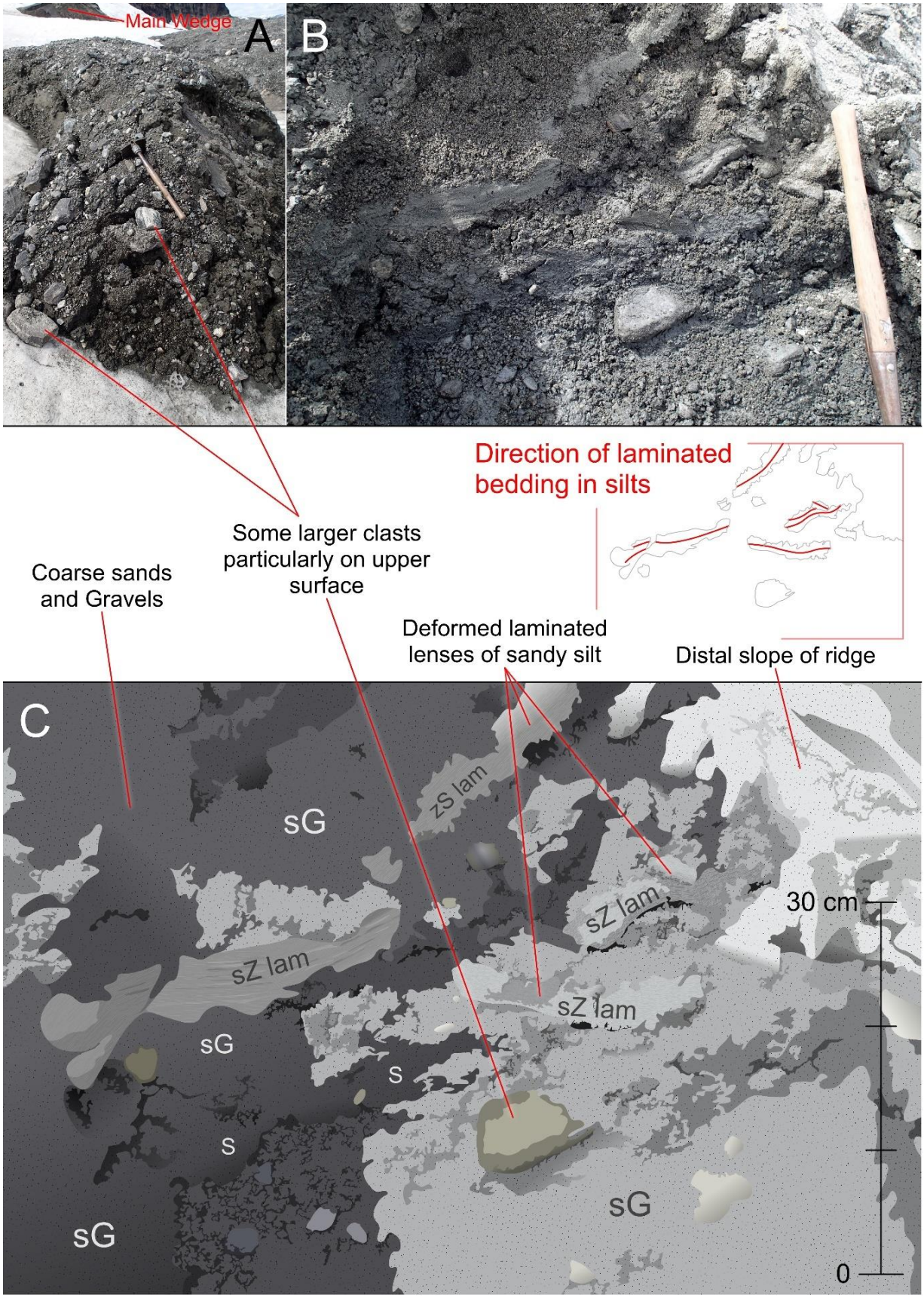

Figure 21 *- Shows the exposure described in the above paragraph. Part A shows the site of the exposure prior to its excavation. Part B shows the photo that the illustration was based on for comparison; Part C shows the illustration of the exposure with universal lithofacies codes (Farrell et al., 2012) S - Sand; sG - Sandy gravel; zS lam - Silty sand, laminated; sZ lam - Sandy silt, laminated.*

4.4 Foreland Evolution Photos

This section briefly documents the changes observed in the foreland through photos taken from the same position in June and September; these photos are displayed below in Figure 22. The purpose of this section is mainly to act as a reference and to support the other results and discussion points by providing photographic evidence of the changes in the foreland. Below, each pair of photos are briefly described.

A - Photo looking north, the changes revealing a number of small flutes and minor moraines. This also illustrates the reverse slope, which is common on the southeast side of the foreland, and the presence of the margin where it is detached from the substratum as noted in section 4.1.1.

B - Photo looking towards the south, focusing on the site of the SfM model 2. The margin retreat revealed further minor moraines to those mapped in June and the large flute in the centre of the September picture. Changes here have been noted in detail in section 4.2.

C - Photo facing north, overlooking the main meltwater portal and the site of the greatest marginal retreat to the extent that it is out of the September frame. In the foreground are the lateral moraines identified in section 4.1.2.

D - Photo looking south back at where photo C was taken. This illustrates the scale of retreat around the main meltwater portal.

E - Photo looking southeast over the sediment wedge, the focus of the site 1 SfM model, and described in greater detail in section 4.2.

F - Photo facing the southeast. The foreground shows the second sediment wedge type feature noted in section 4.3.3 with the main meltwater outlet in the background. The ablation season exposed more of the sedimentary feature and shows the degradation of the sharper wedge form observed in June to a more hummocky ridge by September.

G - Photo looking north, showing the large distance of marginal retreat. Like photo C, the September margin is out of frame. In the foreground of the September, the small flutes are visible that were mapped in Figure 10, exposed by the margin retreat.

H - Photo looking southwards, showing the snowbank push ridge, as illustrated in Figure 17. The September photo shows poor preservation of the original ridge, a slight ridge can still be discerned however it is ambiguous enough to be easily missed had its location not been mapped in June.

Figure 22 *(Overleaf) - This figure runs over the following 2 pages, at the top of each page, the locations of the photos are shown. The June photos are show on the left and the September photos are on the right.*


N
D
C
B
A
H
G
E
F
100m
A
B
C
D

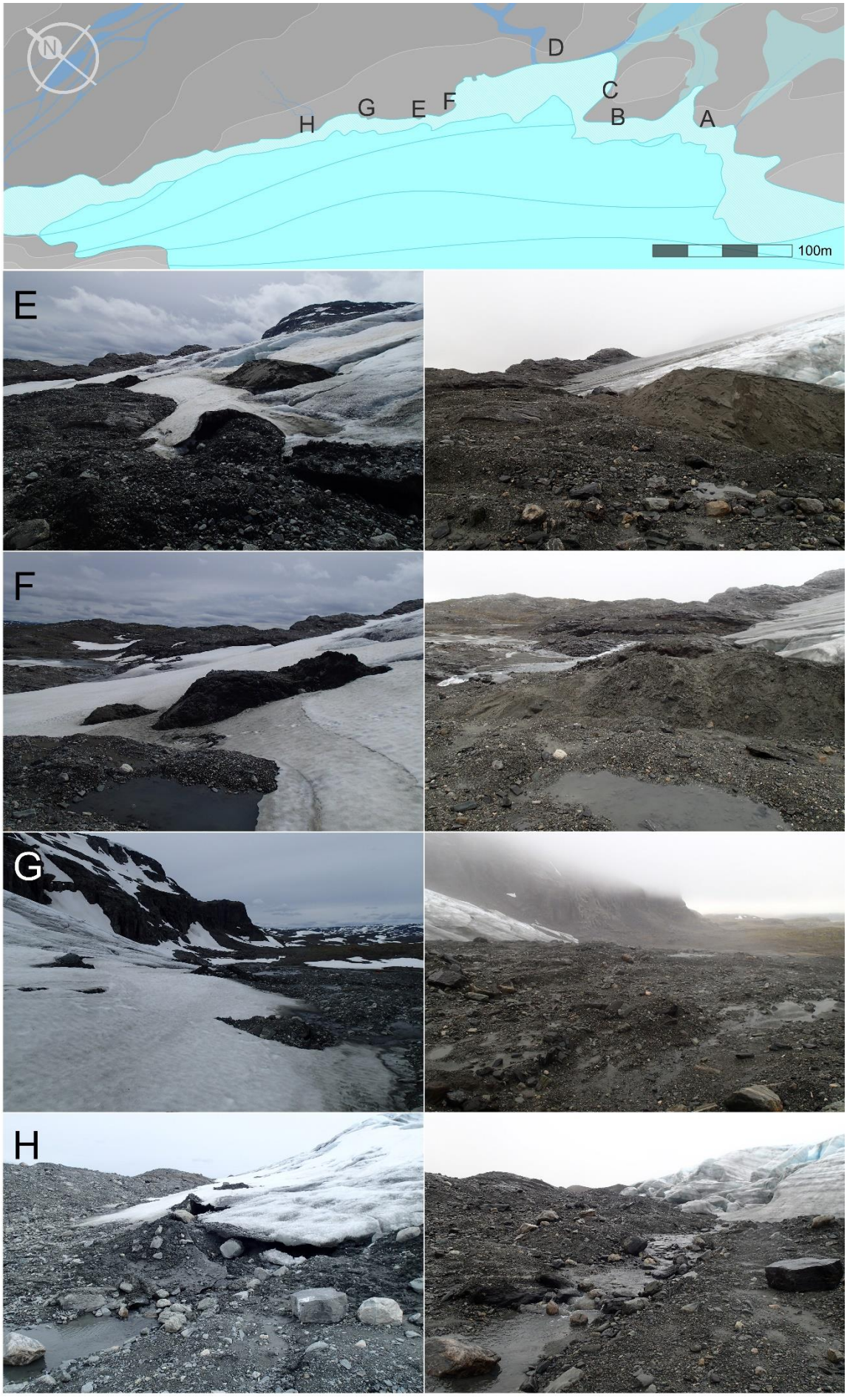
N
D
C
B
A
G
E
F
H
100m
E
F
G
H

4.5. September Ice Cave Observations

In September, ice caves were discovered at numerous locations along the margin. These varied in size from a few decimetres in height, to over a metre. The following section documents a few of the observations made in, and around these caves with this text largely acting as an extended caption for the photographs in Figure 23.

Photo A - Shows the scale of one of the ice caves with Lena Uldal Hansen and Mateusz Zawadzki standing in the opening for scale. Also visible, indicated by the arrow, is water draining back into the glacier following a reverse slope present at the site.

Photo B - Shows a more detailed view of the left-hand side of the cave in Photo A, where the ice is in contact with the sediments. A small ridge is visible, indicated by an arrow, (also visible silhouetted against the cave opening in Photo A). This ridge runs roughly subparallel to the ice flow direction following the curve of the cave. The side proximal to the ice appears steeper, with a more gentle slope on the distal side.

Photo C - View looking into one of the ice caves. Arrow 1 picks out a large boulder with a ridge (arrow 2) on the leeside, composed of more coarse material than the surrounding sediments. This matches the landforms found outside the cave in the foreland which were interpreted as boulder-initiated flutes. Arrow 3 points to an area of finer silty sediments, with a microscale braided drainage system across its surface, flowing back into the glacier. Small, circular water-filled depressions can be seen in this surface, similar to small impact craters, where water was observed dripping from the thawing ice in the roof of the cave onto the floor.

Photo D - Depicts the ice margin near a cave with a ridge protruding directly from the ice, parallel to flow (arrow 1). The shape of the ridge is well defined near the ice but deteriorates distally with slumping and surface cracks observed (arrow 2).

Photo E - Shows the floor inside one of the caves with another microscale drainage system similar to photo C. The surface is comprised of fine, silty sediments which has been dissected by the drainage system leaving miniature plateau areas, mesas (arrow 2) and buttes. Drawing similarities to those found in the mature incised river systems in the western Sun Belt states in the USA such as along the Colorado River (Jain, 2014). In the gully areas the sediment is more poorly sorted with larger clasts up to 5 cm (arrow 1). The upper surface contained some crater marks, resembling those observed in Photo C.

Photo F - Shows the floor of a different cave with different surface features. Small ripple marks are visible in the background composed of fine silty sediments. In the foreground (arrow 1), lines parallel to the contours of a small sediment dune are visible. This resembles an erosional shoreline terraces in miniature similar to those found around evaporating lakes or draining reservoirs.

Figure 23 *(Overleaf) - This figure shows observations from ice caves found along the margin as described in the text above.*

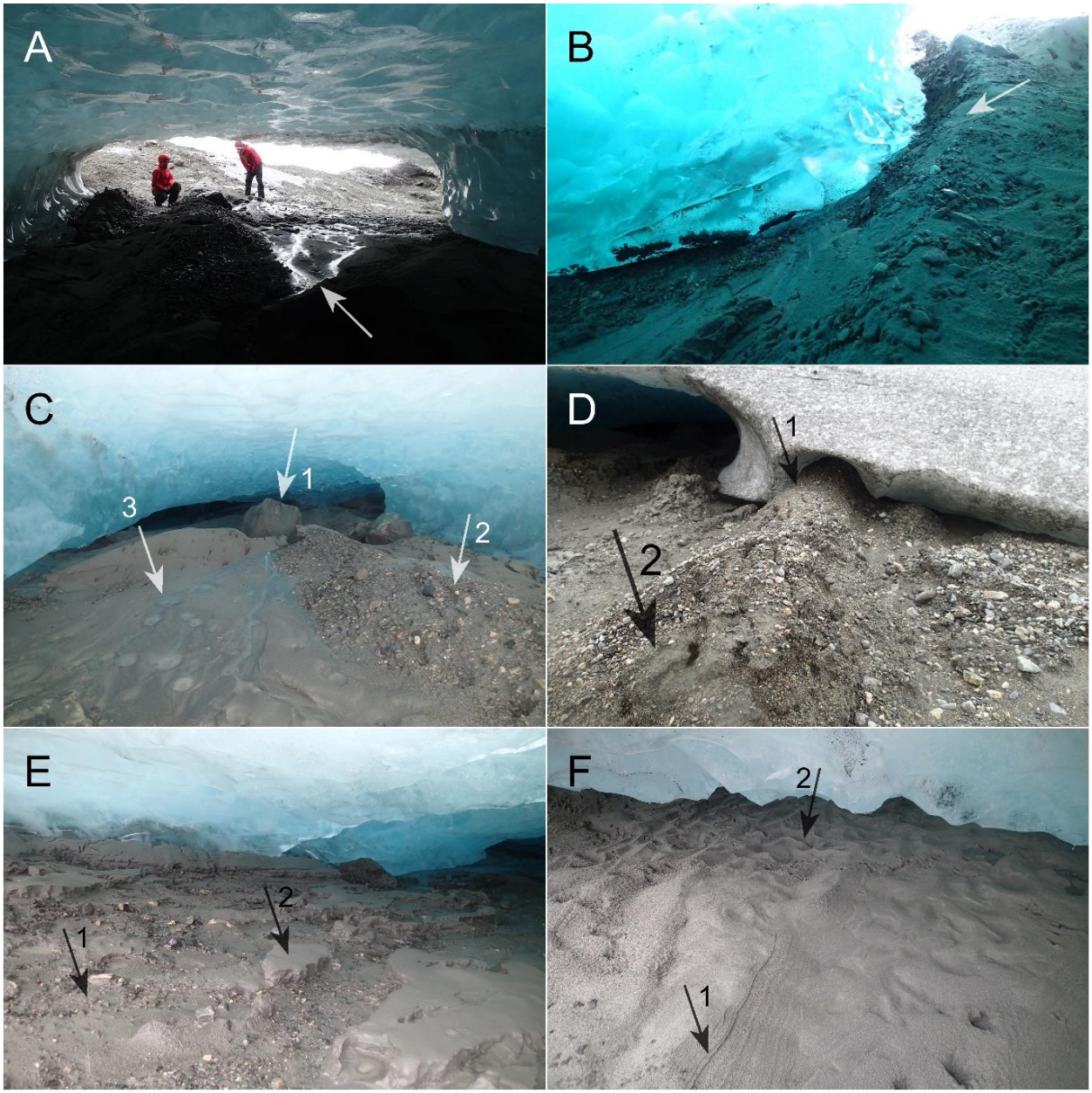
A
B
C
1
2
3
D
1
2
E
1
2
F
2
1

4.6. Geomorphological map

June

Figure 24 shows the interpreted landforms described in section 4.1 compiled into a full geomorphological map. The foreland can be roughly divided into two areas based on distinctive sediment-landform assemblages.

The north-western area which topographically consists of the terrain sloping away from the ice to the north has a thicker sediment cover. The area is divided by several small meltwater channels that form terraces as they drain towards the north. The area is dominated by larger minor moraines of over 50 cm in height, but other landforms are largely absent.

This is in contrast to the south, where the terrain is more undulating and complex, and where there is a much thinner sediment cover and bedrock is frequently at the surface (Fig. 24), either in steeply sloping areas or as topographic highs. The area contains the main meltwater portal in a topographic depression which in June was largely covered by a tongue of snow and ice; aside from the main portal, this area has no other significant outlets as a reverse slope is present for a large portion of the margin. The geomorphology is much more varied when compared to the north-western area. The most prominent landforms are also minor moraines but these are smaller and more closely-spaced ridges than those in the northwest. Flutes are prevalent mainly in the south of the foreland, southeast of the meltwater portal. Apart from a small cluster to the north of the depression, they are largely absent from the northwest of this point. Similarly, lateral moraines, are confined to several clusters, mainly along the flanks of the ice tongue than surrounds the main meltwater outlet.

Figure 24 *(Overleaf)* ***Geomorphological map (June)*** *- This figure shows the interpreted landforms from Section 4.1. Note that the position of the meltwater channels, ponds and exposed bedrock are estimated based on field notes and photographs, as are the local slope indicators. The light blue/off white coloured area along the margin shows the area of change between the June margin and the September margin.*

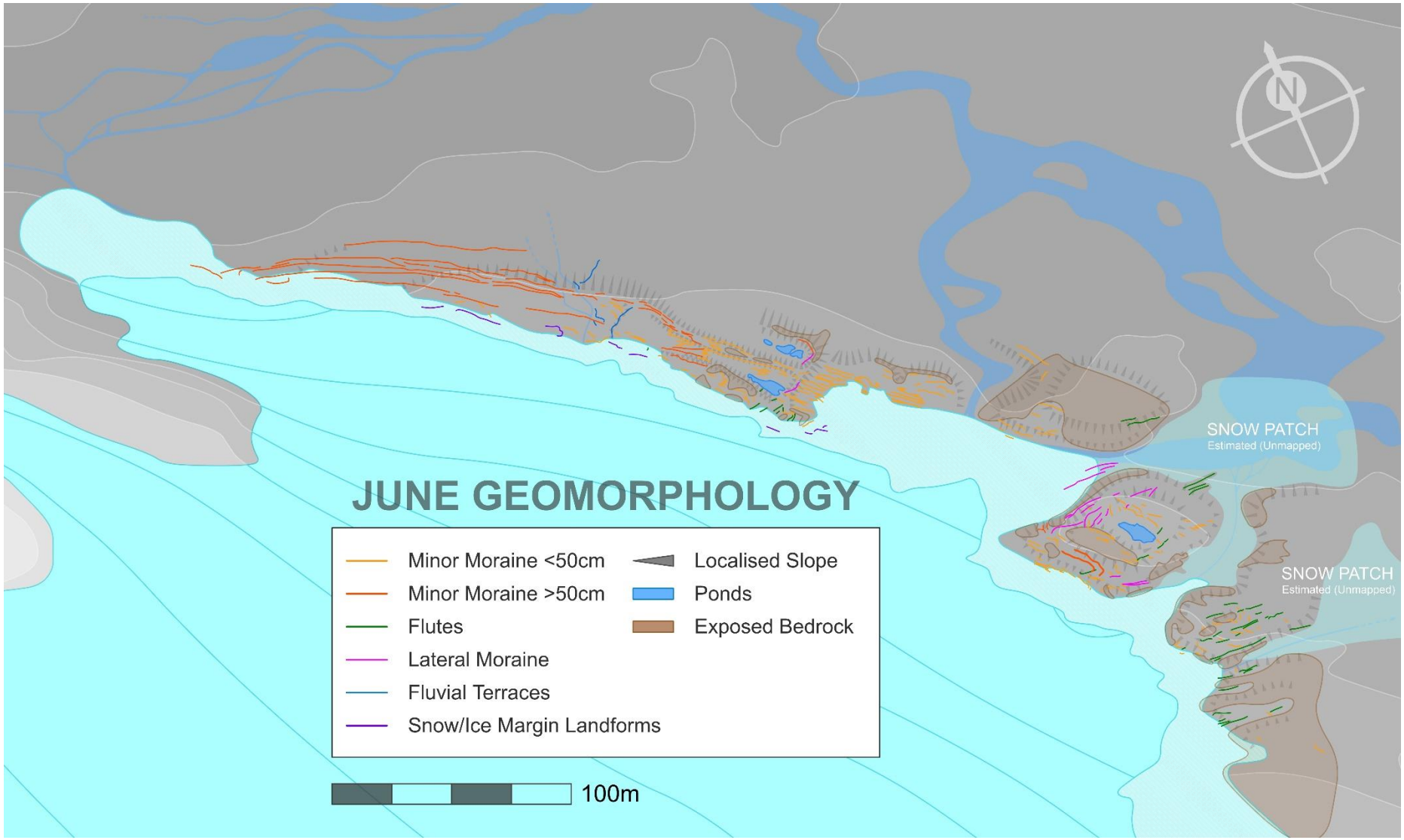
N
SNOW PATCH
Estimated (Unmapped)
SNOW PATCH
Estimated (Unmapped)
JUNE GEOMORPHOLOGY
Minor Moraine <50cm
Minor Moraine >50cm
Flutes
Lateral Moraine
Fluvial Terraces
Snow/Ice Margin Landforms
Localised Slope
Ponds
Exposed Bedrock
100m

September

Comparing the geomorphology to June, the most apparent change is the disappearance of the snowbank that masked much of the glacier margin. Due to the presence of the snow it was difficult to distinguish the exact position of the margin in June and therefore give an estimate for the retreat over the melt season. On average, when treating the snow and ice in June as one entity, the change was between 20-30 m of retreat across the foreland but was up to 40-50 m around the main meltwater portal. It is important to note that this may be skewed by a greater accumulation of snow in the low-lying area around the meltwater outlet that masked the location of the actual margin in June.

In relation to the margin change, the thawing of the snow and margin retreat revealed multiple sets of minor moraines. These were closer to the new margin than those mapped in June which had previously appeared to be the youngest; the September evidence showed this not to be the case.

Elsewhere along the margin, the retreat showed that the main meltwater portal is actually divided in three within the topographic depression, with the southernmost channel bearing the majority of the discharge, coalescing approximately at the point where the margin lay in June.

Further to the northwest of the meltwater portal, where the terrain rises before reaching the ponds, more flutes and minor moraines were recorded. The area where the most dramatic landform evolutionary changes occurred was located at the top of this slope in the area where the 'sediment wedge' was recorded. The retreat of the margin exposed a more complex depositional wedge-shaped landform than that originally observed in June. Much of the original 'wedge' shape had been retained (Fig. 8a); however, to the southwest, a more extensive series of wedges was observed. As this area formed part of SfM Site 1, the changes can be shown in detail using the SfM models (Fig. 9, 10) and the DEMs in (Fig. 13, 16), the latter overlaying the two DEMs to highlight the differences. These changes and the possible formation mechanisms are described further in both the SfM and the discussion sections, with further sedimentary details given in section 4.3.3.

Continuing northwest, a large number of minor moraines (up to eight sets) was recorded in the area previously covered by snow and ice supporting the observation made above that the moraines mapped closest to the margin in June were likely not recently formed. Beyond this, in the area dominated by the larger minor moraines the retreat exposed several flutes but no further moraines in this area.

Figure 25 *(Overleaf)* ***Geomorphological Map (September)*** *- This figure shows the interpreted geomorphology from Section 4.1. Note that the position of the meltwater channels, ponds and exposed bedrock are estimated based of field notes and photographs, as are the local slope indicators. As listed in the key, the greyed geomorphology lines are to make the distinction between the geomorphology mapped in June and the 'new' September geomorphology including some of the June geomorphology that was remapped on the second visit.*

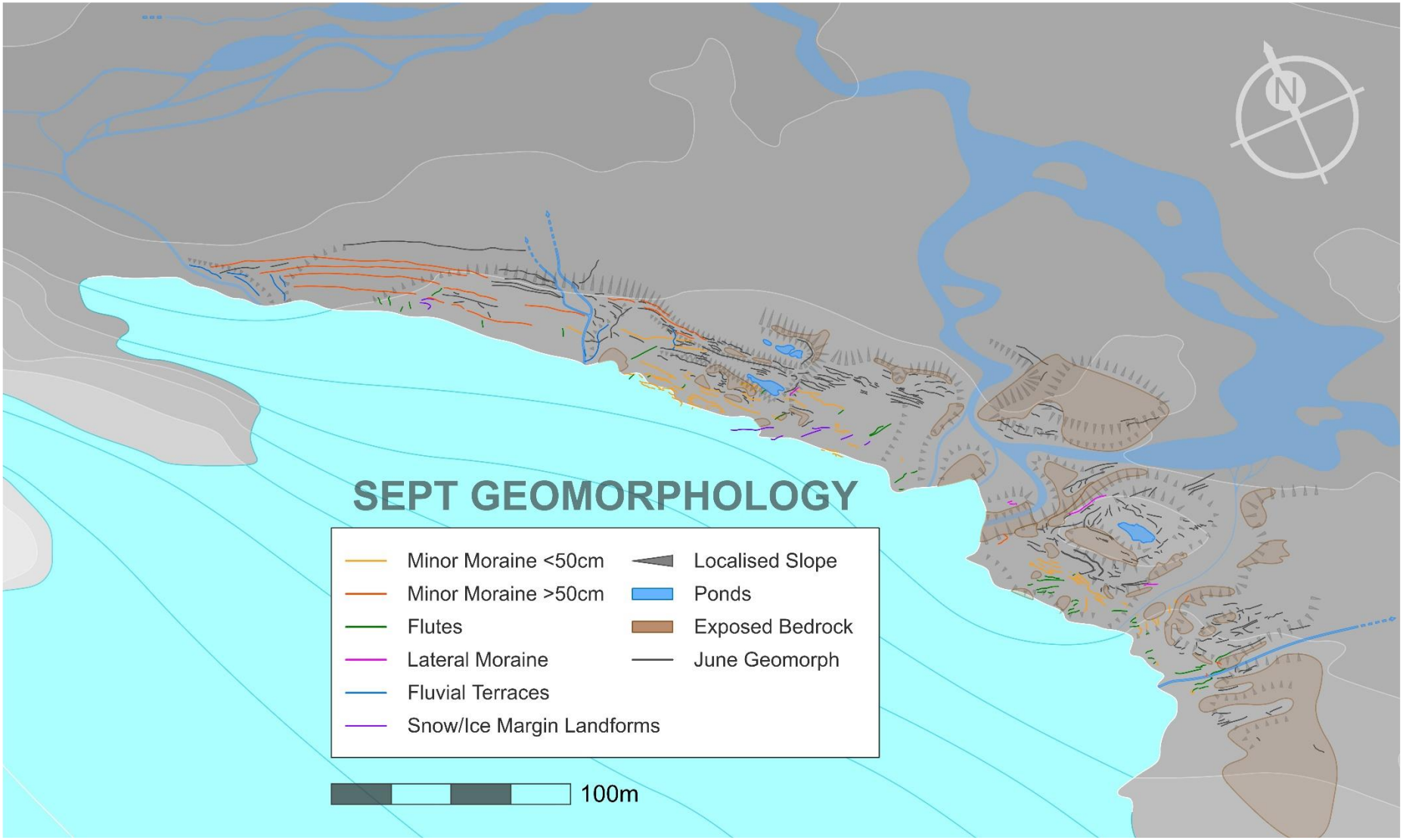
SEPT GEOMORPHOLOGY
Minor Moraine <50cm
Minor Moraine >50cm
Flutes
Lateral Moraine
Fluvial Terraces
Snow/Ice Margin Landforms
Localised Slope
Ponds
Exposed Bedrock
June Geomorph
100m
N

5. Discussion

The discussion is divided into three sections, the first builds directly on the landforms featured in sections 4.2 and 4.3 in the results, considering their genesis and preservation. The second section takes a more holistic view, encompassing how landforms are configured across the foreland and comparing them to other landsystems studies. The final section details limitations to this investigation and the possible areas for further research at Blåisen to address these.

5.1. Discussion of landform processes & evolution

This section focuses on three of the more idiosyncratic landforms recorded in the Blåisen foreland, the sediment wedge feature, multi-crested minor moraine and the snowbank ridge. The possible mechanisms from their formation are discussed, drawing on the morphological and sedimentological evidence. Conditions that may constrain their formation and their preservation over the duration of the study period are also considered.

As a general point across the margin as a whole, it was initially thought in June that many of the marginal features were relatively young, having formed earlier that winter or were even still active, such as shown in Figure 6b where the snow lay just decimetres away from the moraine crests. However, the September visit showed that large areas had just been covered by snow and were inactive. To use the example of the moraine in Figure 6b, the thaw of the snow in that location unearthed a number of landforms including a number of minor moraine ridges.

5.1.1. Formation and evolution of the sediment wedge structures

Drawing on the morphological and sedimentological evidence, the sediment wedge appears to have formed by an englacial debris band or septum approximately 20 cm thick melting out of the ice, brought up by freeze-on. This is most evident from the last panel of Figure 19 which shows a band of sediment appearing to ‘unpeel’ from the underside of the ice margin as it thaws. Freeze-on is a well-documented mechanism prevalent in Norway (e.g. Andersen and Sollid, 1971; Harris and Bothamley, 1984), and is recorded as capable of transporting up to 1 m thick sediment slabs in favourable conditions (Krüger, 1995). Favourable conditions include a thin margin, which allows freezing conditions to penetrate the substratum in winter. Under a thicker margin, the overburden pressure might reduce the depth at which freeze-on could occur or prevent the base of the ice from reaching freezing point entirely. It is also speculated by this study, that poor drainage of meltwater away from the margin, influenced by a reverse slope inhibiting meltwater flow, may also contribute to the thickness of freeze-on by providing highly saturated sediments which can freeze into a more consolidated frozen slab than drier sediments at the base of the ice. This latter point is supported by the observation of very poorly consolidated sandy sediments forming the upper proximal surface of the wedge which might be expected following the thawing of ice that bound the grains together. Freeze-on was also documented on Midtdalsbreen (Andersen and Sollid., 1971; Reinardy et al., 2013), which also exhibits similar ice margin characteristics to Blåisen, particularly a thin margin.

Due to differential melting the underlying ice becomes cut off from the glacier and becomes dead ice, as identified by the dark blue ice in View 1, Figure 19. Similar features have been previously observed in mountain glacial environments (Swift et al., 2006; Kirkbride and Deline, 2013; Swift et al., 2018). As the overlying ice thawed the meltwater winnowed the upper surface/proximal side of the wedge, removing the finer sediments, forming the coarser bands observed in areas on the upper surface of the wedge and also in the repeating bands on the distal and crevasse sides shown in Views 2 and 3, Figure 19. The meltwater followed the slope and so ran backwards towards the glacier resulting in the dendritic incisions observed near the contact between the sediments and the ice on the upper surface.

The presence of multiple layers of the coarser bands on the distal and crevasse side of the wedge could form from one of two processes, or possibly a combination of them. The first, under static margin conditions where the ablation keeps pace with ice flow velocity, likely occurring during the spring months. This transports a continuous band of frozen-on sediment to the surface; the loosely consolidated sediments cause the crest of the wedge to repeatedly fail and slump, as seen on the distal side of the crestline in Views 1 and 3, Figure 19. The slumping sediments are overridden by more sediments forming an unstable stack of sediment bands on the distal side of the wedge. The distal side of this stack continuously collapses over the dead ice below, burying it and further slowing the melt.

The other possible process is comparable, with the difference of the margin fluctuating instead of being static. The process would occur as outlined in the above paragraph, with the approximately 20 cm thick sediment band freezing on and being transported to the surface. Slight marginal retreat would subject the proximal side of the wedge to the winnowing effect described above, before subsequent readvance of the ice bulldozed and

replaced the sediments on top of the wedge forcing them to cascade over the distal slope. It was initially thought that this process may occur over several accumulation-ablation season cycles, however the evidence from the surrounding foreland indicates a much more dynamic margin than what would be required for this mechanism to occur. Additionally, it would be expected that there would be greater evidence of degradation of the underlying dead ice were it a few seasons old.

It is therefore likely that the process that formed the wedge was more akin to the former hypothesis. Sediment would be continuously delivered to the margin (albeit with occasional slight marginal variances), but not as large as those proposed in the second hypothesis and likely occurring instead over one accumulation to ablation season cycle. This inference is supported by the findings encountered during the September fieldwork. The summer ablation exceeded that which would have been required to facilitate the seasonal stacking of the frozen-on sediments.

The September findings support the interpretations drawn from the June fieldwork, with the margin retreat exposing a continuation of the sediment band to the southwest of the original wedge. This formed a series of wedges, similar to the original wedge and dissected where former crevasses were located in June, with the crestlines orientated roughly 45° to the ice margin (illustrated in Figure 16). The preservation of the original wedge is perhaps better than might be expected considering that the core of the landform was comprised of dead ice. The original wedge in September still retained a similar morphology and size, although, without being able to difference the Site 1 SfM DEMs, this is difficult to quantify. The original wedge had lost some of its original 'crisp' geometry and the September crest appears to have migrated towards the ice margin and become less well-defined, likely due to continued slumping of the distal slope and the at least partial thawing of some of the dead ice core. However, the newly exposed wedges retained the appearance of the wedge in June.

.

It is proposed that there is a link between the main sediment wedge formation discussed above, and the smaller feature to the east, pictured in Figure 8B. Although the sedimentary structure of the smaller feature was not recorded in detail, the similarity in sediment composition and morphology as well as the close proximity to the main sediment wedge sequence, leads this study to conclude that they were all formed from the same process, the exposure of an englacial debris septum. In June, the two appeared unrelated with the smaller eastern feature appearing to be aligned more perpendicular to the margin, whereas the main wedge appeared parallel (Fig. 8A, 8B). However, the exposure of more of the main wedge in September revealed that the crestline of the main wedge(s) broadly aligns with the eastern feature. This is illustrated below in Figure 27. The smaller eastern wedge feature would be an older component of the same wedge formation, forming possibly the previous year or earlier during the ablation season.

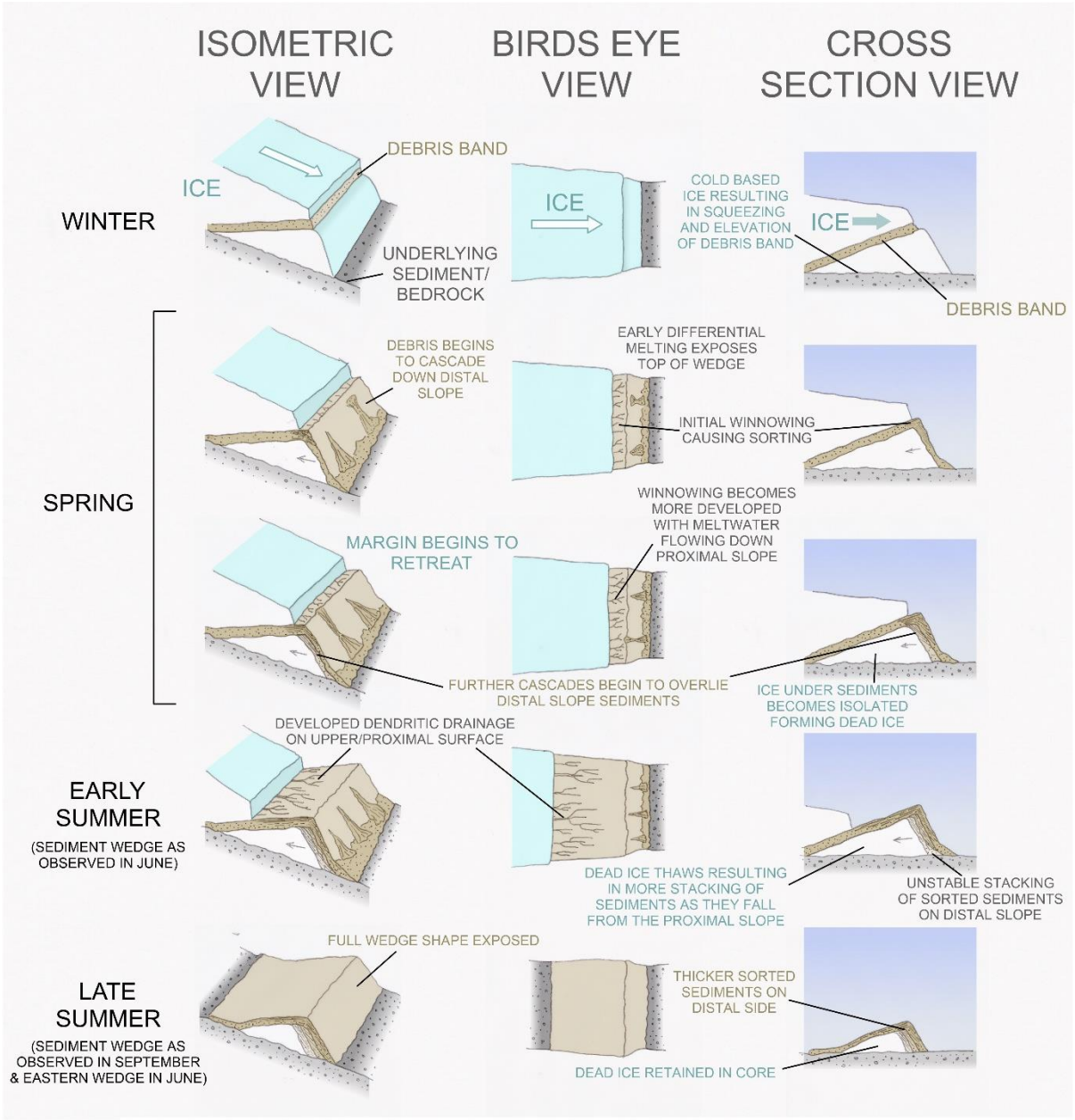

Figure 26 - This shows the hypothesised process forming the sediment wedge features as described above and based on the morphology and sedimentology recorded in the field. The steps relate to the stages discussed in this section.

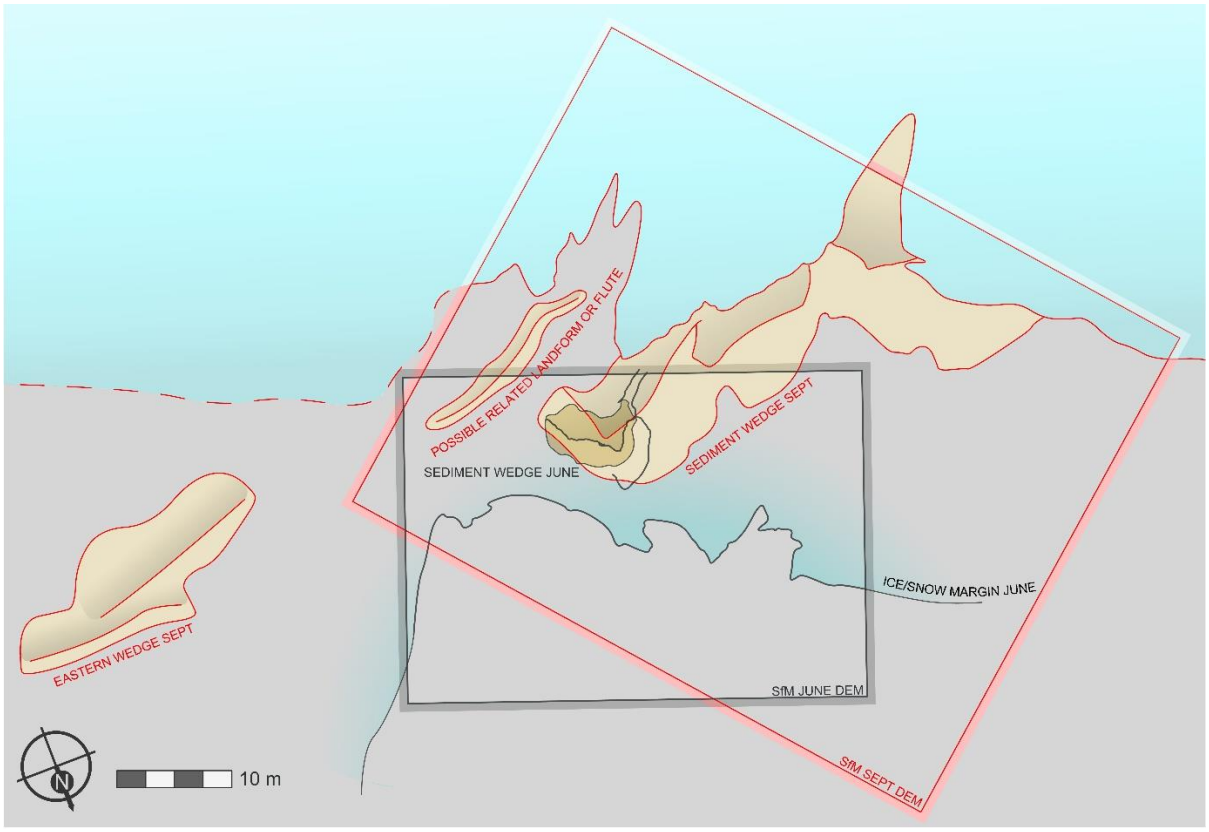

***Figure 27** - This shows a simplified map of the sediment wedges largely based on the SfM DEMs with the eastern wedge added based on GPS data and photographs*

A possible alternative to this configuration, is the smaller landform directly to the south of the main wedge, aligning with the large crevasse-induced embayment in the glacier margin. The landform had the morphology of a flute, however lacked any form of initiation. Its appearance draws similarities with the feature that was the subject of Figure 7a, which was interpreted as a crevasse fill deposit. Were this the case, Figure 27 also appears to show the Eastern Wedge, particularly the southernmost crest, aligning with this smaller ridge. It is therefore also a possibility that the Eastern Wedge formed as part of a crevasse fill rather than in relation to the other wedge features.

The exposure taken into the end of one of the eastern wedges (Fig. 21) revealed finer silts interbedded with coarser sands, aligned parallel to the proximal slope of the landform, very similar in composition to the main wedge, supporting the theory that they are linked in terms of genesis. The eastern wedge was also observed to be underlaid by ice, although this did not form a prominent portion of the landform like the main wedge. The smaller core of ice would also support the idea that the eastern wedge formed an older component of the main wedge, fed by the same debris band emerging from the ice. Its earlier formation would allow the time for the ice core to thaw, possibly causing the faulting and slumping observed on the distal side in the process.

The morphology and sedimentology identified in this study draws parallels with those in Lukas et al. (2005) who identified a similar feature in Svalbard (Fig. 28) describing a 'discrete debris ridge unequivocally associated with an englacial wedge'. The sediments were described as being distinctive from those in the rest of the foreland, comprising of laminated and cross bedded sands. Although cross bedding was not identified in the sediment wedge is this study, faint laminae were observed particularly in View 1, Figure 19. The sediments were also distinctive compared to those of the surrounding foreland, matching the characteristics previously described (Lukas et al., 2005). Lukas et al. (2005) interpreted their sediments as originating from a crevasse-fill formed from supraglacial stream deposits. The band of sediment forms the core of the wedge in the Lukas et al. (2005) study, pointing to a different genesis for the sediment wedge on Blåisen to that outlined by Lukas et al. (2005) above. At Blåisen, there was relatively little supraglacial sediments observed except for those near the margin, so it is unlikely that sediment pathway is the same as that identified in Lukas et al. (2005). A study conducted by Reinardy et al. (2019) at Midtdalsbreen identified very similar features (ice-cored moraines and debris covered dead-ice areas), attributing them to zones of cold-based ice at the margin, supporting the freeze-on mechanism proposed by this study.

***Figure 28** - Comparison between the wedge landform identified in Lukas et al (2005) reproduced here with permission from the author and the wedge from this study.*

In terms of potential sources for the sediment forming the debris band, the debris band recorded at the glacier bed in section 4.3.4 may provide the missing piece of the jigsaw, as it were. The feature was recorded as sediment emerging from the side of a small crevasse in the ice which extended up about 50 cm at 45° before closing to a suture higher up. This is interpreted as a lateral exposure of a debris septum in an early stage of development (Swift et al., 2006). It is proposed that the sediment bands formed sub-glacially, similar to the mechanisms proposed by Swift et al. (2006). In their study investigating the debris bands forming at Kvíárjökull, Iceland, a model was developed based on earlier studies (Goodsell et al., 2002; Spedding and Evans, 2002). In this model, basal sediments are initially folded due to flow compression as ice decelerates. At Kvíárjökull this is identified as occurring at the base of an icefall; a transverse englacial foliation begins to develop. The continued pressure from the ice deceleration results in diagonal transverse shearing, similar to a reverse fault, which begins to entrain debris up the shear zone. This continues as the ice flows, transferring basal material to the surface. The conditions described at Kvíárjökull draw several similarities with Blåisen. At Blåisen this would be likely to occur after the glacier gradient steepened as it flows from the plateau (Weber et al. 2019), then encountered the area of reverse slope identified at the margin. There is some evidence for this deceleration occurring at Blåisen from the longitudinal or splaying crevasses present (e.g. Figure 6A). These were particularly prevalent in September after the overlying snow had thawed. Longitudinal crevasses occur when the ice is compressed, however may also occur when the ice spreads out at the margin. Although the exact origin of the particular sediments forming the wedges cannot be identified, the exposure of the debris band at the glacier bed in section 4.3.4 illustrates the early stage of the Swift et al. (2006) model, providing a possible mechanism for how these sediment bands may have formed. The undulating bedrock topography provides the environment for a range of sorted sediments to collect, forming a mixed patchwork of sediments under the ice as has been recorded at Midtdalsbreen (Killingbeck et al., 2019). It is therefore plausible that sands and gravels from an idiosyncratic area of the ice bed could have been entrained into a debris band of sediments differing to those found on the wider foreland.

5.1.2. Minor moraines

Minor moraines were one of the most frequently observed landforms in the foreland of Blåisen, mapped in both June and September (Fig. 24, 25). As no sedimentological work was performed, mechanisms for their formation is constrained to the geomorphological evidence and existing literature. Existing studies have described a variety of methods for the formation of minor moraines forming different conditions; these have been summarised by Wyshnytzky (2017), who synthesised 35 different studies, covering 41 separate areas. Since the paper by Wyshnytzky, only one paper studying minor moraines has been published (Chandler et al., 2020), therefore this study will largely use Wyshnytzky's synthesis to compare observations while accounting for the more recent publication.

The most common mechanism of formation was found to be pushing and bulldozing (Christiansen, 1956; Hewitt, 1967; Worsley, 1974; Sharp, 1984; Ono, 1985; Evans et al., 1999a; Evans et al., 1999b; Ham and Attig, 2001; Evans and Twigg, 2002; Beedle et al., 2009; Winkler and Matthews, 2010; Lukas, 2012; Bradwell et al., 2013; Chandler et al., 2016a; Chandler et al. 2016b). This occurs when a glacier temporarily readvances over proglacial sediments, briefly interrupting a period of sustained retreat. This forms ridges typically composed of either subglacial traction till previously deposited by the glacier during retreat (e.g. Ham and Attig, 2001; Bradwell et al., 2013; Chandler et al., 2016a); proglacial material (e.g. Winkler and Matthews, 2010; Bradwell et al., 2013); glaciofluvial sediments (e.g. Lukas, 2012; Bradwell et al., 2013); or a combination of the three (Ham and Attig, 2001). There is little direct evidence to support this as a mechanism at Blåisen largely due to absence of sedimentological data. A small ridge was

observed within one of the ice caves (Fig. 23B), formed parallel to the ice contact with the sediment at the side of the cave and sub-parallel to ice flow direction. The highly saturated sediments found in the ice cave and along the margin (Figure 22B, F) would be easily deformable so it is conceivable that under a glacial advance during the accumulation season these could be bulldozed into ridges. The pushing mechanism has been noted in several instances in conjunction with a reverse bedrock slope (Lukas, 2012; Bradwell et al., 2013), a prominent feature of the Blåisen foreland, contributing to the saturation of sediments, so supporting this theory as a possible mechanism for the formation of the minor moraines at Blåisen.

Another mechanism arising in the literature is freeze-on of subglacial sediments (Andersen and Sollid, 1971; Krüger, 1993; Matthews et al., 1995; Ham and Attig, 2001; Evans and Hiemstra 2005; Winkler and Matthews, 2010; Lukas, 2012; Reinardy et al., 2013; Hiemstra et al., 2015; Chandler et al., 2016a; Chandler et al. 2016b). This mechanism occurs when sediments underlying the ice freeze to the glacier and are carried forward often as a 'till slab' when the ice advances (Krüger, 1995; Hiemstra et al., 2015), forming a ridge as the glacier retreats. It is notable that this process has frequently been described in Norway (Matthews et al., 1995; Winkler and Matthews, 2010; Hiemstra et al., 2015) and specifically at Midtdalsbreen, the glacier to the north of Blåsen (Andersen and Sollid, 1971; Reinardy et al., 2013). A common observation often described in association with this process is the presence of a thin ice margin, which is required to allow the freezing front to infiltrate the underlying sediments (Krüger, 1995; Ham and Attig, 2001; Lukas, 2012; Reinardy et al., 2013; Chandler et al., 2016a) and the existence of a reverse bedrock slope. Both features were observed at Blåisen; the thin margin was prominent particularly around the snowbank ridges (Fig. 17), and as already discussed a reverse slope was present across much of the margin. The two factors are also linked in that the reverse slope has the effect of trapping the meltwater against the margin, often requiring drainage back under the ice or through the subglacial sediment, as was observed in the ice caves (Fig. 23). This contributes to the thinning of the ice margin and ensures the sediment is saturated allowing it to be easily frozen-on in winter (Chandler et al., 2016a). A reverse bedrock slope under some of the most prominent moraines was noted by Andersen and Sollid (1971) in the foreland of Midtdalsbreen, further supporting that such processes may occur on Blåisen.

Another method of minor moraine formation is shearing and/or thrusting of basal till occurring when a portion of sediment at the margin becomes detached under glacial advance and in transported a short distance and dumped to form a ridge (Krüger et al, 2010). This process has been recorded in Iceland but not on mountain glaciers in Norway (Sharp, 1984; Schomacker et al., 2012). No evidence was recorded to support this mechanism on Blåisen, but without sedimentological evidence this method cannot be excluded entirely.

Squeezing as a minor moraine formation mechanism occurs when the sediment underlying the glacier deforms under the weight of the ice and is extruded at the terminus. Frequently occurring in conjunction with pushing and bulldozing mechanisms during glacier advances, this forms small ridges which are preserved when the glacier retreats (Worsley, 1974; Sharp, 1984; Bradwell, 2004; Chandler et al., 2016a). Squeezing has been most widely reported in Iceland (Price, 1970; Sharp, 1984; Evans and Twigg, 2002; Bradwell, 2004; Chandler et al., 2016a, Chandler et al., 2020) with only one example studied in Norway (Worsley, 1974). The squeezing mechanism is closely associated with the presence of bedrock reverse slopes (Chandler et al., 2016a; Price, 1970). As the bedrock is impermeable and the reverse slope prevents surface runoff; Chandler et al. (2016a) notes how meltwater is forced to accumulate at the ice margin, resulting in highly saturated subglacial sediments that are more liable to deformation and squeezing. Similar to the bulldozing and freeze-on mechanisms, conditions on Blåisen, notably the reverse slope and saturated sediments around the margin, would support this as a possible theory.

The presence of flutes, particularly in September (Fig. 25), were often observed in close association with the minor moraines (e.g. Fig. 12A) may also support this mechanism. There has been a wealth of papers discussing the formation of flutes (Boulton, 1976; Benn, 1994; Gordon et al., 1992; Eklund and Hart, 1996; Schoof and Clarke, 2008; Evans et al., 2009; Roberson et al., 2011; Hart et al., 2018). The general model is that flutes form when an object, often a boulder or bedrock outcrop, obstructs ice flow causing a cavity to form in its lee (Boulton, 1976; Benn, 1994; Eklund and Hart, 1996). Deforming under the pressure, underlying sediments are forced up into the cavity, similar to the squeezing mechanism of minor moraines. Fluting can then evolve from two mechanisms; through sediments and water refreezing to the ice due to the drop in pressure in a cold-based glacier, being carried down glacier (Gordon et al., 1992; Roberson et al., 2011). The second mechanism is by the cavity migrating down glacier as it is filled with the sediment remaining unfrozen, occurring in a warm-based glacier (Boulton, 1976; Benn, 1994; Eklund and Hart, 1996). In reality, flute formation has shown to be often more complex, and a combination of the two mechanisms (Roberson et al., 2011). Flute development has been shown to vary depending on conditions other than whether the glacier is cold or warm based. For example, the influence of ice velocity (Evans and Rea,

2003; Hart et al., 2018), with the implication being that faster ice flow results in longer flutes with more regular cross section size along their length. Another factor is the size of the initiation obstacle affecting the development with a continuum between flutes and larger mega-scale glacier lineations and rock-cored drumlins (Hart et al., 2018). Till saturation is also discussed as an important factor in allowing the deformation of the sediments under varying pore water pressure, which itself is influenced by the presence of obstacles such as boulders obstructing flow (Hart et al., 2018).

The plan view of the site 2 SfM model, Figure 12A, illustrates this configuration between the flutes and moraines on Blåisen. It shows that the moraine ridges vary along their length. Rather than the same small ridges observed in the section continuing down the length of the moraine, they dwindle, and are replaced by other small ridges aligned slightly differently but orientated the same as the original ridges. This gives the overall appearance of creased fabric rather than a corrugated morphology which might be expected. This might imply that the force creating the moraine was not applied perpendicularly but rather at a slight angle. It is speculated that the cause for this may be the difference between the dip direction of the bedrock and the flow of the glacier which were at a slight offset. Potential further evidence in support of this is the orientation of the flutes on the proximal side of the moraine best shown in Figure 12A. The flutes meet the line of the moraine at a slightly acute angle, rather than at 90°. This is however making the assumption that the flutes and moraines formed around the same time and not in separate occurrences where the ice was flowing locally in slightly different directions.

The final mechanism for minor moraine formation outlined by Wyshnytzky (2017) is dumping (Winkler and Matthews, 2010; Schomacker et al., 2012). This occurs where sediments are deposited from the ice surface or margin due to gravity and accumulate near the terminus during a period where the margin is stationary (Benn and Evans, 2010). They may be subsequently bulldozed into a push moraine if the glacier readvances (Boulton and Eyles, 1979; Lukas, 2005). At Blåisen the ice surface was almost entirely free of sediment, however in certain locations, sediment was delivered to the ice surface by debris septums. Although it was not observed, sediment cascading down the distal slope of the sediment wedges could plausibly form dump-type minor moraines.

In this section, the possible mechanisms for minor moraine formation on Blåisen are outlined, however without sedimentological evidence to study the internal structure of the moraines in is impossible to draw much in the way of conclusions about how the Blåisen moraines may have formed.

5.1.3. Snowbank squeeze moraines

As noted in the interpretation of the snowbank push moraines in the results (section 4.1.3), the morphology of the snowbank push moraines, closely matches those described by Birnie (1977). Drawing on the sedimentological evidence from the exposure in section 4.3.2, the processes identified in this study also draws similarities to those in Birnie (1977) and Krüger et al. (2010). The proposed formation is as follows, with the steps described illustrated in Figure 29 below.

During the ablation season the margin thins both from the upper surface and its contact with the underlying sediment, possibly accelerated by meltwater pooling at the margin and flowing back into the glacier due to the reverse slope preventing drainage. During the winter, the glacier advances (Figure 29 part:2), from this point two theories were initially devised. It was initially hypothesised that the thin ice may deform or fracture as the ice advances, particularly if pre-existing sutures reopen, due to sediments and thick snow impeding the ice at the margin, a factor that may be exacerbated by the reverse slope. Deforming subglacial sediments are squeezed up into the vacated space by the pressure of the surrounding ice - a process first proposed by Clapperton (1971) - as well as some bulldozing which may occur at the snow margin.

During the early spring, differential melting thaws the deformed area, exposing the ridge forming below. The reduction in pressure around the margin may cause freeze-on by reverse regelation, potentially contributing to delivering sediment to the ridge; this was not observed and is therefore speculation based on the fact that freeze-on was observed to be a prominent process in the formation of other features at Blåisen, namely the nearby Sediment Wedges.

By Late Spring/Early Summer, around the time of the first visit in June, the ridge protrudes above the snow, as depicted in Figure 17. The continued flow of the glacier would have bulldozed the original ‘squeeze’ ridge, destroying any potential structures and increasing the height of the ridge. Sediment spilling onto the surrounding ice would accelerate the melt of the ice due to the albedo effect further contributing to the thinning of the ice around the ridge. By the end of the ablation season, around the time of the second visit in September, the margin has retreated, fully exposing the ridge.

The main issue when considering this model as the mechanism behind the formation of the snowbank push ridge, is the initial deformation of the thin glacial ice. Ice was observed on both sides of the ridge, appearing to curve upwards above the ridge, an observation echoed by Birnie (1977). However. an alternative theory is that the ice on the down glacier side of the ridge was not glacier

ice, but rather formed from compacted partially melted snow or firn from early in the accumulation season that had been forced up by the advancing glacier. This interpretation is supported by the absence of ice crystals in the firn, an indicator that it has not undergone the process that constitutes glacial ice (Cuffey and Paterson, 2010). This model is illustrated in Figure 29 and largely follows the previous hypothesis with the replacement of the down-glacier ice with more deformable snow or fern. The appearance of the upwards curving up-glacier side of the ridge is attributed to the prow-like characteristics of the ice margin found across the foreland, hypothesised to be a function of the reverse slope and high ablation rates during summer months. Other snowbank push moraines have been observed besides those recorded by Birnie (1977). Sharp (1984) noted the occurrence of moraines where the glacier advancing against a marginal snowbank, pushes debris up into a ridge on the distal side of the bank. This push mechanism described by Sharp (1984) is also noted by Birnie (1977) who distinguishes between these 'squeeze' and 'push' processes but refers to the overall mechanism as snowbank push. It is perhaps more accurate then to name these landforms 'snowbank squeeze moraines' in this study rather than push. Some push-type snowbank ridges were observed at Blåisen occurring contemporaneously with the squeeze-type ridges, as shown on the distal side of the snowbank in Figures 29 part:4, however these were much smaller in size (<10 cm) with very poor preservation, so were absent by the time of the September visit. The only other study besides Birnie (1977) to record the squeeze form of the snowbank moraines is Krüger et al (2010) suggesting that this type of moraine is more rarely formed or more poorly preserved so is not commonly recorded.

In terms of preservation, the September fieldwork showed that very little remained of the ridges observed in June. Very low relief ridges were observed in September as shown in Figure 22H in the foreland evolution section. These however were only a few centimetres higher than the surrounding foreland and would have been easily missed had the locations of the snowbank push moraines not been mapped in June. It is likely that the surrounding ice and snow acted to buttress the ridge during the spring, forming unstably steep sided slopes which would rapidly collapse once this support had been removed. The sediments were observed to be highly saturated in June, which would have also contributed to the rapid degradation of the ridge form. A final possible contributor to the poor preservation is the potential for snow and ice incorporation within the moraine during formation. Although this was not observed, it is plausible that during the squeezing and bulldozing processes, lenses of snow and ice could become integrated within the ridge as observed by Sharp (1984) and Gordon and Timmis (1992), exacerbating the deterioration of the moraine during the ablation season. The presence of many larger blocky clasts in the initial ridge (Fig. 17), may be significant in providing the longer-term evidence of the snowbank push moraines. Across the foreland of Blåisen, many minor moraines consisted of small ridges composed of pebbles and larger cobbles, with finer sediments absent, these ridges either sat on a thin layer of sediment or directly onto the bedrock. This study speculates that a proportion of these may be the remains of former snowbank push ridges in areas of the margin with poor sediment supply as illustrated in Figure 29 part:6. During the ablation and deterioration processes, much of the finer sediments would have been washed away, especially in areas with a reverse slope. The water following the route of the steepest gradient would flow parallel to, or along the glacier margin itself before either finding a route away from the margin or, more frequently, flowing back into the glacier through ice caves (Fig. 23A, C & E). Small blocky ridges of this nature have a large number of possible formation mechanisms including bulldozing and dumping (Sharp, 1984; Wyshnytzky, 2017), so without direct observational evidence from consecutive years, tracking the evolution of individual moraines, this theory would be hard to test.

Figure 29 *(Overleaf) - This illustrates the final proposed process as described above with the final panel speculating on the potential for longer term preservation.*

1

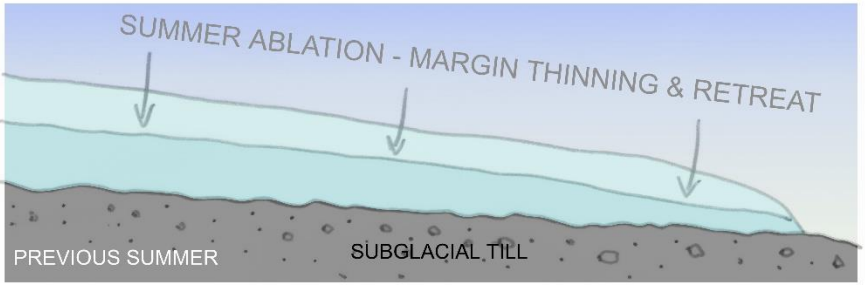
SUMMER ABLATION - MARGIN THINNING & RETREAT
PREVIOUS SUMMER
SUBGLACIAL TILL

2

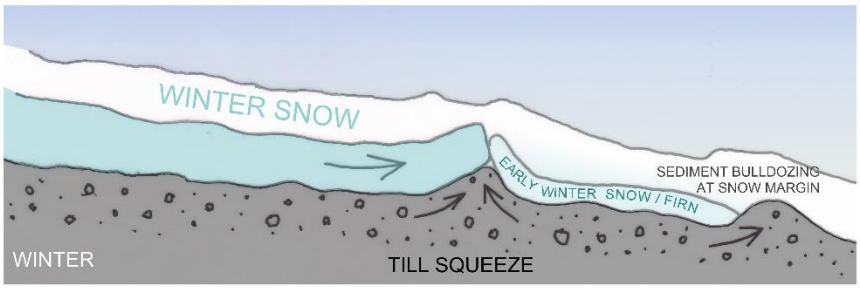
WINTER SNOW
EARLY WINTER SNOW / FIRN
SEDIMENT BULLDOZING AT SNOW MARGIN
WINTER
TILL SQUEEZE

3

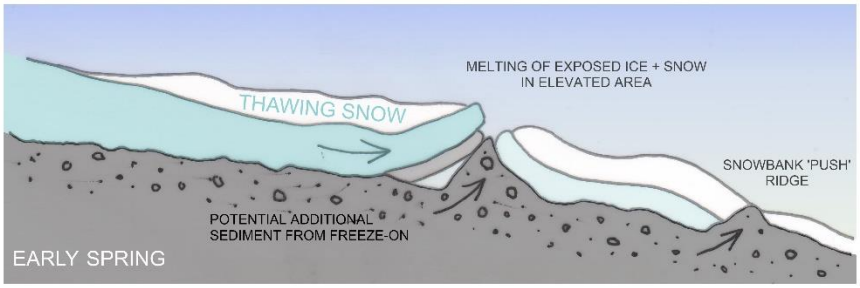
MELTING OF EXPOSED ICE + SNOW IN ELEVATED AREA
THAWING SNOW
SNOWBANK 'PUSH' RIDGE
POTENTIAL ADDITIONAL SEDIMENT FROM FREEZE-ON
EARLY SPRING

4

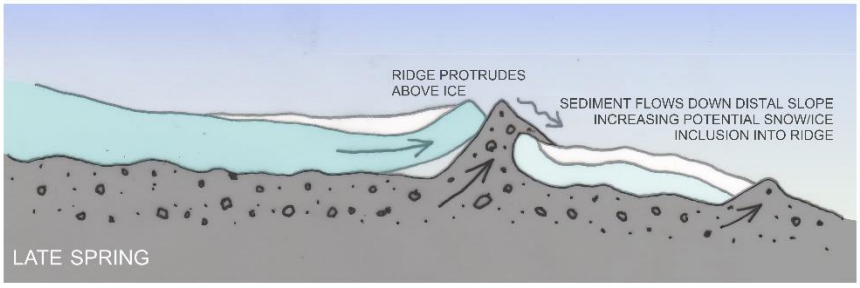
RIDGE PROTRUDES ABOVE ICE
SEDIMENT FLOWS DOWN DISTAL SLOPE INCREASING POTENTIAL SNOW/ICE INCLUSION INTO RIDGE
LATE SPRING

5

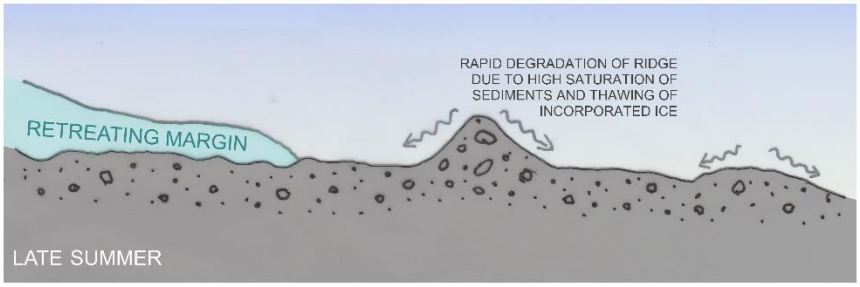
RAPID DEGRADATION OF RIDGE DUE TO HIGH SATURATION OF SEDIMENTS AND THAWING OF INCORPORATED ICE
RETREATING MARGIN
LATE SUMMER

6

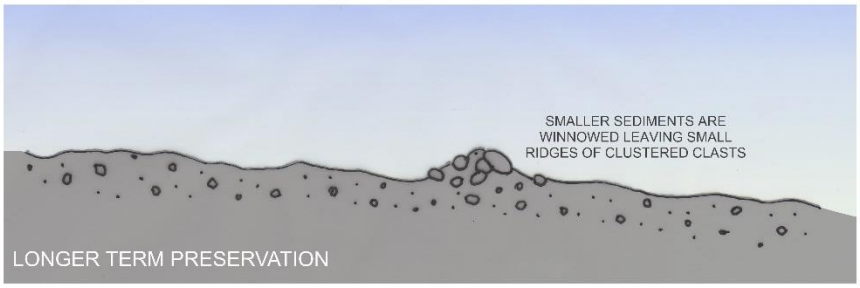
SMALLER SEDIMENTS ARE WINNOWED LEAVING SMALL RIDGES OF CLUSTERED CLASTS
LONGER TERM PRESERVATION

5.2. Landform Assemblages and Landsystems

In this study and the wider literature, there are several governing characteristics that influence the production of landforms for certain areas of the foreland. At Blåisen, this can be broadly condensed down to the availability of sediment at the margin and the bedrock/substratum gradient. Although these two governing factors in turn influence each other, here they are explored in greater detail.

Sediment availability ultimately determines whether a depositional landform can form and also has a strong influence on its size. There are differences in the distribution of sediment in the foreland of Blåisen as illustrated in the geomorphological maps (Fig. 24, 25), by the difference in minor moraine height and the mapped areas of exposed bedrock. Although the latter can also be attributed to cases where bedrock protruded up out of the foreland and the occurrence of small cliffs, frequently the bedrock was exposed on shallow gradient slopes where the sediment covering was very thin or patchy.

This study found that the most prominent mechanism of sediment reaching the margin was likely through debris rich transverse bands or septums which transported material from the ice bed to surface. The sorting and grain size of the sediment cover varied depending on its source area from the glacier bed, although sorting was also found to take place at the margin during deposition (Fig. 26 and accompanying in-text description). No evidence was found of sediment in any significant volume being transported proglacially, making the debris bands process the most likely sediment delivery mechanism operating on Blåisen. Therefore, a prominent influence affecting the sediment quantity at the margin was the ice bed conditions and the amounts of sediment at the base of the ice. Investigations on Midtdalsbreen found a varied ice bed mosaic of bedrock and sediments (Killingbeck et al., 2019) supporting the idea that a similar configuration would exist under Blåisen. Although this was not investigated by this study, it is possible to predict that areas of greater sediment at the margins were likely fed by areas of thicker basal sediments possibly from areas surrounding subglacial streams and rivers or localised topographic lows where sediment had been allowed to accumulate.

Ice bed gradient and drainage appears to be the second overarching factor that governs landform distribution on Blåisen. Its influence has already been touched upon for the local glacier bed topography in the sediment availability section above. Beyond this, the gradient of the bedrock at the margin appeared to have a strong influence on the landforms, particularly where reverse slopes were observed. Reverse slopes were common across the margin and were observed at both SfM sites, particularly site two. The main effect of the reverse slope was to inhibit meltwater drainage away from the margin forcing it to collect and flow along the margin or even back through the glacier. This forced the meltwater to effectively drain through a limited number of confined channels. During the summer of 2019, this was through a gully in the central foreland, identified as the main meltwater portal ([5] in Fig. 1a) and depicted in Figure 22C & D. However, there were several smaller incisions through the bedrock where misfit streams were observed to the south of the main portal (Fig. 24 & 25), which possibly point to them as relict drainage channels.

At the margin, the pooling of meltwater has several effects, firstly it contributes to the sorting of sediments, allowing finer sediments to be deposited (Fig. 23). Secondly, the presence of water at the margin would accelerate the basal melting of the marginal ice, resulting in the creation of the 'boat's prow' configuration and ice caves observed in September. This thin ice margin has been attributed to aiding the freeze-on process in winter across other studies (Krüger, 1995; Ham and Attig, 2001; Lukas, 2012; Chandler et al., 2016a) and on neighbouring Midtdalsbreen where a reverse slope was also recorded (Andersen and Sollid, 1971; Reinardy et al., 2013). The final effect of the meltwater being trapped at the margin, is the creation of saturated sediments. While this aids freeze-on in the winter (Chandler et al., 2016a; Reinardy et al., 2019), it also makes the sediments highly deformable in the summer. This plasticity facilitates the formation of the snowbank squeeze moraines and flutes observed at Blåisen, the latter of which were largely confined to areas with reverse slopes, supporting this link.

The high sediment saturation may also have a strong influence on the preservation of the landforms. This investigation has already discussed how ice-cored features such as the sediment wedge may deteriorate rapidly as the underlying ice thaws (section 5.1.1) and touched on the detrimental impact the saturated sediments forming the snowbank push ridges had on their preservation. This is evident in the foreland evolution photos where a wide, low-amplitude ridge represents the only evidence of the snowbank push ridges in September (Fig. 22H). Another example of the rapid deterioration of landforms composed of the highly saturated sediment is the flute identified in Figure 23D. Closest to the ice the ridge is 'fresh looking' with sharp, clearly distinguishable sides. However, by just over a metre from the margin the form is much less clear. The sides are slumped, and large cracks are visible over the surface. The poor preservation of landforms with saturated sediments may explain why relatively few flutes were observed in June, the majority being found in September

in the areas vacated by the snow and ice. After being exposed, many flutes in the foreland of Blåisen may only last a few months before becoming indistinguishable from the surrounding sediments.

5.3. Discussion of limitations and further research

It is important to consider the limitations to this investigation and the errors encountered when discussing the results. Primarily among these is the margin of error around the GPS as it provided the framework from which the rest of the data is based on. The average accuracy of the GPS unit used had ~3 m error which for mapping very small features was a drawback. However, the waypoints used to map the landforms were marked out in quick succession meaning that the error would have been relatively consistent and so was less important than the precision, which would control how a point taken would relate to the surrounding waypoints that had just been taken. If there was greater duration between waypoints, this would mean that the satellites would have longer to change position, thus decreasing the precision and increasing the error. The issue was compounded by the lack of recent satellite or aerial imagery that could have been used to cross reference the GPS data against.

The error was an especially important consideration for scaling and aligning the SfM models as a small error between GPS points could be perpetuated into the 3D models and impact on how well two models from the same site could be aligned. This is exacerbated by the greater error associated with elevation, the z coordinate. For Site 1, the large change in the margin combined with this error made it difficult to align the models. The models were aligned manually by estimates and matching some of the landforms to produce Figure 16, but the elevations could not be accurately matched due to the extent of change, so the differencing of the DEMs could not be performed.

The poor weather was a significant hinderance during the September fieldwork which reduced time in the field from a planned four full days, down to two and a half short days. While efforts were made to mitigate the impact this had on the overall investigation by prioritising certain elements of the fieldwork - namely the GPS data and SfM data collection - other elements were slightly compromised, mainly field photos and notes, and the recording of landform sections. Field photos and notes accompanying the GPS data were used to support the interpretation of the geomorphology recorded by GPS. The conditions made the coverage of photos and notes more sparse, adding an element of uncertainty to the interpretations made from the September data. The recording of sections in September had to be completely forfeited, which is a further drawback as these would have been valuable to compare how the structures of landforms such as the sediment wedge had developed over the ablation season. Particularly in the case of the sediment wedge, this may have helped identify the role that the dead ice, recorded underlying the sediments in June, had changed and how this was impacting on the preservation of the landform's morphology. The weather also impacted on the quality of the SfM models. Close examination of the models shows small blurred patches, particularly on Site 1's model, Figure 10, which was due to water droplets on the camera lens resulting in the blurring of some of the source photos. While this has mainly affected the quality of the coloured texturing, it had a greater impact on the margins of the model where the terrain was captured by fewer photos, resulting in an increase in the frayed appearance that is present on most of the models, but is particularly prevalent for Site 1 in September.

Another consideration is how effective the method of using GPS to map in the field is, compared to other methods such as remote sensing or a hybrid of the two. The perspective from the ground, while granting the advantage of being able to view the landforms in very high detail to map more obscure, smaller features and view them from different angles, has the drawback of lacking the perspective that remote sensing allows. How different landforms relate to one another and larger features can sometime be too subtle to be recorded while in amongst the topography, so may be missed. The foreland was so dynamic, changing by the day in June, that areas mapped early in the fieldwork had changed by the time an adjacent area was mapped; this particularly applied to the position of the snow at the margin. The snow and glacier margin was mapped on the first day of fieldwork in June but had retreated, revealing new landforms by the final day in the field, giving the impression in the GPS data that more landforms lay within the snow than the few outlined in section 4.1.3. The use of aerial imagery, essentially creating a snapshot of the foreland, would avoid these issues.

The differences between the GPS mapping and the true foreland are apparent when comparing the geomorphological map to the SfM sites which gave a more true representation of the complexity of the different landforms. With the GPS mapping, details such as the height and width of the landforms, i.e, flutes and moraines etc, are largely lost when only the crests are mapped. This presents a major limitation with identifying the variety of forms within landform families. This study, reliant only on the GPS data, can only present these landforms as relatively uniform whereas the SfM shows there was huge variety.

The main problem with using existing aerial imagery instead of, or in addition to mapping in the field, is that it

is dependent on the data that the imagery was taken as outlined in the methods. In a study that is time dependent, investigating changes across the ablation season, it would not have been possible to use such imagery, which would have already been out of date by the time of the fieldtrip. A possible solution to marry the use of aerial imagery and fieldwork would have been to use a drone to collect the imagery during the fieldtrip. This would also have opened up the possibility to perform SfM modelling beyond the two small sites, across the whole foreland as has been performed in numerous other investigations (e.g. Chandler et al., 2016a; Evans et al., 2016a; Ely et al., 2017; Allaart et al., 2018; Chandler et al., 2018; Ewertowski et al., 2019). This would have provided a very powerful tool for both geomorphological mapping and investigating the changes from June to September.

This leads onto the possible avenues for further research on Blåisen; as this study has demonstrated, the foreland of Blåisen is complex and raises several points which would require more investigation, some of which have already been touched upon in the discussion above. A weakness of this study is its lack of in-depth sedimentological data to support the geomorphological work carried out. This is particularly acute when considering the variations in which minor moraines may form on Blåisen. The preservation of snowbank squeeze ridges was also raised as an alternative mechanism, however a much more widescale and detailed sedimentological investigation would have to be carried out to determine this.

Linked to the questions arising from the longer-term preservation, it would be extremely valuable to be able to investigate the evolution of landforms beyond one ablation season. Particularly by comparing the developments at the same time of year, June and September, over successive years would allow for both a more accurate gauge of how the margin is changing without snow masking the 'true' ice position, and whether the summer of 2019 was a typical year for the glacier in terms of retreat and landform formation. The question of how representative the ablation season in 2019 was is also an important consideration. July 2019 saw a very strong heatwave that set temperature records across Europe including Norway (World Meteorological Organization, 2019). This followed a similarly severe heatwave in 2018 (Yiou et al., 2020) raising the possibility that the conditions at Blåisen were exceptional. Therefore, the active landforms that developed during the duration of this study may not be representative analogues of the older landforms in the foreland, even if they may have only formed a few years earlier. A more extensive study over several years would therefore help answer these uncertainties.

6. Conclusions

This study has presented detailed geomorphological process observations and mapping for Blåisen, Hardangerjøkulen in Norway. In this section, the key findings of this study are summarised and the original aims are reviewed.

6.1. Mapping and Field Observations

Geomorphological mapping was undertaken in the foreland of Blåisen in June and September 2019, the ice margin and ridge crests were marked using GPS, while other observations in photo and note form were made on each visit. The mapping of the margin in June included the bank of snow that lay in front of the glacier, as it was impossible to distinguish the exact ice margin position under the snow. The margin retreated by 20-30 m on average but up to 40-50 m in the depression around the main meltwater portal.

The landforms mapped in June, with the exception of those immediately next to the margin, changed little over the ablation season. The retreat revealed multiple sets of minor moraines and flutes. It was initially thought that the landforms at the margin in June were the 'active' landforms from that season, however the mapping of up to ten individual minor moraines on the proximal side of the June ice marginal position disproved this theory.

6.2. Structure from Motion

Structure from Motion (SFM) modelling was implemented at two sites selected to study landform evolution over the ablation season. One site focused on the large sediment wedge recorded in the northeast of the foreland, the other recorded the changes at a section of foreland with a prominent multi-crested minor moraine and reverse bedrock slope. Four 3D models were generated, one from each site in June and September. The initial aim was to perform DEM differencing to quantify the changes in the sites, for example capture the deterioration of ice cored landforms as the ice thawed. The poor weather conditions in September meant that the site one model (of the sediment wedge) was not of sufficient quality to align with its corresponding model from June due to water droplets on the camera lens. The site two DEM models were differenced however as already discussed with the mapping (Section 6.1) little changed in the existing landforms; new landforms were

revealed that had previously been under the snow or ice, including a large number of flutes. Despite the differencing showing relatively little, the 3D SFM models proved instrumental in helping to interpret the processes occurring both in the formation of the landforms and document how they evolved over the melt season, particularly around the complex sediment wedge featured in site 1.

6.3. Landform Genesis and Evolution Models

Referencing the existing literature and field observations, several landform geneses models have been made focusing on the sediment wedge and a snowbank squeeze moraine in particular.

Sediment Wedge: The sediment wedge, so called because of its idiosyncratic shape, was lithologically distinct from the rest of the foreland, composed of sorted sands and gravel beds overlying dead ice. As the name suggests, the feature was wedge shaped with a steeper distal slope formed as sediment brought up in a debris band at the margin and deposited on the proximal slope, slumped down the distal slope as the underlying dead ice thawed. Another wedge shaped feature, nearby to the east of the large wedge, was proposed to have a shared genesis process and presents an older more poorly preserved part of a more extensive ice-cored landform as the debris band was gradually exposed at the margin.

Snowbank Squeeze Moraines: In this study, we present evidence of snowbank squeeze moraines, formed by the compression of deforming sediments between the ice margin and snowbank, a process that is not widely documented in the exiting research. These landforms were observed at the margin in June, but little evidence remained of them in September other than an inconspicuous, low profile ridge.

6.4. Landform Preservation

The repeat visits to the foreland of Blåisen allowed this study to observe the preservation of various ice marginal landforms and how they evolved over the ablation season. This has helped to identify several key factors that influenced preservation, prominent amongst these is the degree of saturation of the sediments that compose the landforms. The snowbank squeeze moraines and flutes in particular require deformable sediments and were found predominantly in areas of reverse bedrock slopes where the gradient prevented drainage of meltwater, forming highly saturated sediments. Few flutes were recorded aside from those mapped in September, indicating that either in past seasons, conditions had not been favourable for formation, or that preservation was poor. The latter is supported by the lack of remaining evidence of the snowbank squeeze ridges in September.

6.5. Further Research

Methodologically, this study follows a relatively standard field mapping procedure, however SFM was used on selected sites to generate 3D models, adding to the growing body of literature on this topic and highlighting the vast potential and versatility of this type of technology. This study also highlights the continued value of field-based studies as standalone investigations or in conjunction with remote sensing. Across many science disciplines, there is an element of technological determinism: using more technologically advanced methods because they exist, when they are not necessarily the best method to use. Remote sensing for glacial geomorphological investigating is a very powerful tool, particularly for use over wider areas that would be impractical in the field. However, it is constrained by the quality and frequency of the images covering a given site, therefore more subtle landforms that do not exist for long periods may be missed entirely. This study has hopefully shown that there is still great value in continuing to use ground-based investigations separately or in tandem with other methods such as SFM or remote sensing.

Overall, this study has demonstrated the value of smaller, ‘shorter-lived’ landforms as part of glacial studies which can give important insights into the glacial behaviour and seasonal changes. This study documents a number of landforms which, particularly in the case of the snowbank squeeze moraines have not been widely studied in existing research. The absence of evidence for the snowbank squeeze ridges in September and the low number of flutes recorded beyond the June margin highlights the poor preservation of these landforms and so how they may easy be missed in other geomorphological studies. As already alluded to in section 5.3, further research is needed to broaden what is known about these landforms with poorer preservation. This study documents one ablation season on one glacier, expanding this type of study over a greater number of glaciers in different years would help establish a more comprehensive catalogue of this type of landforms. It would also help verify if the processes occurring at Blåisen in 2019 are ‘typical’ of an ablation season or a product of the summer of record-breaking temperatures that was experienced that year. As this shows, this study raises a range of questions, more than it answers, so it is hoped that this investigation will stimulate further research of this nature into these glacial landforms with poorer preservation

.

Acknowledgements

I would like to firstly thank my supervisor, Sven Lukas, for his guidance and help on all things glacial, both in the field, and throughout the writing process. Sven, with the help of Lena Uldal Hansen, organised both the fieldtrips and along with Mateusz Zawadzki accompanied me on both occasions; we also enjoyed the company of Benedict Reinardy and Hannah Watts from Stockholm University in June, many thanks to them all. GPS units were borrowed from the Lund Geography Department and Helena Alexanderson for the fieldwork mapping, I would like to thank them for their assistance as well as the wider Lund Geology department for a fantastic two years of education in Sweden.

I would like to thank my family for their support and particularly my partner, Natalie. Without her, this work would not have been possible (or at the very least contain many more spelling and grammatical errors); thanks for putting up with me and wading through this document to correct my butchery of English spellings.

Lastly, I would like to thank my coursemates, I have made some great friends during my time in Sweden; their continued cheer, enthusiasm and good humour has made that time very enjoyable and kept me motivated over the thesis period.

References

Abram, N., Gattuso, J.P., Prakash, A., Cheng, L., Chidichimo, M.P., Crate, S., Enomoto, H., Garschagen, M., Gruber, N., Harper, S. and Holland, E., 2019. Framing and Context of the Report. In IPCC Special Report on the Ocean and Cryosphere in a Changing Climate. [Pörtner, H.O., Roberts, D.C., Masson-Delmotte, V., Zhai, P., Tignor, M., Poloczanska, E., Mintenbeck, K., Alegría, A., Nicolai, M., Okem, A., Petzold, J., Rama, B., Weyer N.M. (eds.)]. In press.

Agisoft LLC (2019) Agisoft Metashape Version 1.6.2 (Software) Retrieved from http://www.agisoft.com/downloads/installer/

Åkesson, H.M., 2014. Simulating the climatic response of Hardangerjøkulen in southern Norway since the Little Ice Age. Master's thesis, Department of Earth Science Faculty of Mathematics and Natural Sciences, University of Bergen.

Åkesson, H., Nisancioglu, K.H. and Morlighem, M., 2017. Simulating the evolution of Hardangerjøkulen ice cap in southern Norway since the mid-Holocene and its sensitivity to climate change. Deglaciation of the Norwegian fjords. The Cryosphere, 11, pp.281–302

Allaart, L., Friis, N., Ingólfsson, Ó., Håkansson, L., Noormets, R., Farnsworth, W.R., Mertes, J. and Schomacker, A., 2018. Drumlins in the Nordenskiöldbreen forefield, Svalbard. Gff, 140(2), pp.170-188.

Allison, M. and Kepple, E., 2001. Modern sediment supply to the lower delta plain of the Ganges-Brahmaputra River in Bangladesh. Geo-Marine Letters, 21(2), pp.66-74.

Andersen, J.L. and Sollid, J.L., 1971. Glacial chronology and glacial geomorphology in the marginal zones of the glaciers, Midtdalsbreen and Nigardsbreen, south Norway. Norsk Geografisk Tidsskrift-Norwegian Journal of Geography, 25(1), pp.1-38.

Andreassen, L.M., Elvehøy, H., Kjøllmoen, B., Engeset, R.V. and Haakensen, N., 2005. Glacier mass-balance and length variation in Norway. Annals of Glaciology, 42, pp.317-325.

Andreassen, L.M., Winsvold, S.H., Paul, F. and Hausberg, J.E., 2012. Inventory of Norwegian glaciers, Report, 38. Oslo: Norwegian Water Resources and Energy Directorate.

Beedle, M.J., Menounos, B., Luckman, B.H. and Wheate, R., 2009. Annual push moraines as climate proxy. Geophysical Research Letters, 36(20).

Bendle, J.M., Thorndycraft, V.R. and Palmer, A.P., 2017. The glacial geomorphology of the Lago Buenos Aires and Lago Pueyrredón ice lobes of central Patagonia. Journal of Maps, 13(2), pp.654-673.

Benn, D.I., 1994. Fluted moraine formation and till genesis below a temperate valley glacier: Slettmarkbreen, Jotunheimen, southern Norway. Sedimentology, 41(2), pp.279-292.

Benn, D.I. and Ballantyne, C.K., 1994. Reconstructing the transport history of glacigenic sediments: a new approach based on the co-variance of clast form indices. Sedimentary Geology, 91(1-4), pp.215-227.

Benn, D.I. and Ballantyne, C.K., 2005. Palaeoclimatic reconstruction from Loch Lomond readvance glaciers in the west Drumochter Hills, Scotland. Journal of Quaternary Science, 20(6), pp.577-592.

Benn, D.I. and Evans, D.J.A., 2010. Glaciers and Glaciation. Hodder Education. London, UK, 802.

Bennett, G.L., Evans, D.J., Carbonneau, P. and Twigg, D.R., 2010. Evolution of a debris-charged glacier landsystem, Kviárjökull, Iceland. Journal of Maps, 6(1), pp.40-67.

Bennett, M.R., and Glasser, N.F., 2009, Glacial Geology: Ice Sheets and Landforms: Chicester, John Wiley & Sons, Ltd, 385 p.

Bennett, M.R., Huddart, D., Glasser, N.F. and Hambrey, M.J., 2000. Resedimentation of debris on an ice-cored lateral moraine in the high-Arctic (Kongsvegen, Svalbard). Geomorphology, 35(1-2), pp.21-40.

Birnie, R.V., 1977. A snow-bank push mechanism for the formation of some "annual" moraine ridges. Journal of Glaciology, 18(78), pp.77-85.

Bishop, M.P., Bonk, R., Kamp Jr, U. and Shroder Jr, J.F., 2001. Terrain analysis and data modeling for alpine glacier mapping. Polar Geography, 25(3), pp.182-201.

Bishop, M.P., Olsenholler, J.A., Shroder, J.F., Barry, R.G., Raup, B.H., Bush, A.B., Copland, L., Dwyer, J.L., Fountain, A.G., Haeberli, W. and Kääb, A., 2004. Global Land Ice Measurements from Space (GLIMS): remote sensing and GIS investigations of the Earth's cryosphere. Geocarto International, 19(2), pp.57-84.

Borisov, D., Hiesinger, H., Reiss, D., Hauber, E. and Scholten, F., 2017. Degradation and daily backwasting rate of an ice-cored lateral moraine in Kongsfjorden, Svalbard. In EGU General Assembly Conference Abstracts (Vol. 19, p. 17263).

Boulton, G.S., 1976. The origin of glacially fluted surfaces-observations and theory. Journal of Glaciology, 17(76), pp.287-309.

Boulton, G.S., 1978. Boulder shapes and grain-size distributions of debris as indicators of transport paths through a glacier and till genesis. Sedimentology, 25(6), pp.773-799.

Boulton, G.S., 1986. Push-moraines and glacier-contact fans in marine and terrestrial environments. Sedimentology, 33(5), pp.677-698.

Boulton, G.S. and Eyles, N., 1979. Sedimentation by valley glaciers: a model and genetic classification. In Schlucher, C. (ed), Moraines and Varves, Balkema, Rotterdam, pp.11-23.

Box, J.E., Fettweis, X., Stroeve, J.C., Tedesco, M., Hall, D.K. and Steffen, K., 2012. Greenland ice sheet albedo feedback: thermodynamics and atmospheric drivers.

Bradwell, T., 2004. Annual moraines and summer temperatures at Lambatungnajökull, Iceland. Arctic, Antarctic, and Alpine Research, 36(4), pp.502-508.

Bradwell, T., Sigurđsson, O. and Everest, J., 2013. Recent, very rapid retreat of a temperate glacier in SE I celand. *Boreas*, *42*(4), pp.959-973.

Brozović, N., Burbank, D.W. and Meigs, A.J., 1997. Climatic limits on landscape development in the northwestern Himalaya. Science, 276(5312), pp.571-574.

Brynjólfsson, S., Schomacker, A. and Ingólfsson, Ó., 2014. Geomorphology and the Little Ice Age extent of the Drangajökull ice cap, NW Iceland, with focus on its three surge-type outlets. Geomorphology, 213, pp.292-304.

Burki, V., Larsen, E., Fredin, O. and Nesje, A., 2009. Glacial remobilization cycles as revealed by lateral moraine sediment, Bødalsbreen glacier foreland, western Norway. The Holocene, 19(3), pp.415-426.

Chandler, B.M., Chandler, S.J., Evans, D.J., Ewertowski, M.W., Lovell, H., Roberts, D.H., Schaefer, M. and Tomczyk, A.M., 2020. Sub-annual moraine formation at an active temperate Icelandic glacier. Earth Surface Processes and Landforms. DOI: 10.1002/esp.4835

Chandler, B.M., Evans, D.J., Roberts, D.H., Ewertowski, M. and Clayton, A.I., 2016a. Glacial geomorphology of the Skálafellsjökull foreland, Iceland: A case study of 'annual'moraines. *Journal of Maps*, *12*(5), pp.904-916.

Chandler, B.M., Evans, D.J. and Roberts, D.H., 2016b. Characteristics of recessional moraines at a temperate glacier in SE Iceland: Insights into

patterns, rates and drivers of glacier retreat. Quaternary Science Reviews, 135, pp.171-205.

Chandler, B.M., Lovell, H., Boston, C.M., Lukas, S., Barr, I.D., Benediktsson, Í.Ö., Benn, D.I., Clark, C.D., Darvill, C.M., Evans, D.J. and Ewertowski, M.W., 2018. Glacial geomorphological mapping: A review of approaches and frameworks for best practice. Earth-Science Reviews, 185, pp.806-846.

Chandler, B.M. and Lukas, S., 2017. Reconstruction of Loch Lomond Stadial (Younger Dryas) glaciers on Ben More Coigach, north-west Scotland, and implications for reconstructing palaeoclimate using small ice masses. Journal of Quaternary Science, 32(4), pp.475-492.

Chevallier, P., Pouyaud, B., Suarez, W. and Condom, T., 2011. Climate change threats to environment in the tropical Andes: glaciers and water resources. Regional Environmental Change, 11(1), pp.179-187.

Chiverrell, R.C. and Thomas, G.S., 2010. Extent and timing of the Last Glacial Maximum (LGM) in Britain and Ireland: a review. Journal of Quaternary Science, 25(4), pp.535-549.

Christiansen, E.A., 1964. Glacial geology of the Moose Mountain area, Saskatchewan. Bulletin of Canadian Petroleum Geology, 12(3), pp.770-770.

Clapperton, C.M., 1971. Geomorphology of the Stromness Bay-Cumberland Bay area, South Georgia (Vol. 70). British Antarctic Survey.

Cuffey, K.M. and Paterson, W.S.B., 2010. The physics of glaciers. Academic Press.

Dahl, S.O. and Nesje, A., 1994. Holocene glacier fluctuations at Hardangerjøkulen, central-southern Norway: a high-resolution composite chronology from lacustrine and terrestrial deposits. The Holocene, 4(3), pp.269-277.

Dahl, S.O. and Nesje, A., 1996. A new approach to calculating Holocene winter precipitation by combining glacier equilibrium-line altitudes and pine-tree limits: a case stud from Hardangerjokulen, central southern Norway. The Holocene, 6(4), pp.381-398.

Eichel, J., Draebing, D. and Meyer, N., 2018. From active to stable: Paraglacial transition of Alpine lateral moraine slopes. Land degradation & development, 29(11), pp.4158-4172.

Eklund, A. and Hart, J.K., 1996. Glaciotectonic deformation within a flute from the Isfallsglaciären, Sweden. Journal of Quaternary Science, 11(4), pp.299-310.

Ely, J.C., Graham, C., Barr, I.D., Rea, B.R., Spagnolo, M. and Evans, J., 2017. Using UAV acquired photography and structure from motion techniques for studying glacier landforms: application to the glacial flutes at Isfallsglaciären. Earth Surface Processes and Landforms, 42(6), pp.877-888.

Ewertowski, M.W., Tomczyk, A.M., Evans, D.J., Roberts, D.H. and Ewertowski, W., 2019. Operational framework for rapid, very-high resolution mapping of glacial geomorphology using low-cost unmanned aerial vehicles and structure-from-motion approach. Remote Sensing, 11(1), p.65.

Evans, D.J., Archer, S., and Wilson, D.J.H., 1999a, A comparison of the lichenometric and Schmidt hammer dating techniques based on data from the proglacial areas of some Icelandic glaciers: Quaternary Science Reviews, v. 18, p. 13–41.

Evans, D.J. and Benn, D.I. eds., 2014. A practical guide to the study of glacial sediments. Routledge.

Evans, D.J., Ewertowski, M. and Orton, C., 2016. Fláajökull (north lobe), Iceland: active temperate piedmont lobe glacial landsystem. Journal of Maps, 12(5), pp.777-789.

Evans, D.J. and Hiemstra, J.F., 2005. Till deposition by glacier submarginal, incremental thickening. Earth surface processes and landforms, 30(13), pp.1633-1662.

Evans, D.J., Lemmen, D.S., and Rea, B.R., 1999b, Glacial landsystems of the southwest Laurentide ice sheet: Modern Icelandic analogues: Journal of Quaternary Science, v. 14, p. 673–691.

Evans, D.J., Nelson, C.D. and Webb, C., 2009. An assessment of fluting and “till esker” formation on the foreland of Sandfellsjökull, Iceland. Geomorphology, 114(3), pp.453-465.

Evans, D.J. and Rea, B.R., 1999. Geomorphology and sedimentology of surging glaciers: a land-systems approach. Annals of Glaciology, 28, pp.75-82.

Evans, D.J. and Rea, B.R., 2003. Surging glacier landsystem. In Evans, D.J. (ed.), Glacial Landsystems. Arnold, London (pp. 259-288)

Evans, D.J. and Twigg, D.R., 2002. The active temperate glacial landsystem: a model based on Breiðamerkurjökull and Fjallsjökull, Iceland.

Quaternary science reviews, 21(20-22), pp.2143-2177.

Eyles, N., 1979. Facies of supraglacial sedimentation on Icelandic and Alpine temperate glaciers. Canadian Journal of Earth Sciences, 16(7), pp.1341-1361.

Eyles, N., 1983. The glaciated valley landsystem. In: Eyles, N. (Ed.), Glacial Geology. Pergamon, Oxford, pp. 91e110.

Farrell, K.M., Harris, W.B., Mallinson, D.J., Culver, S.J., Riggs, S.R., Pierson, J., Self-Trail, J.M. and Lautier, J.C., 2012. Standardizing texture and facies codes for a process-based classification of clastic sediment and rock. Journal of Sedimentary Research, 82(6), pp.364-378.

Förstner, W., 1986. A feature-based correspondence algorithm for image matching. International Archives of Photogrammetry and Remote Sensing 26, 150–166

Fu, P., Heyman, J., Hättestrand, C., Stroeven, A.P. and Harbor, J.M., 2012. Glacial geomorphology of the Shaluli Shan area, southeastern Tibetan Plateau. Journal of Maps, 8(1), pp.48-55.

Giesen, R.H., 2009. The ice cap Hardangerjøkulen in the past, present and future climate. Doctoral dissertation, Institute for Marine and Atmospheric research Utrecht (IMAU) Faculty of Science, Department of Physics and Astronomy Utrecht University.

Giesen, R.H. and Oerlemans, J., 2010. Response of the ice cap Hardangerjøkulen in southern Norway to the 20th and 21st century climates. The Cryosphere, 4, pp.191-213.

Glasser, N.F. and Hambrey, M.J., 2001. Styles of sedimentation beneath Svalbard valley glaciers under changing dynamic and thermal regimes. Journal of the Geological Society, 158(4), pp.697-707.

Goodsell, B., Hambrey, M.J. and Glasser, N.F., 2002. Formation of band ogives and associated structures at Bas Glacier d'Arolla, Valais, Switzerland. Journal of Glaciology, 48(161), pp.287-300.

Gordon, J.E. and Timmis, R.J., 1992. Glacier fluctuations on South Georgia during the 1970s and early 1980s. Antarctic Science, 4(2), pp.215-226.

Gordon, J.E., Whalley, W.B., Gellatly, A.F. and Vere, D.M., 1992. The formation of glacial flutes: assessment of models with evidence from Lyngsdalen, North Norway. Quaternary Science Reviews, 11(7-8), pp.709-731.

Ham, N.R. and Attig, J.W., 2001. Minor end moraines of the Wisconsin Valley Lobe, north-central Wisconsin, USA. Boreas, 30(1), pp.31-41.

Hanáček, M., Flašar, J. and Nývlt, D., 2011. Sedimentary petrological characteristics of lateral and frontal moraine and proglacial glaciofluvial sediments of Bertilbreen, Central Svalbard. Czech Polar Reports, 1(1), pp.11-33.

Harris, C. and Bothamley, K., 1984. Englacial deltaic sediments as evidence for basal freezing and marginal shearing, Leirbreen, southern Norway. Journal of Glaciology, 30(104), pp.30-34.

Hart, J.K., Clayton, A.I., Martinez, K. and Robson, B.A., 2018. Erosional and depositional subglacial streamlining processes at Skálafellsjökull, Iceland: an analogue for a new bedform continuum model. Gff, 140(2), pp.153-169.

Hewitt, K., 1967. Ice-front deposition and the seasonal effect: a Himalayan example. Transactions of the Institute of British Geographers, pp.93-106.

Hiemstra, J.F., Matthews, J.A., Evans, D.J., and Owen, G., 2015, Sediment fingerprinting and the mode of formation of singular and composite annual moraine ridges at two glacier margins, Jotunheimen, southern Norway: The Holocene, v. 25, p. 1–14

Hoppe, G. and Schytt, V., 1953. Some observations on fluted moraine surfaces. Geografiska Annaler, 35, 105–115

Hughes, A.L., Clark, C.D. and Jordan, C.J., 2014. Flow-pattern evolution of the last British Ice Sheet. Quaternary Science Reviews, 89, pp.148-168.

IPCC, 2019: Summary for Policymakers. In: IPCC Special Report on the Ocean and Cryosphere in a Changing Climate [H.-O. Pörtner, D.C. Roberts, V. Masson-Delmotte, P. Zhai, M. Tignor, E. Poloczanska, K. Mintenbeck, A. Alegría, M. Nicolai, A. Okem, J. Petzold, B. Rama, N.M. Weyer (eds.)]. In press.

Jain, S., 2014. Streams. In Fundamentals of Physical Geology (pp. 165-210). Springer, New Delhi.

James, M.R. and Robson, S., 2012. Straightforward reconstruction of 3D surfaces and topography with a camera: Accuracy and geoscience

application. Journal of Geophysical Research: Earth Surface, 117(F3).

Jamieson, S.S., Hulton, N.R. and Hagdorn, M., 2008. Modelling landscape evolution under ice sheets. Geomorphology, 97(1-2), pp.91-108.

Kaser, G., 2001. Glacier-climate interaction at low latitudes. Journal of Glaciology, 47(157), pp.195-204.

Kaser, G., Großhauser, M. and Marzeion, B., 2010. Contribution potential of glaciers to water availability in different climate regimes. Proceedings of the National Academy of Sciences, 107(47), pp.20223-20227.

Killingbeck, S.F., Booth, A.D., Livermore, P.W., West, L.J., Reinardy, B.T. and Nesje, A., 2019. Subglacial sediment distribution from constrained seismic inversion, using MuLTI software: examples from Midtdalsbreen, Norway. Annals of Glaciology, 60(79), pp.206-219.

Kirkbride, M.P. and Deline, P., 2013. The formation of supraglacial debris covers by primary dispersal from transverse englacial debris bands. Earth Surface Processes and Landforms, 38(15), pp.1779-1792.

Krüger, J., 1993. Moraine-ridge formation along a stationary ice front in Iceland. Boreas, 22(2), pp.101-109.

Krüger, J., 1995. Origin, chronology and climatological significance of annual-moraine ridges at Myrdalsjökull, Iceland. The Holocene, 5(4), pp.420-427.

Krüger, J., Schomacker, A. and Benediktsson, Í.Ö., 2010. 6 Ice-Marginal Environments: Geomorphic and Structural Genesis of Marginal Moraines at Mýrdalsjökull. Developments in Quaternary Sciences, 13, pp.79-104.

Lukas, S., 2005. A test of the englacial thrusting hypothesis of 'hummocky' moraine formation: case studies from the northwest Highlands, Scotland. Boreas, 34(3), pp.287-307.

Lukas, S., 2012. Processes of annual moraine formation at a temperate alpine valley glacier: insights into glacier dynamics and climatic controls. Boreas, 41(3), pp.463-480.

Lukas, S., Graf, A., Coray, S. and Schlüchter, C., 2012. Genesis, stability and preservation potential of large lateral moraines of Alpine valley glaciers–towards a unifying theory based on Findelengletscher, Switzerland. Quaternary Science Reviews, 38, pp.27-48.

Lukas, S. and Sass, O., 2011. The formation of Alpine lateral moraines inferred from sedimentology and radar reflection patterns: a case study from Gornergletscher, Switzerland. Geological Society, London, Special Publications, 354(1), pp.77-92.

Lukas, S., Nicholson, L.I., Ross, F.H. and Humlum, O., 2005. Formation, meltout processes and landscape alteration of high-Arctic ice-cored moraines—Examples from Nordenskiold Land, central Spitsbergen. Polar Geography, 29(3), pp.157-187.

Małecki, J., Lovell, H., Ewertowski, W., Górski, Ł., Kurczaba, T., Latos, B., Miara, M., Piniarska, D., Płocieniczak, J., Sowada, T. and Spiralski, M., 2018. The glacial landsystem of a tropical glacier: Charquini Sur, Bolivian Andes. Earth surface processes and landforms, 43(12), pp.2584-2602.

Margold, M. and Jansson, K.N., 2011. Glacial geomorphology and glacial lakes of central Transbaikalia, Siberia, Russia. Journal of Maps, 7(1), pp.18-30.

Margold, M., Jansson, K.N., Kleman, J. and Stroeven, A.P., 2011. Glacial meltwater landforms of central British Columbia. Journal of Maps, 7(1).

Margold, M., Stokes, C.R. and Clark, C.D., 2018. Reconciling records of ice streaming and ice margin retreat to produce a palaeogeographic reconstruction of the deglaciation of the Laurentide Ice Sheet. Quaternary science reviews, 189, pp.1-30.

Marzeion, B., Champollion, N., Haeberli, W., Langley, K., Leclercq, P. and Paul, F., 2017. Observation-based estimates of global glacier mass change and its contribution to sea-level change. In Integrative Study of the Mean Sea Level and Its Components (pp. 107-132). Springer, Cham.

Mather, A.E., Mills, S., Stokes, M. and Fyfe, R., 2015. Ten years on: what can Google Earth offer the geoscience community?. Geology Today, 31(6), pp.216-221.

Matthews, J.A., Mccarroll, D. and Shakesby, R.A. 1995, Contemporary terminal-moraine ridge formation at a temperate glacier: Styggedalsbreen, Jotunheimen, southern Norway. Boreas, 24: 129-139. doi:10.1111/j.1502-3885.1995.tb00633.x

Meier, M.F., 1984. Contribution of small glaciers to global sea level. Science, 226(4681), pp.1418-1421.

Meier, M.F., Dyurgerov, M.B., Rick, U.K., O'neel, S., Pfeffer, W.T., Anderson, R.S., Anderson, S.P. and Glazovsky, A.F., 2007. Glaciers dominate eustatic sea-level rise in the 21st century. Science, 317(5841), pp.1064-1067.

Mukherjee, A., Fryar, A.E. and Thomas, W.A., 2009. Geologic, geomorphic and hydrologic framework and evolution of the Bengal basin, India and Bangladesh. Journal of Asian Earth Sciences, 34(3), pp.227-244.

Nesje, A., Bakke, J., Dahl, S.O., Lie, Ø. and Matthews, J.A., 2008. Norwegian mountain glaciers in the past, present and future. Global and Planetary Change, 60(1-2), pp.10-27.

Nesje, A. and Dahl, S.O., 1991. Holocene glacier variations of Blåisen, Hardangerjøkulen, central southern Norway. Quaternary Research, 35(1), pp.25-40.

Nesje, A., Dahl, S.O., Løvlie, R. and Sulebak, J.R., 1994. Holocene glacier activity at the southwestern part of Hardangerjøkulen, central-southern Norway: evidence from lacustrine sediments. The Holocene, 4(4), pp.377-382.

Ono, Y., 1985. Recent fluctuations of the Yala (Dakpatsen) Glacier, Langtang Himal, reconstructed from annual moraine ridges. Zeitschrift for Gletscherkunde und Glazialgeologie, Universitatsverlag Wagner, Innsbruck, 21, pp.251-258

Ottesen, D. and Dowdeswell, J., 2006. Assemblages of submarine landforms produced by tidewater glaciers in Svalbard. Journal of Geophysical Research-Earth Surface, 111, F01016, doi:10.1029/2005JF000330

Pearce, D.M., Mair, D.W., Rea, B.R., Lea, J.M., Schofield, J.E., Kamenos, N. and Schoenrock, K., 2018. The glacial geomorphology of upper Godthåbsfjord (Nuup Kangerlua) in southwest Greenland. Journal of Maps, 14(2), pp.45-55.

Pellikka, P. and Rees, W.G. eds., 2009. Remote sensing of glaciers: techniques for topographic, spatial and thematic mapping of glaciers. CRC Press.

Price, R.J., 1970. Moraines at fjallsjökull, Iceland. Arctic and Alpine Research, 2(1), pp.27-42.

Radić, V. and Hock, R., 2011. Regionally differentiated contribution of mountain glaciers and ice caps to future sea-level rise. Nature Geoscience, 4(2), pp.91-94.

Reinardy, B., Booth, A., Hughes, A., Boston, C., Akesson, H., Bakke, J., Nesje, A., Giesen, R. and Pearce, D., 2019. Pervasive cold ice within a temperate glacier-implications for glacier thermal regimes, sediment transport and foreland geomorphology. The Cryosphere, 13, 827–843

Reinardy, B.T., Leighton, I. and Marx, P.J., 2013. Glacier thermal regime linked to processes of annual moraine formation at Midtdalsbreen, southern Norway. Boreas, 42(4), pp.896-911.

Roberson, S., Hubbard, B., Coulson, H.R. and Boomer, I., 2011. Physical properties and formation of flutes at a polythermal valley glacier: Midre Lovénbreen, Svalbard. Geografiska Annaler: Series A, Physical Geography, 93(2), pp.71-88.

Rose, J., 1989. Glacier stress patterns and sediment transfer associated with the formation of superimposed flutes. Sedimentary geology, 62(2-4), pp.151-176.

Schomacker, A., Benediktsson, Í.Ö., Ingólfsson, Ó., Friis, B., Korsgaard, N.J., Kjær, K.H. and Keiding, J.K., 2012. Late Holocene and modern glacier changes in the marginal zone of Sólheimajökull, South Iceland. Jökull, 62, pp.111-130.

Schoof, C. G., and Clarke, G. K. C. (2008), A model for spiral flows in basal ice and the formation of subglacial flutes based on a Reiner-Rivlin rheology for glacial ice, J. Geophys. Res., 113, B05204, doi:10.1029/2007JB004957.

Sharp, M., 1984. Annual moraine ridges at Skálafellsjökull, south-east Iceland. Journal of Glaciology, 30(104), pp.82-93.

Small, R.J., 1983. Lateral moraines of glacier de Tsidjiore Nouve: form, development, and implications. Journal of Glaciology, 29(102), pp.250-259.

Small, R.J., 1987. Englacial and supraglacial sediment: transport and deposition. Glacio-Fluvial Sediment Transfer: An Alpine Perspective. John Wiley and Sons, New York New York. 1987. pp. 165-197.

Snavely, N., Seitz, S.M. and Szeliski, R., 2008. Modeling the world from internet photo collections. International journal of computer vision, 80(2), pp.189-210.

Spedding, N. and Evans, D.J., 2002. Sediments and landforms at Kvíárjökull, southeast Iceland: a reappraisal of the glaciated valley landsystem. Sedimentary Geology, 149(1-3), pp.21-42.

Stokes, C.R., Spagnolo, M., Clark, C.D., Cofaigh, C.Ó., Lian, O.B. and Dunstone, R.B., 2013. Formation of mega-scale glacial lineations on the Dubawnt Lake Ice Stream bed: 1. size, shape and spacing from a large remote sensing dataset. Quaternary Science Reviews, 77, pp.190-209.

Swift, D.A., Evans, D.J. and Fallick, A.E., 2006. Transverse englacial debris-rich ice bands at Kvíárjökull, southeast Iceland. Quaternary Science Reviews, 25(13-14), pp.1708-1718.

Swift, D.A., Cook, S.J., Graham, D.J., Midgley, N.G., Fallick, A.E., Storrar, R., Rodrigo, M.T. and Evans, D.J.A., 2018. Terminal zone glacial sediment transfer at a temperate overdeepened glacier system. Quaternary Science Reviews, 180, pp.111-131.

Stroeven, A.P., Hättestrand, C., Kleman, J., Heyman, J., Fabel, D., Fredin, O., Goodfellow, B.W., Harbor, J.M., Jansen, J.D., Olsen, L. and Caffee, M.W., 2016. Deglaciation of fennoscandia. Quaternary Science Reviews, 147, pp.91-121.

Trenbirth, H.E. and Matthews, J.A., 2010. Lichen growth rates on glacier forelands in southern Norway: preliminary results from a 25-year monitoring programme. Geografiska Annaler: Series A, Physical Geography, 92(1), pp.19-39.

Vectorworks Inc., 2017. Vectorworks SP5 (Software). Retrieved from https://www.vectorworks.net/downloads/ServicePack?major=2017&servicepack=5&language=1

Weber, P., Boston, C.M., Lovell, H. and Andreassen, L.M., 2019. Evolution of the Norwegian plateau icefield Hardangerjøkulen since the 'Little Ice Age'. The Holocene, 29(12), pp.1885-1905.

Westoby, M.J., Brasington, J., Glasser, N.F., Hambrey, M.J. and Reynolds, J.M., 2012. 'Structure-from-Motion'photogrammetry: A low-cost, effective tool for geoscience applications. Geomorphology, 179, pp.300-314.

Winkler, S. and Matthews, J.A., 2010. Observations on terminal moraine-ridge formation during recent advances of southern Norwegian glaciers. Geomorphology, 116(1-2), pp.87-106.

World Meteorological Organization (WMO). 2019. European Heatwave Sets New Temperature Records. [online] Available at: <https://public.wmo.int/en/media/news/european-heatwave-sets-new-temperature-records> [Accessed 30 March 2020].

Worsley, P., 1974. Recent "annual" moraine ridges at Austre Okstindbreen, Okstindan, north Norway. Journal of Glaciology, 13(68), pp.265-277.

Wyshnytzky, C.E., 2017. On the mechanisms of minor moraine formation in high-mountain environments of the European Alps. Doctoral dissertation, School of Geography, Queen Mary University of London, pp.329

Yiou, P., Cattiaux, J., Faranda, D., Kadygrov, N., Jézéquel, A., Naveau, P., Ribes, A., Robin, Y., Thao, S., van Oldenborgh, G.J. and Vrac, M., 2020. Analyses of the Northern European summer heatwave of 2018. Bulletin of the American Meteorological Society, 101(1), pp.S35-S40.

Tidigare skrifter i serien ”Examensarbeten i Geologi vid Lunds universitet”:

531. Höglund, Nikolas, 2018: Groundwater chemistry evaluation and a GIS-based approach for determining groundwater potential in Mörbylånga, Sweden. (45 hp)
532. Haag, Vendela, 2018: Studie av mikrostrukturer i karbonatslagkäglor från nedslagsstrukturen Charlevoix, Kanada. (15 hp)
533. Hebrard, Benoit, 2018: Antropocen – vad, när och hur? (15 hp)
534. Jancsak, Nathalie, 2018: Åtgärder mot kusterosion i Skåne, samt en fallstudie av erosionsskydden i Löderup, Ystad kommun. (15 hp)
535. Zachén, Gabriel, 2018: Mesosideriter – redogörelse av bildningsprocesser samt SEM-analys av Vaca Muertameteoriten. (15 hp)
536. Fägersten, Andreas, 2018: Lateral variability in the quantification of calcareous nannofossils in the Upper Triassic, Austria. (15 hp)
537. Hjertman, Anna, 2018: Förutsättningar för djupinfiltration av ytvatten från Ivösjön till Kristianstadbassängen. (15 hp)
538. Lagerstam, Clarence, 2018: Varför svalde svanödlor (Reptilia, Plesiosauria) stenar? (15 hp)
539. Pilser, Hannes, 2018: Mg/Ca i bottenlevande foraminiferer, särskilt med avseende på temperaturer nära 0°C. (15 hp)
540. Christiansen, Emma, 2018: Mikroplast på och i havsbotten - Utbredningen av mikroplaster i marina bottensediment och dess påverkan på marina miljöer. (15 hp)
541. Staahlnacke, Simon, 2018: En sammanställning av norra Skånes prekambriska berggrund. (15 hp)
542. Martell, Josefin, 2018: Shock metamorphic features in zircon grains from the Mien impact structure - clues to conditions during impact. (45 hp)
543. Chitindingu, Tawonga, 2018: Petrological characterization of the Cambrian sandstone reservoirs in the Baltic Basin, Sweden. (45 hp)
544. Chonewicz, Julia, 2018: Dimensionerande vattenförbrukning och alternativa vattenkvaliteter. (15 hp)
545. Adeen, Lina, 2018: Hur lämpliga är de geofysiska metoderna resistivitet och IP för kartläggning av PFOS? (15 hp)
546. Nilsson Brunlid, Anette, 2018: Impact of southern Baltic sea-level changes on landscape development in the Verkeån River valley at Haväng, southern Sweden, during the early and mid Holocene. (45 hp)
547. Perälä, Jesper, 2018: Dynamic Recrystallization in the Sveconorwegian Frontal Wedge, Småland, southern Sweden. (45 hp)
548. Artursson, Christopher, 2018: Stratigraphy, sedimentology and geophysical assessment of the early Silurian Halla and Klinteberg formations, Altajme core, Gotland, Sweden. (45 hp)
549. Kempengren, Henrik, 2018: Att välja den mest hållbara efterbehandlingsmetoden vid sanering: Applicering av beslutsstödsverktyget SAMLA. (45 hp)
550. Andreasson, Dagnija, 2018: Assessment of using liquidity index for the approximation of undrained shear strength of clay tills in Scania. (45 hp)
551. Ahrenstedt, Viktor, 2018: The Neoproterozoic Visingsö Group of southern Sweden: Lithology, sequence stratigraphy and provenance of the Middle Formation. (45 hp)
552. Berglund, Marie, 2018: Basaltkuppen - ett spel om mineralogi och petrologi. (15 hp)
553. Hernnäs, Tove, 2018: Garnet amphibolite in the internal Eastern Segment, Sveconorwegian Province: monitors of metamorphic recrystallization at high temperature and pressure during Sveconorwegian orogeny. (45 hp)
554. Halling, Jenny, 2019: Characterization of black rust in reinforced concrete structures: analyses of field samples from southern Sweden. (45 hp)
555. Stevic, Marijana, 2019: Stratigraphy and dating of a lake sediment record from Lyngsjön, eastern Scania - human impact and aeolian sand deposition during the last millennium. (45 hp)
556. Rabanser, Monika, 2019: Processes of Lateral Moraine Formation at a Debris-covered Glacier, Suldenferner (Vedretta di Solda), Italy. (45 hp)
557. Nilsson, Hanna, 2019: Records of environmental change and sedimentation processes over the last century in a Baltic coastal inlet. (45 hp)
558. Ingered, Mimmi, 2019: Zircon U-Pb constraints on the timing of Sveconorwegian migmatite formation in the Western and Median Segments of the Idefjorden terrane, SW Sweden. (45 hp)
559. Hjorth, Ingeborg, 2019: Paleomagnetisk undersökning av vulkanen Rangitoto, Nya Zeeland, för att bestämma dess utbrottshistoria. (15 hp)
560. Westberg, Märta, 2019: Enigmatic wormlike fossils from the Silurian Waukesha Lagerstätte, Wisconsin, USA. (15 hp)

561. Björn, Julia, 2019: Undersökning av påverkan på hydraulisk konduktivitet i förorenat område efter in situ-saneringsförsök. (15 hp)
562. Faraj, Haider, 2019: Tolkning av georadarprofiler över grundvattenmagasinet Verveln - Gullringen i Kalmar län. (15 hp)
563. Bjermo, Tim, 2019: Eoliska avlagringar och vindriktningar under holocen i och kring Store Mosse, södra Sverige. (15 hp)
564. Langkjaer, Henrik, 2019: Analys av Östergötlands kommande grundvattenresurser ur ett klimtperspektiv - med fokus på förstärkt grundvattenbildning. (15 hp)
565. Johansson, Marcus, 2019: Hur öppet var landskapet i södra Sverige under Atlantisk tid? (15 hp)
566. Molin, Emmy, 2019: Litologi, sedimentologi och kolisotopstratigrafi över krita–paleogen-gränsintervallet i borrningen Limhamn-2018. (15 hp)
567. Schroeder, Mimmi, 2019: The history of European hemp cultivation. (15 hp)
568. Damber, Maja, 2019: Granens invandring i sydvästa Sverige, belyst genom pollenanalys från Skottenesjön. (15 hp)
569. Lundgren Sassner, Lykke, 2019: Strandmorfologi, stranderosion och stranddeposition, med en fallstudie på Tylösand sandstrand, Halland. (15 hp)
570. Greiff, Johannes, 2019: Mesozoiska konglomerat och Skånes tektoniska utveckling. (15 hp)
571. Persson, Eric, 2019: An Enigmatic Cerapodian Dentary from the Cretaceous of southern Sweden. (15 hp)
572. Aldenius, Erik, 2019: Subsurface characterization of the Lund Sandstone – 3D model of the sandstone reservoir and evaluation of the geoenergy storage potential, SW Skåne, South Sweden. (45 hp)
573. Juliusson, Oscar, 2019: Impacts of subglacial processes on underlying bedrock. (15 hp)
574. Sartell, Anna, 2019: Metamorphic paragenesis and P-T conditions in garnet amphibolite from the Median Segment of the Idefjorden Terrane, Lilla Edet. (15 hp)
575. Végvári, Fanni, 2019: Vulkanisk inverkan på klimatet och atmorsfärcirkulationen: En litterarurstudie som jämför vulkanism på låg respektive hög latitud. (15 hp)
576. Gustafsson, Jon, 2019: Petrology of platinum-group element mineralization in the Koillismaa intrusion, Finland. (45 hp)
577. Wahlquist, Per, 2019: Undersökning av mindre förkastningar för vattenuttag i sedimentärt berg kring Kingelstad och Tjutebro. (15 hp)
578. Gaitan Valencia, Camilo Esteban, 2019: Unravelling the timing and distribution of Paleoproterozoic dyke swarms in the eastern Kaapvaal Craton, South Africa. (45 hp)
579. Eggert, David, 2019: Using Very-Low-Frequency Electromagnetics (VLF-EM) for geophysical exploration at the Albertine Graben, Uganda - A new CAD approach for 3D data blending. (45 hp)
580. Plan, Anders, 2020: Resolving temporal links between the Högberget granite and the Wigström tungsten skarn deposit in Bergslagen (Sweden) using trace elements and U-Pb LA-ICPMS on complex zircons. (45 hp)
581. Pilser, Hannes, 2020: A geophysical survey in the Chocaya Basin in the central Valley of Cochabamba, Bolivia, using ERT and TEM. (45 hp)
582. Leopardi, Dino, 2020: Temporal and genetical constraints of the Cu-Co Vena-Dampetorp deposit, Bergslagen, Sweden. (45 hp)
583. Lagerstam Lorien, Clarence, 2020: Neck mobility versus mode of locomotion – in what way did neck length affect swimming performance among Mesozoic plesiosaurs (Reptilia, Sauropterygia)? (45 hp)
584. Davies, James, 2020: Geochronology of gneisses adjacent to the Mylonite Zone in southwestern Sweden: evidence of a tectonic window? (45 hp)
585. Foyn, Alex, 2020: Foreland evolution of Blåisen, Norway, over the course of an ablation season. (45 hp)

LUNDS UNIVERSITET

Geologiska institutionen
Lunds universitet
Sölvegatan 12, 223 62 Lund